Closed-Loop Reference Model Adaptive Control: with Application to Very Flexible Aircraft

by

Travis Eli Gibson

B.S., Georgia Institute of Technology (2006)
S.M., Massachusetts Institute of Technology (2008)

Submitted to the Department of Mechanical Engineering
in partial fulfillment of the requirements for the degree of

Doctor of Philosophy in Mechanical Engineering

at the

MASSACHUSETTS INSTITUTE OF TECHNOLOGY

February 2014

Author .....
Department of Mechanical Engineering
December 30, 2013

Certified by .....
Anuradha M. Annaswamy
Senior Research Scientist
Thesis Supervisor

Accepted by .....
David E. Hardt
Chairman, Department Committee on Graduate Theses

Closed-Loop Reference Model Adaptive Control: with Application to Very Flexible Aircraft

by

Travis Eli Gibson

Submitted to the Department of Mechanical Engineering
on December 30, 2013, in partial fulfillment of the
requirements for the degree of
Doctor of Philosophy in Mechanical Engineering

Abstract

One of the main features of adaptive systems is an oscillatory convergence that exacerbates with the speed of adaptation. Over the past two decades several attempts have been made to provide adaptive solutions with guaranteed transient properties. In this work it is shown that Closed-loop Reference Models (CRMs) can result in improved transient performance over their open-loop counterparts in model reference adaptive control. In addition to deriving bounds on L-2 norms of the derivatives of the adaptive parameters which are shown to be smaller, an optimal design of CRMs is proposed which minimizes an underlying peaking phenomenon. The analytical tools proposed are shown to be applicable for a range of adaptive control problems including direct control, composite control with observer feedback and partial states accessible control. In addition a detailed study of the applicability of CRM adaptive control to very flexible aircraft is presented.

Following the NASA Helios flight mishap in 2003 there has been a push for greater understanding of the aerodynamic–structural coupling that occurs in light, very flexible, flying wings. Previous efforts in that direction revealed that the flexible aircraft had instability in the phugoid mode for large dihedral angles and that including the flexible dynamics was necessary to arrive at an appropriate trim condition. In this thesis, we show how these large dihedral excursions can occur in the presence of turbulence, by constructing an overall nonlinear model that captures the dominant dynamics of a very flexible aircraft. The thesis closes with the application of CRM adaptive control to the VFA model.

Thesis Supervisor: Anuradha M. Annaswamy
Title: Senior Research Scientist

Acknowledgments

I would like to thank the scientific process for being true. The person most responsible for my success is my advisor, Anuradha Annaswamy. Horror stories are passed around of inaccessible advisors, snap funding catastrophes and the like. She has always been available for discussion and has made sure that my funding was always in line, even during the economic crisis of 2008 and the sequestration in early 2013. Another person responsible for my success is Eugene Lavretsky. Eugene, like Anuradha, has always been accessible and was the one who encouraged me to study the specific adaptive structure that became the core of my thesis. I would also like to thank the other members of my PhD committee, Mark Drela and Jean-Jacques Slotine, for their valuable input. Colleagues that have positively influenced my work are Zac Dydek, Yoav Sharon, Yildiray Yildiz, Ross Gadient, David Wilcox, Irene Gregory, Sean Kenny and Luis Crespo. Finally, I have to thank my family: Eddie Gibson, for which hard work is his definition, Lisa Gibson, who made sure that I received the best education possible and even home schooled me when the local schools were not up to par, and Tyler Gibson for buying that motorcycle. If Tyler had not purchased a motorcycle and forced the big brother to man up I would have missed out on, what is now, the biggest passion of my life. A very special thanks is in order for A.G. as well. I leave you with the most important statement made by an individual in my lifetime.

> *[T]he offer of certainty, the offer of complete security, the offer of an impermeable faith that cant give way, is an offer of something not worth having. I want to live my life taking the risk all the time that I dont know anything like enough yet; that I haven't understood enough; that I cant know enough; that I'm always hungrily operating on the margins of a potentially great harvest of future knowledge and wisdom. I wouldn't have it any other way. And I'd urge you to look at those people who tell you, at your age, that you're dead till you believe as they do. What a terrible thing to be telling to children! And that you can only live by accepting an absolute authority, dont think of that as a gift. Think of it as a poisoned chalice. Push it aside, however tempting it is. Take the risk of thinking for yourself. Much more happiness, truth, beauty, and wisdom will come to you that way.*
>
> – Christopher Hitchens, 2010

Contents

1 Introduction **15**
1.1 Contributions by Chapter 17

2 Mathematical Preliminaries and Stability Definitions **21**
2.1 Introduction 21
2.2 Preliminaries 21
2.2.1 Vector Norms 21
2.2.2 Matrix Norms 22
2.2.3 Signal Norms 23
2.2.4 Positive Matrices 24
2.2.5 Continuity 25
2.2.6 Convergence 26
2.3 Definitions of Stability 26
2.4 Conditions for Stability 28
2.5 Linear Systems 32
2.5.1 Transfer Functions 36
2.5.2 Cheap Observer Riccati Equations 37

3 Closed-loop Reference Model Adaptive Control **39**
3.1 Introduction 39
3.2 CRM-Based Adaptive Control of Scalar Plants 41
3.2.1 Stability Properties of CRM-adaptive systems 41
3.2.2 Transient Performance of CRM-adaptive systems 42
3.2.3 Effect of Projection Algorithm 46
3.3 Bounded Peaking with CRM adaptive systems 47
3.3.1 Bounds on x_m 47
3.3.2 Bounds on parameter derivatives and oscillations 50
3.3.3 Simulation Studies for CRM 51
3.4 CRM for States Accessible Control 51
3.5 CRM Composite Control with Observer Feedback 57
3.5.1 Stability 58
3.5.2 Transient performance of CMRAC-CO 59
3.5.3 Robustness of CMRAC–CO to Noise 61
3.5.4 Simulation Study 63
3.5.5 Comments on CMRAC and CMRAC–CO 65

3.6 CRMs in other Adaptive Systems . . . 66
3.6.1 Adaptive Backstepping with Tuning Functions . . . 66
3.6.2 Adaptive Control in Robotics . . . 67
3.7 Conclusions . . . 68

4 Closed-loop Reference Models in SISO Adaptive Control 71
4.1 Introduction . . . 71
4.2 Notation . . . 72
4.3 The Control Problem . . . 73
4.4 Classical $n^* = 1$ case (ORM $n^* = 1$) . . . 73
4.4.1 Stability for $n^* = 1$ . . . 74
4.5 CRM $n^* = 1$ . . . 75
4.5.1 Performance . . . 77
4.6 CRM SISO $n^* = 2$ . . . 78
4.6.1 Performance . . . 79
4.7 CRM Arbitrary n^* . . . 79
4.7.1 Stability for known high frequency gain . . . 79
4.7.2 Performance when k_p known . . . 83
4.7.3 Stability in the case of unknown high frequency gain . . . 85
4.8 Conclusion . . . 88

5 Control Oriented Modeling of Very Flexible Aircraft 89
5.1 Introduction . . . 89
5.2 Modeling . . . 91
5.2.1 Vector Notation . . . 91
5.2.2 Forces and Frames for Aircraft Dynamics . . . 91
5.2.3 Linear and Angular Momentum for Very Flexible Aircraft . . . 93
5.2.4 Forces and Moments acting on VFA in Stability Axis Frame . . . 96
5.3 Effect of Large Dihedral Angles . . . 98
5.3.1 Trim Analysis . . . 98
5.4 Control of Dihedral Angles . . . 101
5.4.1 Control Design . . . 101
5.4.2 Controllability and Observability . . . 103
5.4.3 Controllability and Observability Measures applied to VFA Model 104
5.5 Analysis of Helios Crash . . . 105
5.5.1 Part I: . . . 105
5.5.2 Part II: . . . 106
5.5.3 Part III: . . . 107
5.5.4 Part IV: . . . 107
5.6 Conclusions . . . 108

6 Modern Output Feedback Adaptive Control 111
6.1 SISO: Zero Annihilation . . . 112
6.2 MIMO Square: Zero Annihilation . . . 114
6.3 MIMO LQG/LTR . . . 116

6.4 Adaptive Control for Very Flexible Aircraft 118
6.4.1 Comparison of linear and adaptive controllers 122

7 Conclusions **129**
7.1 Future Work 129

A Projection Algorithm **131**
A.1 Properties of Convex Sets and Functions 131
A.2 Projection 132
A.3 Γ–Projection 135

B Bounds for Signals in SISO Adaptive System **137**
B.1 Norm of $e_\chi(t)$ 137
B.2 Norm of $e_a(t)$ 139

C MIMO Adaptive Control Squaring Up Example **141**
C.1 Creating SPR Transfer Functions for Square Systems Using Observer Feedback 141
C.2 Squaring Up 142
C.3 Mixing the Outputs 143
C.4 Adaptive Control Example 143

List of Figures

1-1 Centrifugal governor [55]. 15
1-2 Open–loop reference model (top) does not use feedback from the error state to modify the reference trajectory. The closed–loop reference model (bottom) uses the error signal as an extra input into the reference model. 16
1-3 (a) Helios flying at normal dihedral. (b) Helios flying at large dihedral. (c) Helios breaking apart mid flight. 17

2-1 Norms in $\mathbb{R}^2$. 22
2-2 Asymptotic stability, adapted from [35]. 28
2-3 Lyapunov stability, adapted from [35]. 30
2-4 Asymptotic stability, adapted from [35]. 30

3-1 Trajectories of the ORM adaptive system $\gamma = 1$. 52
3-2 Trajectories of the ORM adaptive system $\gamma = 10$. 52
3-3 Trajectories of the ORM adaptive system $\gamma = 100$. 52
3-4 Trajectories of the CRM adaptive system $\gamma = 100$, $\ell = -10$. 53
3-5 Trajectories of the CRM adaptive system $\gamma = 100$, $\ell = -100$. 53
3-6 Trajectories of the CRM adaptive system $\gamma = 100$, $\ell = -1000$. 53
3-7 (top) reference model trajectories x_m, (middle) state x, and (bottom) model following e. 64
3-8 (top) Control input u, (middle–top) discrete rate of change of control input $\Delta u/\Delta t$, (middle–bottom) adaptive parameter $\theta(t)$ and (bottom) adaptive parameter $\hat{\theta}(t)$. 65

5-1 NASA Helios in flight. 90
5-2 Reference frames important for describing aircraft motion. 92
5-3 Artistic rendering of VFA. 93
5-4 Schematic of VFA. 94
5-5 Eigenvalues for trim points. At zero dihedral angle the short period mode is lightly damped and the phugoid mode is stable. As the dihedral angle increases the short period mode damping increases and the phugoid mode becomes unstable. 100
5-6 Initial condition perturbation from trim input for dihedral angle of 5 degrees. 101
5-7 Helios flight mishap data (adapted from [65]). 102

5-8 LQG Control Structure. 103
5-9 Measure of controllability as a function of input selection and dihedral angle. 104
5-10 Measure of controllability as a function of input selection and dihedral angle, semilog plot. 105
5-11 Simulation in the presence of turbulence with $\Delta_t = 0.1$ and $D = 1$ for the three test case scenarios in Table 5.3. 107
5-12 Comparison of dihedral measured in ft for Helios mishap and VFA sim Case (i), $D = 1$, and $\Delta_t \in \{0.1, 0.05, 0.01\}$. 108
5-13 Comparison of dihedral measured in ft for Helios mishap and VFA sim Case (i), $\Delta_t = 0.1$, and $D \in \{1, \sqrt{0.5}, \sqrt{0.1}\}$. 109
5-14 Comparison of dihedral measured in ft for Helios mishap and VFA sim Case (i). 109

6-1 PZ Map for MIMO system with feedback gain L chosen as in Lemma 6.2. 114
6-2 Comparison of adaptive and linear controller to dihedral disturbance. 121
6-3 Comparison of adaptive and linear controller to dihedral disturbance $t \in [0, 20]$. 123
6-4 Comparison of adaptive and linear controller to dihedral disturbance $t \in [0, 80]$. 124
6-5 Adaptive gains without turbulence $t \in [0, 80]$. 125
6-6 Comparison of adaptive and linear controller in the presence of turbulence over $t \in [0, 20]$. 126
6-7 Comparison of adaptive and linear controller to dihedral disturbance in the presence of turbulence over $t \in [0, 800]$. 127
6-8 Adaptive gains in the presence of turbulence $t \in [0, 800]$. 128

A-1 Visualization of Projection Operator in $\mathbb{R}^2$. 133

List of Tables

3.1 Test Case Equations 63
3.2 Simulation Parameters 64

5.1 Constants. 99
5.2 Controllability/Observability Study. 104
5.3 Simulation Cases. 106
5.4 Simulation Cases. 106

6.1 Control Design Parameters. 122

C.1 Definitions 141

Chapter 1

Introduction

Control systems arise anytime the output of a system needs to be regulated or forced to track a command. The first instances of control systems appeared in the first century A.D., in the form of water clocks. [7] The most cited modern example of a mechanical control system is that of the fly-ball governor, see Figure 1-1. [3] The fly-ball governor was first used to regulate the speed of the output shaft on a steam engine. The output shaft of the steam engine is connected to the shaft that the ball governors rotate on. As the speed of the output shaft increases, the the scissor arms spread, and the linkage at the top of figure then decreases the throttle setting on the righthand side of the figure. This illustrates the defining feature of automatic control, the notion of *feedback*. [80] That is, a system output is measured and then fed back into the input of the system. Feedback control systems are ever-present occurring naturally or engineered into our machines.

The basic premise of any adaptive control system is to have the output of a plant follow a prescribed reference model through the online adjustment of control parameters. [4, 32, 37, 41, 47, 61, 73] Adaptive control originated in 1958 [79] and was popular in aircraft control for most of the 60's until the X-15 flight mishap in 1967 [17, 25]. It was clear that adaptive control was in its infancy and it would take two more

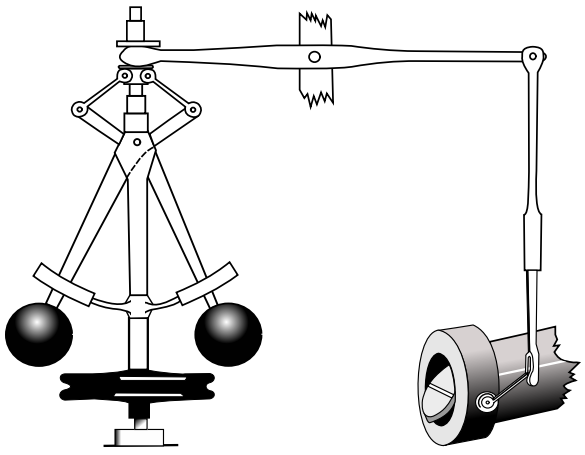

Figure 1-1: Centrifugal governor [55].

decades until the stability of adaptive systems was fully understood [18,26,58,62,63]. Following stability of adaptive control systems in the 80s and their robustness into the 90s [31, 36, 59, 60, 67], several attempts have been made to quantify transient performance (see for example, [10, 38, 81]).

Historically, the reference models in MRAC have been open-loop in nature (see for example, [32, 61]), with the reference trajectory generated by a linear dynamic model, and unaffected by the plant output. The notion of feeding back the model following error into the reference model was first reported in [49] and more recently in [20–23, 44, 45, 74, 75]. We denote adaptive systems with an Open-loop Reference Model as ORM-adaptive systems and those with closed-loop reference models as CRM-adaptive systems, see Figure 1-2.

Combined/composite direct and indirect Model Reference Adaptive Control (CMRAC) [16,72], is another class of adaptive systems in which a noticeable improvement in transient performance was demonstrated. While the results of these papers established stability of combined schemes, no rigorous guarantees of improved transient performance were provided, and have remained a conjecture [43]. This thesis is concerned with rigorously proving how one can design CRM adaptive systems with improved transient performance over their ORM counterparts.

In keeping with tradition our application of interest is that of aircraft control. Re-

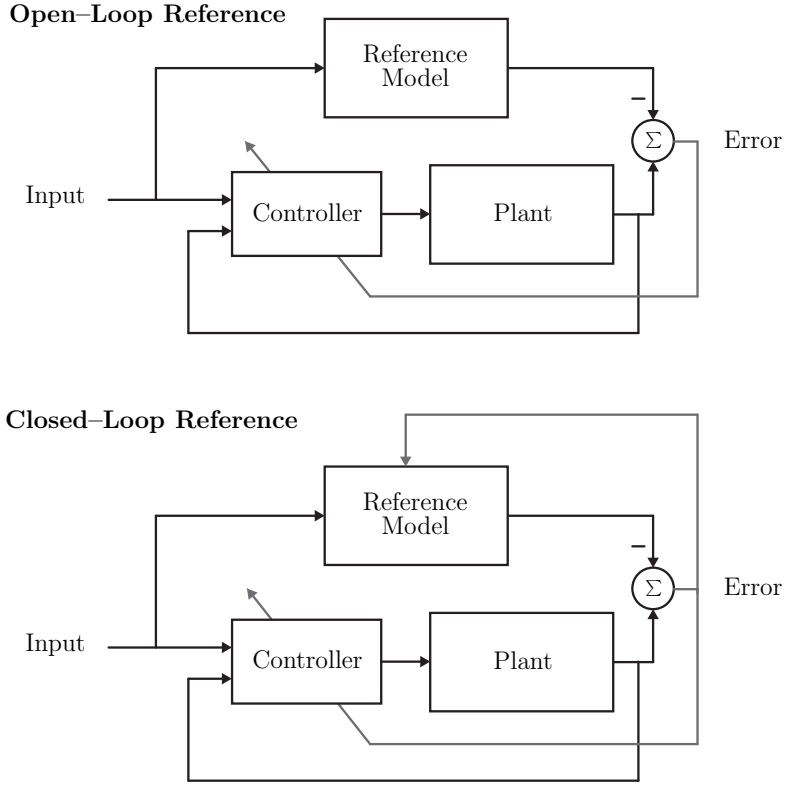

Figure 1-2: Open–loop reference model (top) does not use feedback from the error state to modify the reference trajectory. The closed–loop reference model (bottom) uses the error signal as an extra input into the reference model.

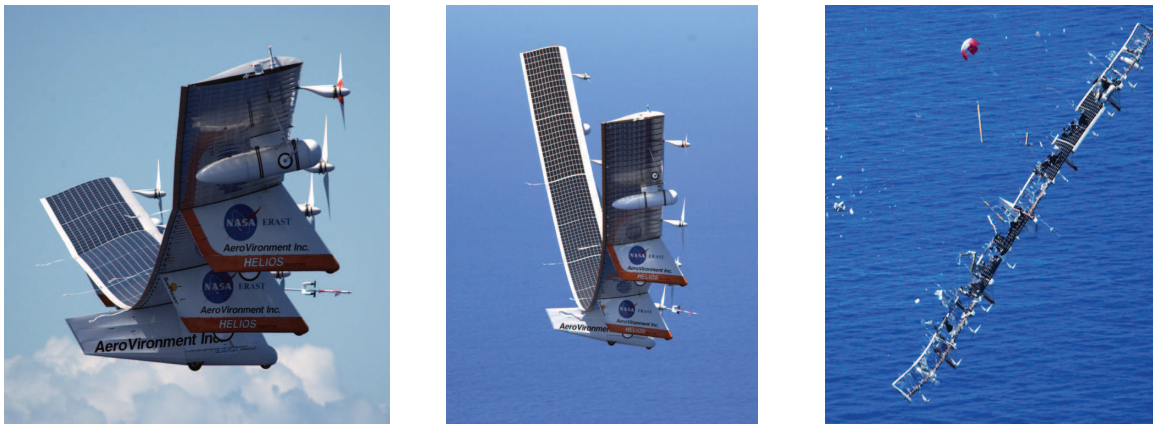

(a) (b) (c)

Figure 1-3: (a) Helios flying at normal dihedral. (b) Helios flying at large dihedral. (c) Helios breaking apart mid flight.

cently the control of very flexible aircraft has become of interest. One such example is the Helios aircraft, depicted in Figure 1-3. On June 26$^{\text{th}}$ 2003 the aircraft broke apart mid–flight during testing. Throughout the flight the aircraft encountered turbulence. After approximately 30 minutes of flight time a larger than expected wing dihedral formed and the aircraft began a slowly diverging pitch oscillation. The oscillations never subsided and led to flight speeds beyond the design specifications for Helios. The loading on the aircraft compromised the structure of the aircraft and the skin of the aircraft pulled apart. One of the key recommendations that came from the flight mishap investigation was to, "Develop more advanced, multidisciplinary (structures, aeroelastic, aerodynamics, atmospheric, materials, propulsion, controls, etc) "time-domain" analysis methods appropriate to highly flexible, "morphing" vehicles" [65]. This thesis addresses this recommendation directly with a control oriented model of very flexible aircraft and an adaptive control design.

The thesis is organized as follows: Chapter 2 contains the mathematical preliminaries, Chapter 3 contains the main theoretical components of transient response and CRM systems, Chapter 4 analysis's the benefits of CRMs in SISO adaptive control, Chapter 5 presents a model for control design of very flexible aircraft, Chapter 6 contains the adaptive control design for very flexible aircraft, and Chapter 7 ends with conclusions and future directions.

1.1 Contributions by Chapter

Chapter 2

Very little in this chapter is original. All of the definitions pertaining to real analysis were taken from [69]. The functional analysis results were taken from MIT 18.102 course notes. The stability definitions originated in [52] with the necessary conditions from stability coming from [51, 61].

Chapter 3

The main contribution of this thesis comes in this chapter. It is shown how one can design adaptive systems with improved transients in terms of model following error and a reduced L-2 norm of the derivative of the adaptive parameters. It is then shown that reducing the L-2 norm of the derivative of a signal directly correlates into a reduction of the high frequency oscillations of the system. Another major contribution from this chapter is the introduction of adaptive systems with filtered regressor vectors. It is shown that introducing CRMs into CMRAC results in the recovery of a separation like principle.

Chapter 4

This chapter extends the results of Chapter 3 to the SISO case. There are three contributions from this chapter: 1) Using CRM, one can follow reference models that are not SPR. 2) Using CRMs in SISO control one can choose the feedback gain such that the error model reduces to a first order decay, 3) Analysis of adaptive systems always comes in the form of non-minimal state analysis. This chapter illustrates that much tighter performance bounds can be achieved when analyzing the minimal state-space models. This chapter also shows that the results for the scalar adaptive system in Chapter 3 were not a fluke.

Chapter 5

This chapter introduces a first principles simple model of very flexible aircraft. A trend in the literature surrounding VFA is that complicated CFD models are needed to explain why the Helios flight mishap occurred. However a simple understudying of controllability could have predicted the demise of he Helios aircraft. It is shown through simulation that VFA can suffer from turbulence induced dihedral drift, the catalyst for the Helios crash.

Chapter 6

This chapter analyzes a modern interpretation of output feedback adaptive control. This is accomplished via a zero annihilation technique and an LQG/LTR technique first realized in [44]. A different stability analysis is presented for the LQG/LTR technique as compared to that in [47] where $\lim_{t\to\infty} e(t) = 0$. Also, the need for a prescribed degree of stability is relaxed. The Chapter is closed with the application of LQG/LTR adaptive control to the VFA model presented in Chapter 5.

Chapter 7

This chapter contains the conclusions and future directions.

Chapter 2

Mathematical Preliminaries and Stability Definitions

2.1 Introduction

This chapter introduces the basic mathematical principles and theorems necessary to discuss the stability and transient performance of adaptive systems.

2.2 Preliminaries

2.2.1 Vector Norms

A norm on a vector space V, usually denoted as $\| \ \|$, maps from a vector space V to the real numbers and is always greater than or equal to zero. Our vector spaces of interest are $\mathbb{R}^n$ (vectors containing all real elements) and possibly $\mathbb{C}^n$ (vectors of complex elements).

Definition 2.1 (Norm)**.** V is a vector space over the field K. Let the norm be defined as $\|\cdot\| : V \longrightarrow [0, \infty)$. Let $a \in K$ and $x, y \in V$. All norms satisfy

(a) $\|x\| = 0$ if and only if $x = 0$

(b) $\|ax\| = |a| \, \|x\|$

(c) $\|x + y\| \leq \|x\| + \|y\|$

With the following subscript definition,

$$x^T = \begin{bmatrix} x_1 & x_2 & \cdots & x_n \end{bmatrix}$$

for all $x \in \mathbb{R}^n$, $1 \leq p < \infty$

$$\|x\|_p \triangleq \left(\sum_{i=1}^{n} |x_i|^p \right)^{1/p}$$

and

$$\|x\|_\infty \triangleq \sup_i |x_i| .$$

The norms are referred to as p-norms (1-norm, 2-norm, ..., ∞-norm). It will always be assumed that when the subscript on the p-norm is not given, we are assuming $p = 2$,

$$\|x\| \triangleq \|x\|_2.$$

A visualization of these norms is given in Figure 2-1.

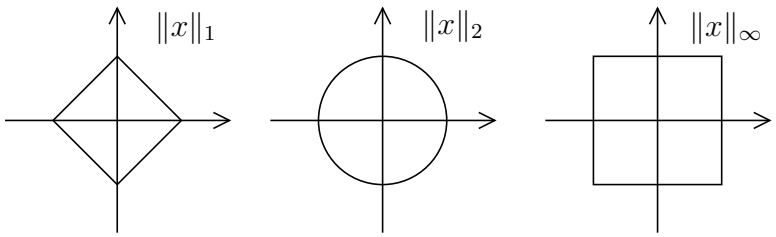

Figure 2-1: Norms in $\mathbb{R}^2$.

2.2.2 Matrix Norms

Let $A \in \mathbb{R}^{m\times n}$ then the induced p-norm is defined as

$$\|A\|_p \triangleq \sup_{\|x\|=1} \frac{\|Ax\|_p}{\|x\|_p}.$$

when the Euclidean norm is used, i.e. $p = 2$ we have that

$$\|A\|_2 = \sqrt{\lambda_{\max}(A^T A)}$$

where $\lambda_{\max}$ denotes the maximum eigenvalue. Also as before, when no p value is denoted, it is assumed that $p = 2$,

$$\|A\| = \|A\|_2.$$

Property 2.1. *The induced p-norms have two special properties. Let $x \in \mathbb{R}^n$, $A \in \mathbb{R}^{m\times n}$ and $B \in \mathbb{R}^{n\times d}$*

$$\begin{aligned} \|Ax\|_p &\le \|A\|_p \|x\|_p \\ \|AB\|_p &\le \|A\|_p \|B\|_p. \end{aligned} \tag{2.1}$$

Note that this property need not hold for all matrix norms.

Definition 2.2. When a norm satisfies the second property above, $\|AB\|_p \le \|A\|_p \|B\|_p$ it is called a sub-multiplicative norm.

Definition 2.3. Let $A \in \mathbb{R}^{n\times n}$, the Frobenius norm is defined as

$$\|A\|_F = \sqrt{\text{trace}(A^T A)}$$

Property 2.2. *The Frobenius norm is a sub-multiplicative norm.*

2.2.3 Signal Norms

Let $x(t) : \mathbb{R} \to \mathbb{R}^n$ and $1 \leq p < \infty$

$$\|x(t)\|_{L_p} \triangleq \left(\lim_{t\to\infty} \int_0^t \|x(\tau)\|^p d\tau \right)^{1/p}. \tag{2.2}$$

and

$$\|x(t)\|_{L_\infty} \triangleq \sup_t \|x(t)\| \tag{2.3}$$

Note that we are not using the essential supremum here, but just the supremum. If the essential supremum were being used, then we would allow the signal to be unbounded on a set of measure zero, and it would still be in $\mathcal{L}_\infty$. With our definition, if a signal is in $\mathcal{L}_\infty$ then the signal is bounded for all time.

The above norm is called the L_p-norm. The p-norm was used on a time varying signal $x(t)$ giving us a time dependent "norm" $\|x(t)\|$. At each fixed t, $\|x(t)\|$ is a norm, but it is not true to say that for all t, $\|x(t)\|$ is a norm. We need a scalar value for all t, so we resorted to integration or using the supremum operator. The above definitions also hold for the induced matrix norms.

It is notationally equivalent to write L_p, L^p, $\mathcal{L}_p$, $\mathcal{L}^p$. Its just a preference of superscript, subscript, and or calligraphic text.

Lemma 2.1. *For $a, b \geq 0$ and $t \in [0, 1]$ the following holds*

$$\mathbf{e}^{ta+(1-t)b} \leq t\mathbf{e}^a + (1-t)\mathbf{e}^b.$$

Proof. This proof follows from the fact that the exponential function is concave up and any secant line is always necessarily above the exponential function between the two points of intersection. □

Theorem 2.1 (Young's Inequality)**.** *For $a, b \geq 0$ and $p, q \geq 1$ the following holds*

$$ab \leq \frac{a^p}{p} + \frac{b^q}{q}$$

where

$$\frac{1}{p} + \frac{1}{q} = 1.$$

Proof. Begin with the equality

$$\begin{aligned} ab &= \mathbf{e}^{\log a + \log b} \\ &= \mathbf{e}^{\frac{1}{p}p\log a + \frac{1}{q}q\log b} \end{aligned}$$

From the fact that $1/p = 1 - 1/q$ and using Lemma 2.1 we have that

$$\begin{aligned} ab &\leq \frac{1}{p}\mathbf{e}^{p\log a} + \frac{1}{q}\mathbf{e}^{q\log b} \\ &= \frac{1}{p}a^p + \frac{1}{q}b^q \end{aligned}$$

□

Theorem 2.2 (Hoelder's Inequality)**.** *Let $f(t)$ and $g(t)$ be scalar functions of time with bounded L_p and L_q norms respectively where $1 = 1/p + 1/q$, then*

$$\|f(t)g(t)\|_{L_1} \leq \|f(t)\|_{L_p}\|g(t)\|_{L_q} \tag{2.4}$$

Proof. Starting with the triangle inequality we have

$$\frac{\|f(t)g(t)\|}{\|f(t)\|_{L_p}\|g(t)\|_{L_q}} \leq \frac{\|f(t)\|}{\|f(t)\|_{L_p}}\frac{\|g(t)\|}{\|g(t)\|_{L_q}}.$$

Application of Theorem leads to

$$\frac{\|f(t)g(t)\|}{\|f(t)\|_{L_p}\|g(t)\|_{L_q}} \leq \left(\frac{\|f(t)\|}{\|f(t)\|_{L_p}}\right)^p + \left(\frac{\|g(t)\|}{\|g(t)\|_{L_q}}\right)^q.$$

Integrating both sides we have

$$\begin{aligned} \frac{1}{\|f(t)\|_{L_p}\|g(t)\|_{L_q}}\int\|f(t)g(t)\|dt &\leq \int\frac{1}{p}\left(\frac{\|f(t)\|}{\|f(t)\|_{L_p}}\right)^p dt + \int\frac{1}{q}\left(\frac{\|g(t)\|}{\|g(t)\|_{L_q}}\right)^q dt \\ &= \frac{1}{p} + \frac{1}{q} \\ &= 1. \end{aligned}$$

Multiplying both sides by $\|f(t)\|_{L_p}\|g(t)\|_{L_q}$ gives us the result. □

Proposition 2.1 (Cauchy-Schwarz Inequality)**.** *Holder's inequality with $p = 2$.*

2.2.4 Positive Matrices

Definition 2.4. A matrix $M \in \mathbb{R}^{n\times n}$ is positive definite if $z^T Mz > 0 \forall z \neq 0$ and is often denoted as $M > 0$.

Lemma 2.2. *Let M be a symmetric matrix with the following decomposition:*

$$M = \begin{bmatrix} A & B \\ B^T & C \end{bmatrix}$$

$A = A^T$ and $C = C^T$ is full rank. $M > 0$ if and only if

- $C > 0$

- $A - BC^{-1}B^T > 0$

Proof. Given that C is full rank, the inverse of C exists and therefore the following relation holds

$$M = \begin{bmatrix} A & B \\ B^T & C \end{bmatrix} = \begin{bmatrix} I & BC^{-1} \\ 0 & I \end{bmatrix} \begin{bmatrix} A - BC^{-1}B^T & 0 \\ 0 & C \end{bmatrix} \begin{bmatrix} I & BC^{-1} \\ 0 & I \end{bmatrix}^T .$$

A block diagonal matrix is positive definite iff all diagonal blocks are positive definite. This concludes the proof, thus $M > 0$ off $C > 0$ and $A - BC^{-1}B^T$. □

2.2.5 Continuity

We start with the definition of a metric space.

Definition 2.5 (Metric)**.** A set X whose elements are called points, is said to be a metric space, if with any two points p and q in X there is associated a real number $d(p, q)$, called the distance from p to q, such that

- $d(p, q) > 0$ if $p \neq q$; $d(p, p) = 0$
- $d(p, q) = d(q, p)$
- $d(p, q) \leq d(p, r) + d(r, q)$, for any $r \in X$

A function with these three properties is called a distance function or a metric.

Note that a norm on any subset of the real or complex numbers is a metric, but not all metrics are norms. Norms have two extra properties as compared to distance functions, and those are translation invariance and scaling.

Definition 2.6 (Limit Point)**.** Let X and Y be metric spaces; supposes $E \subset X$, f maps E into Y, and p is a limit point of E,

$$\lim_{x \to p} f(x) = q$$

if there is a point $q \in Y$ with the following property: For every $\epsilon > 0$, there exists a $\delta > 0$ s.t.

$$d_Y(f(x), q) < \epsilon$$

for all points $x \in E$ for which

$$0 < d_X(x, p) < \delta$$

where d_X and d_Y are distance functions in X and Y respectively.

Definition 2.7 (Continuity)**.** Let X and Y be metric spaces; supposes $E \subset X$, $p \in E$ and f maps E into Y. Then f is continuous at p, if for every $\epsilon > 0$ there exists a $\delta > 0$ such that

$$d_Y(f(x), f(p)) < \epsilon$$

for all point $x \in E$ for wich $d_x(x, p) < \delta$.

Definition 2.8 (Uniform Continuity)**.** Let f be a mapping of a metric space X into a metros space Y. If for every $\epsilon > 0$ there exists a $\delta > 0$ such that

$$d_Y(f(p), f(q)) < \epsilon$$

for all p and q in X for which $d_x(p, q) < \delta$.

2.2.6 Convergence

Theorem 2.3. *Let $\{p_n\}$ be a sequence in a metric space X. Then,*

1. *$\{p_n\}$ converges to $p \in X$ iff every neighborhood of p contains all but finitely many of the terms of $\{p_n\}$.*
2. *If $p \in X$ and $p' \in X$ and if $\{p_n\} \to p$ and $\{p_n\} \to p'$, then $p = p'$.*
3. *If $\{p_n\}$ converges, then $\{p_n\}$ is bounded.*
4. *If $E \subset X$ and if p is a limit point of E, then there is a sequence $\{p_n\} \in E$ such that $p = \lim_{n\to\infty} p_n$*

Theorem 2.4. *Suppose $\{s_n\}$ is monotonic. Then $\{s_n\}$ converges iff it is bounded.*

Proof. Suppose $s_n \leq s_{n+1}$. Let E be the range of $\{s_n\}$ If $\{s_n\}$ is bounded, let s be the least upper bound of E. Then $s_n < s$ and for every $\epsilon > 0$, there exists and integer N such that $s - \epsilon < s_N \leq s$ for otherwise $s - \epsilon$ would be the least upper bound of E. Since $\{s_n\}$ increases, $s - \epsilon < s_n \leq s, \quad \forall n \geq N$, which shows that $\{s_n\}$ converges to s. The converse follows from Theorem 2.3. □

Definition 2.9. A sequence of functions $\{f_n(x)\}, n = 1, 2, 3, \ldots$ converges point wise on set E to f, if for each $x \in E$ there exists an $\epsilon(x)$ such that $n \geq N$ implies

$$\|f(x) - f_n(x)\| \leq \epsilon.$$

The convergence is uniform if ϵ is independent of x.

Theorem 2.5. *Suppose $f_n \to f$ uniformly on a set E in a metric space. Let x be a limit point of E, then*

$$\lim_{t\to x} \lim_{n\to\infty} f_n(t) = \lim_{n\to\infty} \lim_{t\to x} f_n(t)$$

Proof. See [69, Theorem 7.11]. □

2.3 Definitions of Stability

Consider a dynamical system of time, $t \in \mathbb{R}$, varying state $x \in \mathbb{R}^n$ satisfying

$$\begin{aligned} x(t_0) &= x_0 \\ \dot{x}(t) &= f(x(t), t). \end{aligned} \tag{2.5}$$

We are only interested in systems with equilibrium at $x = 0$, so that $f(0,t) = 0\ \forall t$. The solution to the differential equation in (2.5) is a transition function $\phi(t; x_0, t_0)$ such that

$$\phi(t_0; x_0, t_0) = x_0. \tag{2.6}$$

Below we give the various definitions of stability as defined in [27, 35, 52, 61]

Definition 2.10 (Stability)**.** Let $t_0 \geq 0$, the equilibrium is

(i) *Stable*, if for all $\epsilon > 0$ there exists a $\delta(\epsilon, t_0) > 0$ s.t. $\|x_0\| \leq \delta$ implies $\|\phi(t_0; t_0, x_0)\| \leq \epsilon\ \forall\ t \geq t_0$.

(ii) *Attracting*, if there exists a $\rho(t_0) > 0$ such that for all $\eta > 0$ there exists a $T(\eta, x_0, t_0)$ such that $\|x_0\| \leq \rho$ implies $\|\phi(t; x_0, t_0)\| \leq \eta$ for all $t \geq t_0 + T$.

(iii) *Asymptotically Stable*, if it is stable and attracting, see Figure 2-2.

(iv) *Equiasymptotically Attracting*, if the T in (ii) is uniform in x_0 and takes the form $T(\eta, \rho(t_0), t_0)$.

(v) *Equiasymptotically Stable*, if it is stable and equiasymptotically attracting.

(vi) *Uniformly Stable*, if the δ in (i) is uniform in t_0, thus taking the form $\delta(\epsilon)$.

(vii) *Uniformly Attracting*, is equiasymptotic attracting where the ρ, T do not depend on t_0.

(viii) *Uniformly Asymptotically Stable*, (UAS) if it is uniformly stable and uniformly attracting.

(ix) *Exponentially Asymptotically Stable* (EAS) If the there exists a $\nu > 0$, and for all $\zeta > 0$ there exists a $\delta(\zeta)$ such that $\|x_0\| \leq \delta$ implies that $\|\phi(t; x_0, t_0)\| \leq \zeta \mathbf{e}^{-\nu(t-t_0)}$ [52].

(x) *Exponentially Stable* If the there exists a $\nu > 0$ and $\mu > 0$ such that $\|\phi(t; x_0, t_0)\| \leq \mu\|x_0\|\mathbf{e}^{-\nu(t-t_0)}$

Definition 2.11 (Topology of Stability)**.** The following define the neighborhoods around the equilibrium for which the stability results hold.

(i) *Global*, if the results hold for all x_0.

(ii) *Local*, if the results only hold for x_0 in a neighborhood around the equilibrium.

(iii) *Semi–global*, if the results hold globally for only a subset of the state space and locally for the other subset of the state space.

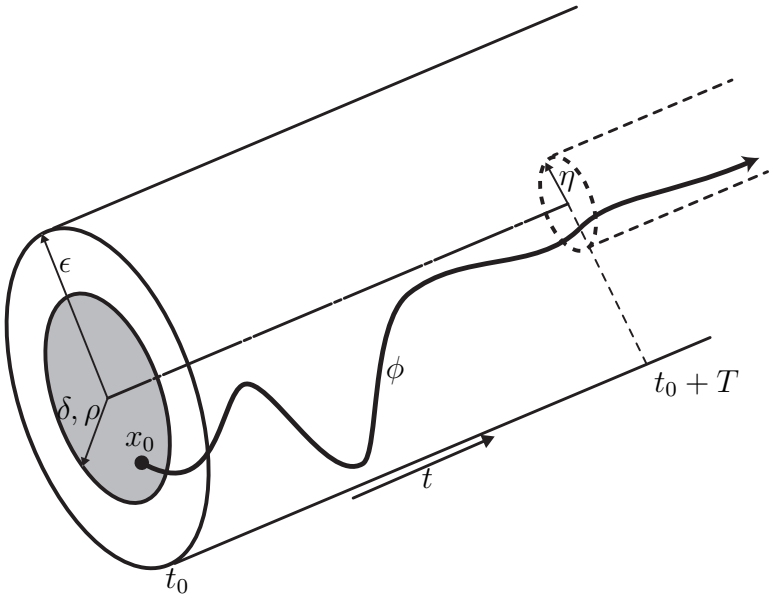

Figure 2-2: Asymptotic stability, adapted from [35].

2.4 Conditions for Stability

Consider dynamics of the form

$$\dot{x} = f(t, x), \qquad x(t_0) = x_0. \tag{2.7}$$

where $f(0, t) = 0 \ \forall t > 0$.

Theorem 2.6 (Lyapunov's Direct (The Second) Method)**.** *The equilibrium state of* (2.7) *is uniformly asymptotically stable in the large if a scalar function* $V(x, t)$ *with continuous first partial derivatives with respect to* x *and* t *exists such that* $V(0, t) = 0$ *and if the following conditions are satisfied*

1. $V(x, t)$ *is positive definite, i.e. there exists a non–decreasing scalar function* α *such that* $\alpha(0) = 0$ *and, for all* t *and all* $x \neq 0$

$$0 < \alpha\left(\|x\|\right) \leq V(x, t)$$

2. *There exist a continuous scalar function* γ *s.t.* $\gamma(0) = 0$ *and the derivative* $\dot{V}$ *of* V *along all system directions, satisfies for all* t

$$\dot{V} = \frac{\partial V}{\partial t} + (\nabla V)^T f(x, t) \leq -\gamma\left(\|x\|\right) < 0, \qquad \forall x \neq 0.$$

3. *There exist as a continuous non–decreasing scalar function such that* $\beta(0) = 0$ *and for all* t

$$V(x, t) \leq \beta\left(\|x\|\right).$$

This is commonly referred to as "V is decrescent" (western literature) or "V has an infinitely small upper bound" (Russian literature).

4. $\lim_{\|x\|\to\infty} \beta(\|x\|) = \infty$

Proof. The proof follows from [35], and is only here for completeness. From Theorem 2.6.2 it follows

$$V(\phi(t; x_0, t_0), t) - V(x_0, t_0) = \int_{t_0}^{t} \dot{V}(\phi(\tau; x_0, t_0), \tau) d\tau < 0, \tag{2.8}$$

and thus V is strictly decreasing along any trajectory.

Proof of uniform stability: For any $\epsilon > 0$ there exists a $\delta(\epsilon)$ such that $\beta(\delta) < \alpha(\epsilon)$, see Figure 2-3. Therefore, if $\|x_0\| \leq \delta$ where t_0 is arbitrary, from 2.6.2 and (2.8) it follows that

$$\alpha(\epsilon) > \beta(\delta) \geq V(x_0, t_0) \geq V(\phi(t; x_0, t_0), t) \geq \alpha(\|\phi(t; x_0, t_0)\|).$$

Given that α is positive and nondecreasing, we have the following,

$$\|\phi(t; x_0, t_0)\| < \epsilon \quad \forall\ t \geq t_0,\ \|x_0\| \leq \delta,$$

for arbitrary t_0. Thus we have proved uniform stability.

Proof of uniform asymptotic stability: From Theorem 2.6.2, for any constant $c_1 > 0$ there exists an $r > 0$ such that $\beta(r) \leq \alpha_(c_1)$. For any x_0 such that $\|x_0\| \leq r$, by uniform stability, $\|\phi(t; x_0, t_0)\| < c_1$ for all $t \geq t_0$, where t_0 is arbitrary. For any $0 < \mu \leq \|x_0\|$, there exists a $\nu(\mu) > 0$ such that $\beta(\nu) < \alpha(\mu)$, see Figure 2-3. Set $c_2(\mu, r)$ as the minimum of the continuous function $\gamma(\|x\|)$ on the compact set $\nu(\mu) \leq \|x\| \leq c_1(r)$, and define $T(\mu, r) \triangleq \beta(r)/c_2(\mu, r) > 0$. Now assume for proof by contraction that $\|\phi(t; x_0, t_0)\| > \nu$ over the interval $t_0 \leq t \leq t_1 = t_0 + T$. From 2.6.2 and (2.8) it follows that

$$\begin{aligned} 0 < \alpha(\nu) \leq & V(\phi(t_1; x_0, t_0), t_1) \\ \leq & V(x_0, t_0) - (t_1 - 1_0)c_2 \\ \leq & \beta(r) - Tc_2 = 0. \qquad \Rightarrow\Leftarrow \end{aligned}$$

Therefore, for some $t = t_2$ in the interval $[t_0, t_1]$, it follows that $\|x_2\| = \|\phi(t; x_0, t_0)\| = \nu$. Therefore

$$\begin{aligned} \alpha(\|\phi(t; x_2, t_2)\|) \leq & V(\phi(t; x_2, t_2), t) \\ \leq & V(x_2, t_2) \\ \leq & \beta(\nu) < \alpha(\mu) \end{aligned}$$

for all $t \geq t_2$. Therefore,

$$\|\phi(t; x_0, t_0)\| < \mu \quad \forall\ t \geq t_0 + T(\mu, r) \geq t_2,\ \|x_0\| \leq r$$

which is the definition of uniform asymptotic stability.

Proof of uniform asymptotic stability in the large: From Condition 4 in Theorem 2.6, the r in the proof of uniform asymptotic stability can be arbitrary large. Uniform boundedness also holds. □

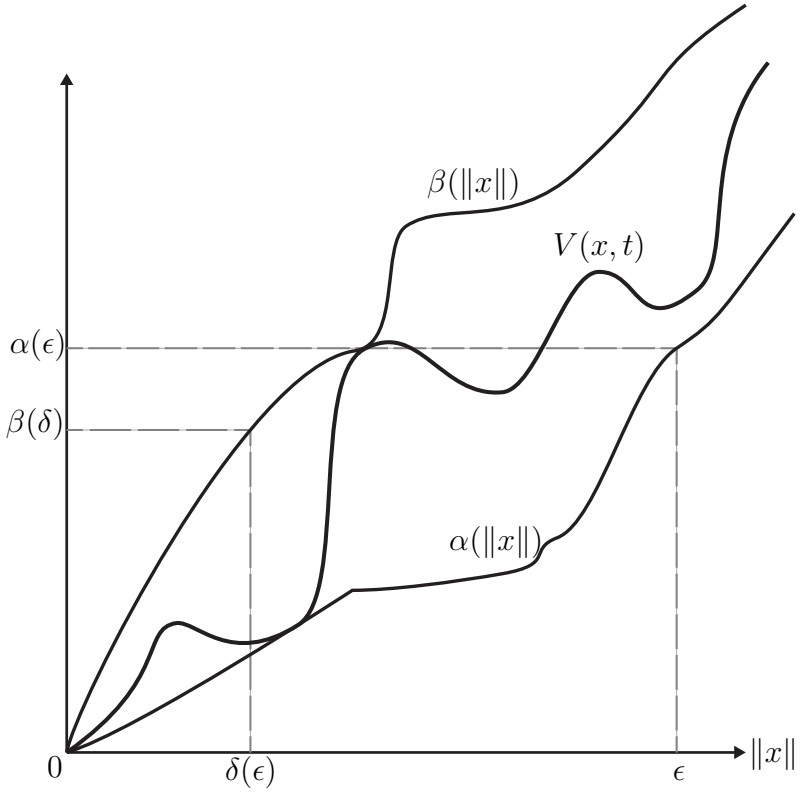

Figure 2-3: Lyapunov stability, adapted from [35].

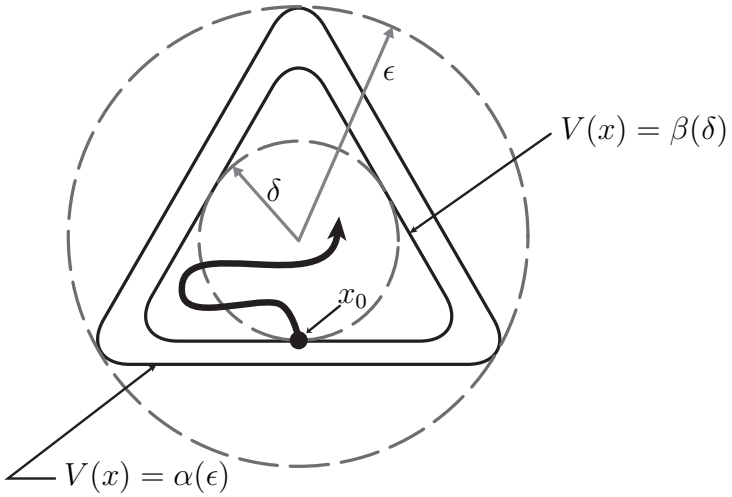

Figure 2-4: Asymptotic stability, adapted from [35].

Proposition 2.2. *If $V(x,t)$ in Theorem 2.6 is positive definite and $\dot{V}(x,t) \leq 0$, then $x(t)$ is bounded for all time.*

Proof. Given that $\dot{V}$ is negative semidefinite, $V(x,t) \leq V(x_0,t_0) < \infty$. From the fact that $V(x,t)$ is positive definite it follows that $\|x(t)\| < \infty$. □

Lemma 2.3. *If $f : \mathbb{R}^+ \to \mathbb{R}$ is uniformly continuous for $t \geq 0$ and if*

$$\lim_{t\to\infty} \int_0^t |f(\tau)|\, d\tau < \infty$$

thus $f(t) \in \mathcal{L}_1$, then

$$\lim_{t\to\infty} f(t) = 0.$$

Proof. See [61, Lemma 2.12] □

Corollary 2.1. *If $g \in \mathcal{L}_2 \cap \mathcal{L}_\infty$ and $\dot{g}$ is bounded, then $\lim_{t\to\infty} g(t) = 0$.*

Proof. Choose $f(t) = g^2(t)$ and the conditions of Lemma 2.3 are satisfied. □

Lemma 2.4. *If $g \in \mathcal{L}_2$ and $\dot{g}$ is bounded, then $\lim_{t\to\infty} g(t) = 0$.*

Proof. This follows by contradiction. Assume $\lim_{t\to\infty} e(t) \neq 0$. Then there exists an infinite unbounded sequence $\{t_n\}_{n\in\mathbb{N}}$ and $\varepsilon > 0$ such that $|e(t_i)| > \varepsilon$. And because $\dot{e}$ is bounded, e is uniformly continuous, and so $|e(t) - e(t_i)| \leq k|t - t_i| \;\forall\; t, t_i \in \mathbb{R}^+$ for some $k > 0$, and we have $|e(t)| \geq \varepsilon - |e(t) - e(t_i)|$. From the reverse triangle inequality

$$|e(t_i)|^2 - 2|e(t) - e(t_i)|^2 \leq 2|e(t)|^2$$

and integrate both sides from t_i to $t_i + \delta$

$$\int_{t_i}^{t_i+\delta} (e(t_i))^2 d\tau - 2\int_{t_i}^{t_i+\delta} (e(\tau) - e(t_i))^2 d\tau \leq 2\int_{t_i}^{t_i+\delta} |e(\tau)|^2 d\tau.$$

Substituting in $\varepsilon < |e(t_i)|$ and the definition from uniform continuity

$$\int_{t_i}^{t_i+\delta} \varepsilon^2 d\tau - 2\int_{t_i}^{t_i+\delta} k^2(\tau - t_i)^2 d\tau \leq \int_{t_i}^{t_i+\delta} (e(t_i))^2 d\tau - 2\int_{t_i}^{t_i+\delta} (e(\tau) - e(t_i))^2 d\tau$$

and thus

$$\int_{t_i}^{t_i+\delta} \varepsilon^2 d\tau - 2k^2 \int_{t_i}^{t_i+\delta} \left(\tau^2 - 2\tau t_i + t_i^2\right) d\tau \leq 2\int_{t_i}^{t_i+\delta} |e(\tau)|^2 d\tau.$$

Integrating the left hand side

$$\frac{\varepsilon^2\delta}{2} - k^2\left(\frac{\delta^3}{3}\right) \leq \int_{t_i}^{t_i+\delta} |e(\tau)|^2 d\tau.$$

Choosing $\delta = \frac{\varepsilon}{k}$,

$$\int_{t_i}^{t_i+\delta} |e(\tau)|^2 d\tau \geq \frac{\varepsilon^2 \delta}{6}$$

Taking the limit as $\delta \to \infty$ implies that $\lim_{t\to\infty} \int_0^t |e(\tau)|^2 d\tau$ is not finite. This contradicts the assumption that $e \in \mathcal{L}^2$ and so we have $\lim_{t\to\infty} e(t) = 0$. □

2.5 Linear Systems

Definition 2.12. A matrix $A \in \mathbb{R}^{n\times n}$ is Hurwitz if all the eigenvalues of A are in the open left half plane of $\mathbb{C}$.

Theorem 2.7 (Lyapunov Equation)**.** *$A \in \mathbb{R}^{n\times n}$ is Hurwitz if and only if, for any $Q = Q^T > 0$ there exists a unique $P = P^T > 0$ satisfying*

$$A^T P + PA = -Q. \tag{2.9}$$

Proof. See [61, Theorem 2.10] □

Example 2.1. The linear system

$$\dot{x}(t) = Ax(t) \tag{2.10}$$

where $x \in \mathbb{R}^n$ and $A \in \mathbb{R}^{n\times n}$ is Hurwizt, is uniformly asymptotically stable in the large. This can be proved as follows: Consider the Lyapunov candidate

$$V(x,t) = x(t)^T P x(t).$$

Taking the time derivative along the system trajectories in (2.10) results in $\dot{V}(x,t) = -x(t)^T(A^T P + PA)x(T)$. Using Theorem 2.7 we have

$$\dot{V}(x,t) = -x(t)^T Q x(t).$$

From Theorem 2.6, $x = 0$ is uniformly asymptotically stable in the large.

Consider the linear time–varying system

$$\dot{x}(t) = F(t)x(t), \tag{2.11}$$

which has solutions

$$\phi(t; x_0, t_0) = \Phi(t, t_0)x_0, \tag{2.12}$$

where Φ is the state transition matrix.

Theorem 2.8. *Given the system dynamics in* (2.11)*, the following three statements are equivalent*

(a) The equilibrium is uniformly asymptotically stable.

(b) The system is exponentially asymptotically stable.

(c) The system is exponentially stable.

Proof. This proof follows from [35, Theorem 3]. For any system, $(c) \to (b) \to (a)$ trivially. We now prove that (a) implies (b). Given that uniform asymptotic stability implies uniform stability we note that for all $\epsilon > 0$, $0 \leq \|x_0\| \leq \delta(\epsilon)$ which by linearity in (2.12), implies that

$$\delta^{-1}\|\phi(t; x_0, t_0)\| \leq \|\Phi(t, t_0)\|\delta^{-1}\|x_0\| \leq \|\phi(t, t_0)\| \leq \delta^{-1}\epsilon \tag{2.13}$$

By uniform asymptotic stability choose $T(2^{-1}, 1)$ so that $\|\Phi(t_0 + T, t_0)\| \leq 1/2$ independent of t_0. It can be shown by induction that

$$\begin{aligned} \|\Phi(t_0 + kT, t_0)\| \leq & \|\Phi(t_0 + kT, t_0 + (k-1)T)\| \dots \\ & \|\Phi(t_0 + T, t_0\| \\ \leq & 2^{-k}. \end{aligned} \tag{2.14}$$

Therefore we have that

$$\|\Phi(t, t_0)\| \leq 2\delta^{-1}\epsilon \mathbf{e}^{-\frac{\log(2)}{T}(t-t_0)}.$$

In order to prove that this is the same as Exponential Asymptotic Stability, $\zeta = 2\epsilon\delta^{-1}$ and $\nu = \log(2)T^{-1}$. Note that T is a fixed constant and therefore ν is a constant for all initial conditions. Given that the dynamics in (2.11) are linear, in order for stability to hold, there must exist a finite upper bound on Φ independent of t. Therefore, for all $\epsilon > 0$, there exists a μ such that $2\delta^{-1}\epsilon \leq \mu < \infty$. This completes the proof. □

Example 2.2. Consider the scaler dynamical system

$$\dot{x}(t) = -c(x)x(t).$$

where

$$c(x) = \begin{cases} 1 & \text{if } x \leq d_0 \\ 0 & \text{else} \end{cases}$$

The system is globally uniformly stable, but only locally uniformly attracting. Therefore, the system is not Exponentially Stable. For all $\zeta > 0$, define

$$\delta \triangleq \begin{cases} \zeta & \text{if } \zeta \leq d_0 \\ d_0 & \text{else} \end{cases}$$

Thus, for all $\|x_0\| \leq \delta$,

$$\|\phi(t; x_0, t_0)\| \leq \zeta \mathbf{e}^{-(t-t_0)}.$$

Therefore, the system is Exponentially Asymptoticaly Stable.

Example 2.3. Consider the time response of the dynamical system $x(t) \in \mathbb{R}^n$ and

$u(t) \in \mathbb{R}$,

$$\dot{x}(t) = Ax(t) + bu(t) \tag{2.15}$$

where A is Hurwitz and further more we are told that $u(t) \in L_2$, i.e. there exists a $c_1 \geq 0$ such that$\|u(t)\|_{L_2} \leq c_1 < \infty$. Given that A is hurwitz, there exists $c_2, c_3 > 0$ such that

$$\|\mathbf{e}^{At}\| \leq c_2 \mathbf{e}^{-c_3 t}. \tag{2.16}$$

Details on bounding the matrix exponential can be found in [57]. The time series response of $x(t)$ is

$$x(t) = \mathbf{e}^{At}x(0) + \int_0^t \mathbf{e}^{A(t-\tau)}u(\tau)d\tau \tag{2.17}$$

Using the bound in (2.16) and taking the 2-norm for fixed t we have

$$\|x(t)\| \leq c_2 \mathbf{e}^{-c_3 t}x(0) + \int_0^t c_2 \mathbf{e}^{-c_3(t-\tau)}\|u(\tau)\|d\tau. \tag{2.18}$$

Using Holder's inequality on the last term we have that

$$\|x(t)\| \leq c_2 \mathbf{e}^{-c_3 t}x(0) + \sqrt{\int_0^t c_2^2 \mathbf{e}^{-2c_3(t-\tau)}d\tau}\sqrt{\int_0^t \|u(\tau)\|^2 d\tau}. \tag{2.19}$$

Using the bound given to us for $u(t)$ we can say

$$\|x(t)\| \leq c_2 \mathbf{e}^{-c_3 t}x(0) + c_1 c_2\sqrt{\int_0^t \mathbf{e}^{-2c_3(t-\tau)}d\tau}. \tag{2.20}$$

Lemma 2.5 (Gronwall-Bellman)**.** *For $u, v \geq 0$ and c_1 a positive constant, and if*

$$u(t) \leq c_1 + \int_0^t u(\tau)v(\tau)d\tau \tag{2.21}$$

then

$$u(t) \leq c_1 \mathbf{e}^{\int_0^t v(\tau)d\tau}.$$

Proof. From (2.21) we have

$$\frac{u(t)v(t)}{c_1 + \int_0^t u(\tau)v(\tau)d\tau} \leq v(t).$$

Integrating both sides between 0 and t we have

$$\log\left(c_1 + \int_0^t u(\tau)v(\tau)d\tau\right) - \log c_1 \leq \int_0^t v(\tau)d\tau.$$

Adding $\log c_1$ to both sides and taking the exponent we have

$$u(\tau) \leq c_1 + \int_0^t u(\tau)v(\tau)d\tau \leq c_1 \mathbf{e}^{\int_0^t v(\tau)d\tau}. \qquad \square$$

Theorem 2.9. *The scalar dynamical system described by*

$$\dot{x} = (a + b(t))x \tag{2.22}$$

with $a < 0$, $b \in \mathcal{L}_2$ results in bounded trajectories for x.

Proof. The solutions to (2.22) is

$$x(t) = \mathbf{e}^{at}x(0) + \int_0^t \mathbf{e}^{a(t-\tau)}b(\tau)x(\tau)d\tau.$$

First note that $\mathbf{e}^{at}x(0) \leq x(0)$, then we can conclude that

$$x(t) \leq x(0) + \int_0^t \mathbf{e}^{a(t-\tau)}b(\tau)x(\tau)d\tau,$$

and taking 2-norms

$$\|x(t)\| \leq \|x(0)\| + \int_0^t \|\mathbf{e}^{a(t-\tau)}b(\tau)\|\|x(\tau)\|d\tau,$$

Applying Lemma 2.5 where

$$\begin{aligned} c_1 =& \|x(0)\| \\ u =& \|x(\tau)\| \\ v =& \|\mathbf{e}^{a(t-\tau)}b(\tau)\| \end{aligned}$$

results in

$$\begin{aligned} \|x(t)\| \leq& \|x(0)\|\mathbf{e}^{\int_0^t \|\mathbf{e}^{a(t-\tau)}b(\tau)\|d\tau} \\ \leq& \|x(0)\|\mathbf{e}^{\int_0^t \|\mathbf{e}^{a(t-\tau)}\|\|b(\tau)\|d\tau} \end{aligned}$$

Application of Cauchy Schwarz inequality results in

$$\|x(t)\| \leq \|x(0)\|\mathbf{e}^{\sqrt{\int_0^t \|\mathbf{e}^{(a(t-\tau))}\|^2 d\tau}\sqrt{\int_0^t \|b(\tau)\|^2 d\tau}}.$$

The quantity $\int_0^t \|\mathbf{e}^{a(t-\tau)}\|^2 d\tau \leq \frac{1}{2|a|}$ and we are told that $b \in \mathcal{L}_2$. Thus

$$\|x(t)\| \leq \|x(0)\|\mathbf{e}^{\sqrt{\frac{1}{2|a|}}\|b(t)\|_{L_2}}. \qquad \square$$

Through out the following subsections we will make use the following system as a

baseline example:

$$\dot{x}(t) = Ax + Bu \qquad y = C^T x \tag{2.23}$$

where $x \in \mathbb{R}^n$, $y \in \mathbb{R}^m$ and $u \in \mathbb{R}^p$ with A, B, C of appropriate dimension in the reals. The transfer function is then defined as

$$Z(s) = C^T(sI - A)^{-1}B. \tag{2.24}$$

2.5.1 Transfer Functions

Definition 2.13. A rational transfer function $H(s)$ is a transfer function defined as $H(s) = p(s)/q(s)$ where p and q are polynomials.

Definition 2.14. A rational transfer function $H(s)$ is analytic in Ω if $H(s)$ is bounded for all $s \in \Omega$.

Definition 2.15. Given a transfer function $H(s) = (a_m s^m + \cdots + a_1 s + a_0)/(b_n s^n + \cdots + b_1 s + b_0)$ the relative degree is defined as

$$n^* \triangleq n - m.$$

Definition 2.16 ([33])**.** A rational function $H(s)$ is Strictly Positive Real (SPR) iff

- $H(s)$ is analytic in $\mathrm{Re}[s] \geq 0$,
- $\mathrm{Re}[H(j\omega)] > 0 \; \forall \; \omega \in (-\infty, \infty)$ and,
- $\lim_{\omega^2 \to \infty} \omega^2 \mathrm{Re}[H(j\omega)] > 0$ when the relative degree is 1.

When $n^* = 0$ the third condition is not needed.

Lemma 2.6 (Meyers Kalman Yakubovich (MKY))**.** *Given a scalar $\gamma \geq 0$, vectors b and h, and asymptotically stable matrix A, and symmetric positive-definite matrix L, if*

$$Re[H(i\omega)] = Re\left[\frac{\gamma}{2} + h^T(i\omega I - A)^{-1}b\right] > 0 \quad \forall \; \omega \in (-\infty, \infty),$$

then there exists a scalar $\epsilon > 0$, a vector q and $P = P^T > 0$ such that

$$A^T P + PA = -qq^T - \epsilon L$$
$$Pb - h = \sqrt{\gamma} q.$$

Proof. See [61, Lemma 2.4] □

Lemma 2.7 (Anderson Kalman Yakubovich (AKY))**.** *Define $Z(s) = c^T(sI - A)^{-1}b$. The poles of $Z(s)$ satisfy $Re[s] < -\mu$. $Z(s)$ is SPR iff there exists $P = P^T > 0$ and L s.t.*

$$A^T P + PA = -LL^T - \mu P = -Q$$
$$Pb = c.$$

Proof. This follows from Lemma 2.6 □

Definition 2.17. The matrix pencil of the triple $\{A, B, C\}$ for the system in (2.23) is defined as

$$P(s) = \begin{bmatrix} sI - A & -B \\ C^T & 0 \end{bmatrix} \tag{2.25}$$

Definition 2.18. The transmission zeros of $Z(s)$ in (2.24) are defined as the set

$$\mathcal{Z}_t = \{s | \text{rank } P(s) < n + \min(m, p)\}$$

where $P(s)$ is the matrix pencil of (2.23) defined in (2.25)

Lemma 2.8. *If the system in* (2.23) *is square (p=m), and $C^T B$ is full rank, then there are exactly $n - m$ transmission zeros.*

Proof. See [11]. □

2.5.2 Cheap Observer Riccati Equations

Consider $A \in \mathbb{R}^{n\times n}$ and $B, C \in \mathbb{R}^{n\times m}$ where (A, C^T) is observable. For any $Q_0 = Q_0^T > 0$ in $\mathbb{R}^n$ and $R_0 = R_0^T > 0$ in $\mathbb{R}^m$ and for all $\nu > 0$, with

$$Q_\nu = Q_0 + \left(1 + \frac{1}{\nu}\right) BB^T, \quad R_\nu = \frac{\nu}{\nu + 1} R_0$$

the solution $P_\nu = P_\nu^T > 0$ to the well known observer Riccati Equation:

$$P_\nu A^T + A P_\nu - \left(1 + \frac{1}{\nu}\right) P_\nu C R_0^{-1} C^T P_\nu + Q_0 + \left(1 + \frac{1}{\nu}\right) BB^T = 0 \tag{2.26}$$

always exists. Another way of representing the Riccati Equation when the $1/\nu$ terms are collected is given below

$$P_\nu A^T + A P_\nu - P_\nu C R_0^{-1} C^T P_\nu + Q_0 + BB^T + \frac{1}{\nu}\left(BB^T - P_\nu C R_0^{-1} C^T P_\nu\right) = 0 \tag{2.27}$$

If in addition we assume that the transfer function $Z(s)$ is minimum phase and $C^T B$ is full rank. Then it is well known that the asymptotic expansion

$$P_\nu = P_0 + P_1 \nu + O(\nu^2) \tag{2.28}$$

approximates P_ν with $P_0 = P_0^T > 0$. That is $\lim_{\nu\to 0} P_\nu = P_0$ and is positive definite, even in the limit of a cheap observer, i.e. ν goes to 0. [40]

Theorem 2.10 (Corollary 13.1 to Theorem 13.2 in [47])**.** *For the triple $\{A, B, C^T\}$, minimum phase, fully observable, square and $C^T B$ full rank*

1. *P_0 and P_1 are symmetric positive definite.*

2. *There exists a unitary matrix* $W \in \mathbb{R}^{m\times m}$ *such that*

$$\begin{aligned} P_0 C &= B W^T \sqrt{R_0} \\ C &= \tilde{P}_0 B W^T \sqrt{R_0} \\ \tilde{P}_0 B &= C R_0^{-1/2} W \end{aligned} \tag{2.29}$$

where $\tilde{P}_0 = P_0^{-1}$ *and* $W = (UV)^T$ *with*

$$B^T C R_0^{-1/2} = U \Sigma V.$$

3. *The following two asymptotic relations hold:*

$$\begin{aligned} P_\nu C &= B W^T \sqrt{R_0} + O(\nu) \\ C &= \tilde{P}_\nu B W^T \sqrt{R_0} + O(\nu) \\ \tilde{P}_\nu B &= C R_0^{-1/2} W + O(\nu) \end{aligned} \tag{2.30}$$

where $\tilde{P}_\nu = P_\nu^{-1}$

Proof. See §13.3 in [47]. □

Chapter 3

Closed-loop Reference Model Adaptive Control

3.1 Introduction

A universal observation in all adaptive control systems is a convergent, yet oscillatory behavior in the underlying errors. These oscillations increase with adaptation gain, and as such, lead to constraints on the speed of adaptation. The main obvious challenge in quantification of transients in adaptive systems stems from their nonlinear nature. A second obstacle is the fact that most adaptive systems possess an inherent trade-off between the speed of convergence of the tracking error and the size of parametric uncertainty. In this chapter, we provide a solution to this long standing problem, and overcome these challenges by proposing an adaptive control design that judiciously makes use of an underlying linear time-varying system, and introduces design changes that decouple speed of adaptation from parametric uncertainty.

The basic premise of any adaptive control system is to have the output of a plant follow a prescribed reference model through the online adjustment of control parameters. Historically, the reference models in Model Reference Adaptive Control (MRAC) have been open-loop in nature (see for example, [32,61]), with the reference trajectory generated by a linear dynamic model, and unaffected by the plant output. The notion of feeding back the model following error into the reference model was first reported in [49] and more recently in [20–23,44,45,74,75]. Denoting the adaptive systems with an Open-loop Reference Model as ORM-adaptive systems and those with closed-loop reference models as CRM-adaptive systems, our goal in this paper is to show how CRM-adaptive systems can be designed to alleviate the oscillatory property observed in ORM-adaptive systems, and obtain a satisfactory transient response.

Following stability analysis of adaptive control systems in the 80s and their robustness in the 90s, several attempts have been made to quantify transient performance (see for example, [10, 38, 81]). The performance metric of interest in these papers stems from either supremum or L-2 norms of key errors within the adaptive system. In [38] supremum and L-2 norms are derived for the model following error, the filtered model following error and the zero dynamics. In [10] L-2 norms are derived for the

the model following error in the context of output feedback adaptive systems in the presence of disturbances and un-modeled dynamics. The authors of [81] analyze the interconnection structure of adaptive systems and discuss scenarios under which key signals can behave poorly.

In addition to references [10,38,81], transient performance in adaptive systems has been addressed in the context of CRM adaptive systems in [20–23, 44, 45, 74, 75]. The results in [44, 45] focused on the tracking error, with emphasis mainly on the initial interval where the CRM-adaptive system exhibits fast time-scales. In [74] and [75], transient performance is quantified using a damping ratio and natural frequency type of analysis. However, assumptions are made that the initial state error is zero and that the closed-loop system state is independent of the feedback gain in the reference model, both of which may not hold in general.

The central contribution of the chapter is the quantification of transient performance in CRM adaptive systems. This is accomplished by deriving L-2 bounds on key signals and their derivatives in the adaptive system. These bounds are then related to the corresponding frequency content using a Fourier analysis, thereby leading to an analytical basis for the observed reduction in oscillations with the use of CRM. The underlying tools used to achieve these results are CRM, projection algorithm, L-2 bounds, and fundamental principles of real and functional analysis. It is also shown that in general, a peaking phenomenon can occur with CRM-adaptive systems, which then is shown to be minimized through an appropriate design of the CRM-parameters. Extensive simulation results are provided, illustrating the conspicuous absence of these oscillations in CRM-adaptive systems in contrast to their dominant presence in ORM-adaptive systems. The results of this paper build on preliminary versions in [20–22] where the bounds obtained were conservative. While all results derived in this paper are applicable to plants whose states are accessible for measurement, we refer the reader to [23] for extensions to output feedback.

This chapter also addresses Combined/composite direct and indirect Model Reference Adaptive Control (CMRAC) [16, 72], which is another class of adaptive systems in which a noticeable improvement in transient performance was demonstrated. While the results of these papers established stability of combined schemes, no rigorous guarantees of improved transient performance were provided, and have remained a conjecture [43]. We introduce CRMs into the CMRAC and show how improved transients can be guaranteed. We close this paper with a discussion of CRM and related concepts that appear in other adaptive systems as well, including nonlinear adaptive control [37] and adaptive control in robotics [73].

This chapter is organized as follows. Section 3.2 contains the basic CRM structure with L-2 norms of the key signals in the system. Section 3.3 investigates the peaking in the reference model. Section 3.4 contains the multidimensional states accessible extension. Section 3.5 investigates composite control structures with CRM. Section 3.6 explores other forms of adaptive control where closed loop structures appear.

3.2 CRM-Based Adaptive Control of Scalar Plants

Let us begin with a scalar system,

$$\dot{x}_p(t) = a_p x_p(t) + k_p u(t) \tag{3.1}$$

where $x_p(t) \in \mathbb{R}$ is the plant state, $u(t) \in \mathbb{R}$ is the control input, $a_p \in \mathbb{R}$ is an unknown scalar and only the sign of $k_p \in \mathbb{R}$ is known. We choose a closed-loop reference model as

$$\dot{x}_m(t) = a_m x_m(t) + k_m r(t) - \ell(x(t) - x_m(t)). \tag{3.2}$$

All of the parameters above are known and scalar, $x_m(t)$ is the reference model state, $r(t)$ is a bounded reference input and $a_m, \ell < 0$ so that the reference model and the subsequent error dynamics are stable. The open-loop reference model dynamics

$$\dot{x}_m^o(t) = a_m x_m^o(t) + k_m r(t) \tag{3.3}$$

is the corresponding true reference model that we actually want x_p to converge to.

The control law is chosen as

$$u(t) = \bar{\theta}^T(t)\phi(t) \tag{3.4}$$

where we have defined $\bar{\theta}^T(t) = \begin{bmatrix}\theta(t) & k(t)\end{bmatrix}^T$ and $\phi^T(t) = \begin{bmatrix}x_p(t) & r(t)\end{bmatrix}^T$ with an update law

$$\dot{\bar{\theta}} = -\gamma \text{sgn}(k_p) e \phi \tag{3.5}$$

where $\gamma > 0$ is a free design parameter commonly referred to as the adaptive tuning gain and $e(t) = x_p(t) - x_m(t)$ is the state tracking error. From this point forward we will suppress the explicit time dependance of parameters accept for emphasis.

We define the parameter error $\tilde{\bar{\theta}}(t) = \bar{\theta}(t) - \bar{\theta}^*$, where $\bar{\theta}^* \in \mathbb{R}^2$ satisfies $\bar{\theta}^{*T} = \begin{bmatrix}\frac{a_m - a_p}{k_p} & \frac{k_m}{k_p}\end{bmatrix}^T$. The corresponding closed loop error dynamics are:

$$\dot{e}(t) = (a_m + \ell)e + k_p \tilde{\bar{\theta}}^T \phi. \tag{3.6}$$

3.2.1 Stability Properties of CRM-adaptive systems

Theorem 3.1 establishes the stability of the above adaptive system with the CRM:

Theorem 3.1. *The adaptive system with the plant in* (3.1)*, with the controller defined by* (3.4)*, the update law in* (3.5) *with the reference model as in* (3.2) *is globally stable,* $\lim_{t\to\infty} e(t) = 0$*, and*

$$\|e\|_{L_2}^2 \leq \frac{1}{|a_m + \ell|}\left(\frac{1}{2}e(0)^2 + \frac{|k_p|}{2\gamma}\tilde{\bar{\theta}}^T(0)\tilde{\bar{\theta}}(0)\right). \tag{3.7}$$

Proof. Consider the lyapunov candidate function

$$V(e(t), \tilde{\theta}(t)) = \frac{1}{2}e^2 + \frac{|k_p|}{2\gamma}\tilde{\bar{\theta}}^T\tilde{\bar{\theta}}.$$

Taking the time derivative of V along the system directions we have $\dot{V} = (a_m + \ell)e^2 \leq 0$. Given that V is positive definite and $\dot{V}$ is negative semi-definite we have that $V(e(t), \tilde{\bar{\theta}}(t) \leq V(e(0), \tilde{\bar{\theta}}(0)) < \infty$. Thus V is bounded and this means in turn that e and $\tilde{\bar{\theta}}$ are bounded, with

$$\|e(t)\|_{L_\infty}^2 \leq 2V(0). \tag{3.8}$$

Given that r and e are bounded and the fact that $a_m < 0$, the reference model is stable. Thus we can conclude x_m, and therefore x_p, are bounded. Given that $\bar{\theta}^*$ is a constant we can conclude that $\bar{\theta}$ is bounded from the boundedness of $\tilde{\bar{\theta}}$. This can be compactly stated as $e, x_p, \tilde{\bar{\theta}}, \bar{\theta} \in \mathcal{L}_\infty$, and therefore all of the signals in the system are bounded.

In order to prove asymptotic stability in the error we begin by noting that $-\int_0^t \dot{V} = V(e(0), \tilde{\theta}(0)) - V(e(t), \tilde{\theta}(t)) \leq V(e(0), \tilde{\theta}(0))$. This in turn can be simplified as

$$|a_m + \ell| \int_0^t e(t)^2 \leq V(0) \ \forall \ t \geq 0.$$

Dividing by $|a_m + \ell|$ and taking the limit as $t \to \infty$ we have

$$\|e\|_{L_2}^2 \leq \frac{V(0)}{|a_m + \ell|} \tag{3.9}$$

which implies (3.7). Given that $e \in \mathcal{L}_2 \cap \mathcal{L}_\infty$ and $\dot{e} \in \mathcal{L}_\infty$, Lemma 2.4 is satisfied and therefore $\lim_{t\to\infty} e(t) = 0$ [61]. □

Theorem 1 clearly shows that CRM ensures stability of the adaptive system. Also, from the fact that $e \in \mathcal{L}_2$ we have that $x_m(t) \to x_m^o(t)$ as $t \to \infty$ [12, §IV.1, Theorem 9(c)]. The question therefore is if any improvement is possible in the transient response with the inclusion of ℓ. This is discussed in the following section.

3.2.2 Transient Performance of CRM-adaptive systems

The main impact of the CRM is a modification in the realization of the reference trajectory, from the use of a linear model to a nonlinear model. This in turn produces a more benign target for the adaptive closed-loop system to follow, resulting in better transients. It could be argued that the reference model meets the closed-loop system half-way, and therefore reduces the burden of tracking on the adaptive system and shifts it partially to the reference model. In what follows, we precisely quantify this effect.

As Equation (3.7) in Theorem 3.1 illustrates, the L-2 norm of e has two components, one associated with the initial error in the reference model, $e(0)$, and the other

with the initial error in the parameter space, $\tilde{\bar{\theta}}(0)$. The component associated with $\tilde{\bar{\theta}}(0)$ is inversely proportional to the product $\gamma\,|\ell|$ and the component associated with the initial model following error $e(0)$ is inversely proportional to $|\ell|$ alone. Therefore, without the use of the feedback gain ℓ it is not possible to uniformly decrease the L-2 norm of the model following error. This clearly illustrates the advantage of using the CRM over the ORM, as in the latter, $\ell = 0$.

While CRM-adaptive systems bring in this obvious advantage, they can also introduce an undesirable peaking phenomenon. In what follows, we introduce a definition and show how through a proper choice of the gain ℓ, this phenomenon can be contained, and lead to better bounds on the parameter derivatives. As mentioned in the introduction, we quantify transient performance in this paper by deriving L-2 bounds on the parameter derivative $\dot{\bar{\theta}}$, which in turn will correlate to bounds on the amplitude of frequency oscillations in the adaptive parameters. For this purpose, we first discuss the L-2 bound on e and supremum bound for x_m. We then describe a peaking phenomenon that is possible with CRM-adaptive systems.

L-∞ norm of x_m

The solution to the ODE in (3.2) is

$$x_m(t) = \mathbf{e}^{a_m t}x_m(0) + \int_0^t \mathbf{e}^{a_m(t-\tau)}r(\tau)d\tau - \ell\int_0^t \mathbf{e}^{a_m(t-\tau)}e(\tau)d\tau. \tag{3.10}$$

The solution to the ODE in (3.3) is

$$x_m^o(t) = \mathbf{e}^{a_m t}x_m^o(0) + \int_0^t \mathbf{e}^{a_m(t-\tau)}r(\tau)d\tau. \tag{3.11}$$

For ease of exposition and comparison, $x_m(0) = x_m^o(0)$ and thus

$$x_m(t) = x_m^o(t) - \ell\int_0^t \mathbf{e}^{a_m(t-\tau)}e(\tau)d\tau. \tag{3.12}$$

Denoting the difference between the open-loop and closed-loop reference model as $\Delta x_m = x_m - x_m^o$, using Cauchy Schwartz Inequality on $\int_0^t \mathbf{e}^{a_m(t-\tau)}\|e(\tau)\|d\tau$, and the bound for $\|e(t)\|_{L_2}$ from (3.9), we can conclude that

$$\|\Delta x_m(t)\| \leq |\ell|\sqrt{\frac{1}{|2a_m|}}\sqrt{\frac{V(0)}{|a_m+\ell|}}. \tag{3.13}$$

We quantify the peaking phenomenon through the following definition:

Definition 3.1. Let $\alpha \in \mathbb{R}^+$, a_1, a_2 are fixed positive constants, $x : \mathbb{R}^+ \times \mathbb{R}^+ \to \mathbb{R}$ and $x(\alpha;t) \in \mathcal{L}_2$,

$$y(\alpha;t) \triangleq \alpha\int_0^t \mathbf{e}^{-a_1(t-\tau)}x(\alpha;\tau)d\tau,$$

Then the signal $y(\alpha;t)$ is said to have a peaking exponent s with respect to α if

$$\|y(t)\|_{L_\infty} \leq a_1\alpha^s + a_2.$$

Remark 3.1. We note that this definition of peaking differs from that of peaking for linear systems given in [77], and references there in. In these works, the underlying peaking behavior corresponds to terms of the form $\kappa\mathbf{e}^{-\alpha t}$, $\alpha, \kappa > 0$, where any increase in α is accompanied by a corresponding increase in κ leading to peaking. This can occur in linear systems where the Jacobian is defective [57]. In contrast, the peaking of interest in this paper occurs in adaptive systems where efforts to decrease the L_2 norm of x through the increase of α leads to the increase of y causing it to peak. This is discussed in detail below.

From Eq. (12), it follows that Δx_m can be equated with y and e with x in Definition 1. Expanding $V(0)$, the bound on $\Delta x_m(t)$ in (3.13) can be represented as

$$\|\Delta x_m(t)\| \leq b_1|\ell|^{1/2} + b_2\left(\frac{|\ell|}{\gamma}\right)^{1/2}$$

where $b_1 = \sqrt{\frac{e(0)^2}{2|a_m|}}$ and $b_2 = \sqrt{\frac{\|\tilde{\theta}(0)\|^2}{2|a_m|}}$. We note that γ is a free design parameter in the adaptive system. Therefore, one can choose $\gamma = |\ell|$ and achieve the bound

$$\|\Delta x_m(t)\| \leq b_1|\ell|^{1/2} + b_2. \tag{3.14}$$

From (3.14) and Definition 1, it follows that with $\gamma = O(|\ell|)$, Δx_m has a peaking exponent of 0.5 with respect to $|\ell|$. Similar to (3.14) the following bound holds for x_m:

$$\|x_m(t)\|_{L_\infty} \leq b_1|\ell|^{1/2} + b_3 \tag{3.15}$$

where $b_3 = b_2 + \|x_m^o(t)\|_{L_\infty}$ and $\gamma = |\ell|$. That is the bounds in (3.14) and (3.15) increase with $|\ell|$, which implies that $\Delta x_m(t)$ and therefore $x_m(t)$ can exhibit peaking.

While it is tempting to simply pick $e(0) = 0$ so that $b_1 = 0$, as is suggested in [6], [7] to circumvent this problem, it is not always possible to do so, as $x(0)$ may not be available as a measurement because of noise or disturbance that may be present. In Section III, we present an approach where tighter bounds for $x_m(t)$ are derived, which enables us to reduce the peaking exponent of Δx_m from 0.5 to zero.

Before moving to the L-2 bounds on $\dot{k}$ and $\dot{\theta}$, we motivate the importance of L-2 bounds on signal derivatives and how they relate to the frequency characteristic of the signals of interest. We use a standard property of Fourier series and continuous functions [48, 69] summarized in Lemma 3.1 and Theorem 3.2 below:

Lemma 3.1. *Consider a periodic signal $f(t) \in \mathbb{R}$ over a finite interval $\mathbb{T} = [t_1, t_1 + \tau]$ where τ is the period of $f(t)$. The Fourier coefficients of $f(t)$ are then given by $F(n) = \frac{1}{\tau}\int_{\mathbb{T}} f(t)\mathbf{e}^{-i\omega(n)t}dt$ with $\omega(n) = 2\pi n/\tau$. If $f(t) \in \mathcal{C}^1$, given $\epsilon_1 > 0$, there exists an integer N_1 such that*

(i) $\left\| f(t) - \sum_{n=-N_1}^{N_1} F(n)\mathbf{e}^{i\omega(n)t} \right\| \leq \epsilon_1, \qquad \forall t \in \mathbb{T}.$

If in addition $f(t) \in \mathcal{C}^2$, then for all $\epsilon_2 > 0$ there exists an integer N_2 such that

(ii) $\left\| \frac{d}{dt} f(t) - \sum_{n=-N_2}^{N_2} i\omega(n) F(n) \mathbf{e}^{i\omega(n)t} \right\| \leq \epsilon_2, \forall t \in \mathbb{T}.$

Theorem 3.2. *If $f(t) \in \mathcal{C}^2$ and periodic with period τ, then the following equality holds*

$$\int_{\mathbb{T}} \|\dot{f}(t)\|^2 dt = \sum_{n=-\infty}^{\infty} |F(n)|^2 |\omega(n) 2\pi n| \tag{3.16}$$

where $F(n) = \frac{1}{\tau} \int_{\mathbb{T}} f(t) \mathbf{e}^{-i\omega(n)t} dt$, $\omega(n) = 2\pi n/\tau$ and $\mathbb{T} = [t_1, t_1 + \tau]$.

Proof. This follows from Parseval's Theorem. From Lemma 3.1(ii), $\int_{\mathbb{T}} \|\dot{f}(t)\|^2 dt = \int_{\mathbb{T}} \left\| \sum_{n=-\infty}^{\infty} i\omega(n) F(n) \mathbf{e}^{i\omega(n)t} \right\|^2 dt$. Using the orthogonality of $\mathbf{e}^{i\omega(n)t}$ we have that $\int_{t_1}^{t_1+\tau} \mathbf{e}^{i\omega(n)t} \mathbf{e}^{-i\omega(m)t} dt = 0$ for all integers $m \neq n$. It also trivially holds that

$$\int_{t_1}^{t_1+\tau} \mathbf{e}^{i\omega(n)t} \mathbf{e}^{-i\omega(n)t} dt = \tau.$$

Using these two facts along with the fact that the convergence in Lemma 3.1(ii) is uniform, the integral above can be simplified as $\int_{\mathbb{T}} \|\dot{f}(t)\|^2 dt = \sum_{n=-\infty}^{\infty} \omega(n)^2 |F(n)|^2 \tau$. Expanding one of the $\omega(n)$ terms and canceling the τ term gives us (3.16). □

Remark 3.2. From Theorem 3.2 it follows that when the L-2 norm of the derivative of a function is reduced, the product $|F(n)|^2 |\omega(n) 2\pi n|$ is reduced for all $n \in \mathbb{Z}$. Given that $\omega(n)$ is the natural frequency for each Fourier approximation and $|F(n)|$ their respective amplitudes, reducing the the L-2 norm of the derivative of a function implicitly reduces the the amplitude of the high frequency oscillations.

L-2 norm of $\dot{k}, \dot{\theta}$

With the bounds on e and x_m in the previous sections, we now derive bounds on the adaptive parameter derivatives. From (3.5) we can deduce that $\|\dot{k}\|^2 = \gamma^2 e^2 r^2$. Integrating both sides and taking the supremum of r we have

$$\int_0^t \|\dot{k}(\tau)\|^2 d\tau \leq \gamma^2 \|r(t)\|_{L_\infty}^2 \|e(t)\|_{L_2}^2. \tag{3.17}$$

Using the bound on $\|e\|_{L_2}$ from (3.9) we have that

$$\|\dot{k}(t)\|_{L_2}^2 \leq \frac{2\gamma^2 \|r(t)\|_{L_\infty}^2 V(0)}{|a_m + \ell|}. \tag{3.18}$$

Similarly, from (3.5) we can derive the inequality

$$\int_0^t \|\dot{\theta}(\tau)\|^2 d\tau \leq 2\gamma^2 \|e(t)\|_{L_\infty}^2 \int_0^t e(\tau)^2 d\tau + 2\gamma^2 \|x_m(t)\|_{L_\infty}^2 \int_0^t e(\tau)^2 d\tau. \tag{3.19}$$

Using the bounds for $\|e(t)\|_{L_\infty}$ in (3.8), $\|e(t)\|_{L_2}$ in (3.9), and the following bound on

$$\|x_m(t)\|_{L_\infty}^2 \leq 2\|x_m^o(t)\|_{L_\infty}^2 + \frac{|\ell|^2 V(0)}{|a_m|\,|a_m+\ell|}, \tag{3.20}$$

which follows from the bound on $\Delta x_m(t)$ in (3.13), the bound in (3.19) can be simplified as

$$\|\dot{\theta}(t)\|_{L_2}^2 \leq 4\gamma^2 \frac{V(0)\|x_m^o(t)\|_{L_\infty}^2}{|a_m+\ell|} + 4\gamma^2 \frac{V(0)^2}{|a_m+\ell|} + 2\gamma^2 \frac{|\ell|^2}{|a_m|} \frac{V(0)^2}{|a_m+\ell|^2}. \tag{3.21}$$

From (3.18) it is clear that by increasing $|\ell|$ one can arbitrarily decrease the L-2 norm of $\dot{k}$. The same is not true, however, for the L-2 norm of $\dot{\theta}$ given in (3.21). Focusing on the first two terms we see that their magnitude is proportional to $\gamma^2/|a_m+\ell|$. Letting ℓ approach negative infinity, the first and second second terms in (3.21) approaches zero and the third term converges to a bound which is proportional to $\gamma^2 V(0)^2$. When $\ell = 0$, the second term becomes proportional to $\gamma^2 V(0)^2$ and the last term in (3.21) becomes zero. From the previous discussion it is clear that regardless of our choice of ℓ, the only way to uniformly decrease the L-2 norms of the derivatives of the adaptive terms is by decreasing γ. This leads to the classic trade-off present in adaptive control. One can reduce the high frequency oscillations in the adaptive parameters by choosing a small γ, this however leads to poor reference model tracking. This can be seen by expanding the bound on $\|e(t)\|_{L_\infty}$ in (3.8),

$$\|e(t)\|_{L_\infty}^2 \leq e(0)^2 + \frac{1}{\gamma}\tilde{\bar{\theta}}(0)^T\tilde{\bar{\theta}}(0). \tag{3.22}$$

If one chooses a small γ, then poor state tracking performance can occur, as the second term in (3.22) is large for small γ. Therefore it still remains to be seen as to how and when CRM leads to an advantage over ORM. As shown in the following subsection and subsequent section, this can be demonstrated through the introduction of projection in the adaptive law and a suitable choice of ℓ and γ. This in turn will allow the reduction of high frequency oscillations.

3.2.3 Effect of Projection Algorithm

It is well known that some sort of modification of the adaptive law is needed to ensure boundedness in the presence of perturbations such as disturbances or unmodeled dynamics. We use a projection algorithm [67] with CRMs as

$$\dot{\bar{\theta}} = \text{Proj}_\Omega(-\gamma \text{sgn}(k_p) e\phi, \bar{\theta}) \tag{3.23}$$

where $\bar{\theta}(0), \bar{\theta}^* \in \Omega$, with $\Omega \in \mathbb{R}^2$ a closed and convex set centered at the origin whose size is dependent on a known bound of the parameter uncertainty $\bar{\theta}^*$. Equation (3.23)

assures that $\bar{\theta}(t) \in \Omega \; \forall \; t \geq 0$ [67]. The following definition will be used throughout:

$$\Theta_{\max} \triangleq \sup_{\bar{\theta},\bar{\theta}^* \in \Omega} \|\tilde{\bar{\theta}}\|. \tag{3.24}$$

Beginning with the already proven fact that $\dot{V} \leq (a_m + \ell)e^2$, we note that the following bound holds as well with the use of (3.23):

$$\dot{V}(t) \leq -2|a_m + \ell|V + \frac{|a_m + \ell|}{\gamma} |k_p| \, \Theta^2_{\max}. \tag{3.25}$$

Using Gronwall-Bellman [6] it can be deduced that

$$V(t) \leq \left(V(0) - \frac{|k_p|}{2\gamma}\Theta^2_{\max} \right) \mathbf{e}^{-2|a_m+\ell|t} + \frac{|k_p|}{2\gamma}\Theta^2_{\max} \tag{3.26}$$

which can be further simplified as

$$V(t) \leq \frac{1}{2}\|e(0)\|^2 \mathbf{e}^{-2|a_m+\ell|t} + \frac{|k_p|}{2\gamma}\Theta^2_{\max} \tag{3.27}$$

which informs the following exponential bound on $e(t)$:

$$\|e(t)\|^2 \leq \|e(0)\|^2 \mathbf{e}^{-2|a_m+\ell|t} + \frac{|k_p|}{\gamma}\Theta^2_{\max}. \tag{3.28}$$

The discussions in Section 3.2 show that with a projection algorithm, the CRM adaptive system is not only stable but satisfies the transient bounds in (3.9), (3.15), (3.18), (3.21), (3.27) and (3.28). The bounds in (3.15), (3.18) and (3.21) leave much to be desired however, as it is not clear how the free design parameters ℓ and γ can be chosen so that the bounds on $\|\dot{k}\|_{L_2}$ and $\|\dot{\theta}\|_{L_2}$ can be systematically reduced while simultaneously controlling the peaking in the reference model output x_m. Using the bounds in (3.27) and (3.28), in the following section, we propose an "optimal" CRM design that does not suffer from the peaking phenomena, and show how the bounds in (3.15), (3.18) and (3.21) can be further improved. We also make a direct connection between the L-2 norm of the derivative of a signal, and the frequency and amplitude of oscillation in that signal.

3.3 Bounded Peaking with CRM adaptive systems

3.3.1 Bounds on x_m

We first show that the peaking that $\|x_m(t)\|$ was shown to exhibit in Section II-A can be reduced through the use of a projection algorithm in the update law as in (3.23), and a suitable choice of γ and ℓ. For this purpose we derive two different bounds, one over the time interval $[0, t_1]$ and another over $[t_1, \infty)$.

Lemma 3.2. *Consider the adaptive system with the plant in* (3.1)*, with the controller defined by* (3.4)*, the update law in* (3.23) *with the reference model as in* (3.2)*. For all* $\delta > 1$ *and* $\epsilon > 0$*, there exists a time* $t_1 \geq 0$ *such that*

$$\begin{aligned} \|x_p(t)\| &\leq \delta \|x_p(0)\| + \epsilon \|r(t)\|_{L_\infty} \\ \|x_m(t)\| &\leq \delta \|x_p(0)\| + \epsilon \|r(t)\|_{L_\infty} + \sqrt{2V(0)} \end{aligned} \tag{3.29}$$

$\forall\ 0 \leq t \leq t_1$.

Proof. The plant in (3.1) is described by the dynamical equation

$$\dot{x}_p = (a_m + k_p \tilde{\theta}) x_p + k_p \tilde{k} r$$

where we note that $(a_m + k_p \tilde{\theta})$ can be positive. This leads to the inequality

$$\|x_p(t)\| \leq \|x_p(0)\| \mathbf{e}^{(a_m + |k_p| \Theta_{\max})t} + \int_0^t \mathbf{e}^{(a_m + |k_p| \Theta_{\max})(t-\tau)} \, |k_p| \, \Theta_{\max} \|r(\tau)\|_{L_\infty} d\tau.$$

For any $\delta > 1$ and any $\epsilon > 0$, it follows from the above inequality that a t_1 exists such that $\mathbf{e}^{(a_m + |k_p| \Theta_{\max})t} \leq \delta$ and $\int_0^t \mathbf{e}^{(a_m + |k_p| \Theta_{\max})(t-\tau)} \, |k_p| \, \Theta_{\max} d\tau \leq \epsilon$, $\forall\ t \leq t_1$. The bound on $x_m(t)$ follows from the fact that $\|x_m\| \leq \|x_p\| + \|e\|$ and from (3.8). □

Remark 3.3. The above lemma illustrates the fact that if t_1 is small, the plant and reference model states cannot move arbitrarily far from their respective initial conditions over $[0,\ t_1]$.

Lemma 3.3. *For any* $a \geq 0$ $\exists$ *an* $x^* < 0$ *such that for all* $x \leq x^* < 0$

$$\mathbf{e}^{xa} \leq |x|^{-\frac{1}{2}} \quad \forall\ x \leq x^* < 0.$$

Proof. Exponential functions with negative exponent decay faster than any fractional polynomial. □

We now derive bounds on $x_m(t)$ when $t \geq t_1$. For this purpose a tighter bound on the error e than that in (3.9) is first derived.

Lemma 3.4. *Consider the adaptive system with the plant in* (3.1)*, with the controller defined by* (3.4)*, the update law in* (3.23) *with the reference model as in* (3.2)*. Given a time* $t_1 \geq 0$*, there exists an* ℓ^* *s.t.*

$$\sqrt{\int_{t_1}^{\infty} \|e\|^2 d\tau} \leq \frac{\|e(0)\|}{\sqrt{2}\,|a_m + \ell|} + \sqrt{\frac{|k_p|}{2\gamma\,|a_m + \ell|}} \Theta_{max} \tag{3.30}$$

for all $\ell \leq \ell^*$.

Proof. Substitution of $t = t_1$ in (3.27) and using the fact that $\dot{V}(t) = -|a_m + \ell| \|e(t)\|^2$, the following bound is obtained:

$$\int_{t_1}^{\infty} \|e\|^2 d\tau \leq \frac{\|e(0)\|^2 \mathbf{e}^{-2|a_m + \ell| t_1}}{2\,|a_m + \ell|} + \frac{|k_p|}{2\gamma\,|a_m + \ell|} \Theta_{\max}^2. \tag{3.31}$$

Noting that $\sqrt{\mathbf{e}^{-2|a_m+\ell|t_1}} = \mathbf{e}^{-|a_m+\ell|t_1}$, and using the result from Lemma 3.3, we know that there exists an ℓ^* such that for all $\ell < \ell^*$, $\mathbf{e}^{(a_m+\ell)t_1} \leq |a_m+\ell|^{-1/2}$. This leads to (3.30). $\square$

Similar to the definition of $\Delta x_m(t)$ in Section II.B we define

$$\Delta \bar{x}_m(t) \triangleq |\ell| \int_{t_1}^{t} \mathbf{e}^{-|a_m|(t-\tau)} \|e(\tau)\| d\tau$$

for all $t \geq t_1$. Choosing $\ell \leq \ell^*$ with ℓ^* defined in Lemma 3.4, using the bound on $e(t)$ in (3.30) and the Cauchy Schwartz inequality, we have that

$$\|\Delta \bar{x}_m(t)\|_{L_\infty} \leq b_4 + b_5 \left(\frac{|\ell|}{\gamma}\right)^{1/2} \quad \forall t \geq t_1$$

where $b_4 = \frac{\|e(0)\|}{2\sqrt{|a_m|}}$ and $b_5 = \frac{\sqrt{|k_p|}\Theta_{\max}}{2\sqrt{|a_m|}}$. Choosing $\gamma = |\ell|$ the bound above becomes

$$\|\Delta \bar{x}_m(t)\|_{L_\infty} \leq b_4 + b_5 \quad t \geq t_1. \tag{3.32}$$

Comparing the bound in (3.32) to the bound in (3.14), we note that the peaking exponent (Definition 1) has been reduced from 1/2 to 0 for the upper bound on the convolution integral of interest. Thus, as $|\ell|$ is increased, the term $\Delta \bar{x}_m(t)$ will not exhibit peaking. This result allows us to obtain a bound on the closed-loop reference model $x_m(t)$ that does not increase with increasing $|\ell|$. This is explored in the following theorem and subsequent remark in detail.

Theorem 3.3. *Consider the adaptive system with the plant in* (3.1)*, the controller defined by* (3.4)*, the update law in* (3.23) *with the reference model as in* (3.2)*, with* t_1 *chosen as in Lemma 3.2 and* $\ell \leq \ell^*$ *where* ℓ^* *satisfies* (3.30)*. It can then be shown that*

$$\|x_m(t)\|^2_{t\geq t_1} \leq c_1(t) + \frac{\|e(0)\|^2}{|a_m|} + \frac{|\ell|\,|k_p|\,\Theta^2_{max}}{\gamma\,|a_m|} \tag{3.33}$$

where

$$c_1 \triangleq 2\left(\|x_m^o\|_{L_\infty} + \|x_m(t_1)\|\mathbf{e}^{-|a_m|(t-t_1)}\right)^2.$$

Proof. The solution of (3.2) for $t \geq t_1$ is given by

$$\|x_m(t)\| \leq \|x_m^o\|_{L_\infty} + \|x_m(t_1)\|\mathbf{e}^{-|a_m|(t-t_1)} + |\ell| \int_{t_1}^{\infty} \mathbf{e}^{-|a_m|(t-\tau)} \|e(\tau)\| d\tau.$$

Using the Cauchy Schwartz Inequality and (3.30) from Lemma 3.4, we have that

$$\begin{aligned}\|x_m(t)\|_{t\geq t_1} \leq &\|x_m^o\|_{L_\infty} + \| x_m(t_1)\|\mathbf{e}^{-|a_m|(t-t_1)} \\ &+ \frac{|\ell|}{\sqrt{2\,|a_m|}}\left(\frac{\|e(0)\|}{\sqrt{2}\,|a_m+\ell|} + \frac{\sqrt{|k_p|}\Theta_{\max}}{\sqrt{2\gamma\,|a_m+\ell|}}\right),\end{aligned}$$

for all $\ell < \ell^*$. Squaring leads to (3.33). $\square$

Corollary 3.1. *Following the same assumptions as Theorem 3.3, with* $\gamma = |\ell|$

$$\|x_m(t)\|^2_{t\leq t_1} \leq 2(\delta\|x_p(0)\| + \epsilon\|r(t)\|_{L_\infty})^2 + 4V(0) \tag{3.34}$$

$$\|x_m(t)\|^2_{t\geq t_1} \leq c_1(t) + \frac{\|e(0)\|^2}{|a_m|} + \frac{|k_p|\,\Theta^2_{max}}{|a_m|} \tag{3.35}$$

Remark 3.4. Through the use of a projection algorithm in the adaptive law, the exploitation of finite time stability of the plant in Lemma 1, and through the use of the extra degree of freedom in the choice of ℓ, we have obtained a bound for $\|x_m(t)\|^2_{t\leq t_1}$ in (3.34) which is only a function of the initial condition of the plant and controller. Similarly for $\|x_m(t)\|^2_{t\geq t_1}$, we have derived a bound in (3.34) which is once again a function of the initial condition of the plant and controller alone. The most important point to note is that unlike (3.15), the bound on x_m in (3.34) and (3.35) is no longer proportional to ℓ in any power. This implies that even for large $|\ell|$, an appropriate choice of the adaptive tuning parameter γ can help reduce the peaking in the reference model. This improvement was possible only through the introduction of projection and the use of the Gronwall-Bellman inequality.

3.3.2 Bounds on parameter derivatives and oscillations

We now present the main result of this paper.

Theorem 3.4. *The adaptive system with the plant in* (3.1)*, the controller defined by* (3.4)*, the update law in* (3.23) *with the reference model as in* (3.2)*, with* t_1 *chosen as in Lemma 3.2 and* $\ell \leq \ell^*$ *where* ℓ^* *is given in Lemma 3.4 and* $\gamma = |\ell|$*, the following bounds are satisfied for all* $\gamma \geq 1$*:*

$$\begin{aligned}
&\int_{t_1}^{\infty} \|\dot{k}\|^2 d\tau \leq \left(\|e(0)\|^2 + |k_p|\,\Theta^2_{max}\right)\|r(t)\|_{L_\infty} \\
&\int_{t_1}^{\infty} \|\dot{\theta}\|^2 d\tau \leq \left(\|e(0)\|^2 + |k_p|\,\Theta^2_{max}\right) c_2 + \left(\|e(0)\|^2 + |k_p|\,\Theta^2_{max}\right)\left(\frac{c_3}{\sqrt{|\ell|}} + \frac{c_4}{\gamma}\right)
\end{aligned} \tag{3.36}$$

where c_2, c_3, c_4 *are independent of* γ *and* ℓ*, and are only a function of the initial conditions of the system and the fixed design parameters.*

Proof. Using (3.17) and (3.30), together with the fact that $\gamma = |\ell|$, we obtain the first inequality in (3.36). To prove the bound on $\dot{\theta}$ we start with (3.19), and note that

$$\gamma^2 \int_{t_1}^{\infty} e(\tau)^2 d\tau \leq \left(\|e(0)\|^2 + |k_p|\,\Theta^2_{\max}\right). \tag{3.37}$$

Using the bound in (3.37) and setting $c_2 = \|x_m(t)\|^2_{t\geq t_1}$ from (3.33) we have the first term in the bound on $\dot{\theta}$ in (3.36).

We note from (3.28) and Lemma 3.3 that

$$\|e(t)\| \leq \frac{e(0)^2}{\sqrt{|a_m + \ell|}} + \frac{|k_p|\,\Theta_{\max}}{\gamma} \qquad \forall t \geq t_1.$$

This together with (3.37) leads to the second term in the bound on $\dot{\theta}$ in (3.36). Therefore, c_2, c_3 and c_4 are independent of γ and ℓ. □

Remark 3.5. From the above Theorem it is clear that if γ and $|\ell|$ are increased while holding $\gamma = |\ell|$, the L-2 norms of the derivatives of the adaptive parameters can be decreased significantly. Two important points should be noted. One is that the bounds in (3.36) are much tighter than those in (3.21), with terms of the form γ^2/ℓ no longer present. Finally, from Theorem 3.2, it follows that the improved L-2 bounds in (3.36) result in a reduced high frequency oscillations in the adaptive parameters.

3.3.3 Simulation Studies for CRM

Simulation studies are now presented to illustrate the improved transient behavior of the adaptive parameters and the peaking that can occur in the reference model. For these examples the reference system is chosen such that $a_m = -1, k_m = 1$ and the plant is chosen as $a_p = 1, k_p = 2$. The adaptive parameters are initialized to be zero. Figures 1 through 3 are for an ORM adaptive system with the tuning gain chosen as $\gamma \in \{1, 10, 100\}$. Walking through Figures 1 through 3 it clear that as the tuning gain is increased the plant tracks the reference model more closely, at the cost of increased oscillations in the adaptive parameters. Then the CRM is introduced and the resulting responses are shown in Figures 4 through 6, for $\gamma = 100$, and ℓ=-10, -100, and -1000 respectively. First, it should be noted that no high frequency oscillations are present in these cases, and the trajectories are smooth, which corroborates the inequalities (3.36) in Theorem 3.4. As the ratio $|\ell|/\gamma$ increases, as illustrated in Figures 4 through 6, the reference trajectory x_m starts to deviate from the open-loop reference x_m^o, with the peaking phenomenon clearly visible in Figure 6 where $|\ell|/\gamma = 10$. This corroborates our results in section 3.3 as well.

3.4 CRM for States Accessible Control

In this section we show that the same bounds shown previously easily extend to the states accessible case. Consider the n dimensional linear system

$$\dot{x}_p = Ax_p + B\Lambda u \tag{3.38}$$

with B known, A, Λ are unknown. An a priori upper bound on Λ is known and therefore we define

$$\bar{\lambda} \triangleq \max_i \lambda_i(\Lambda),$$

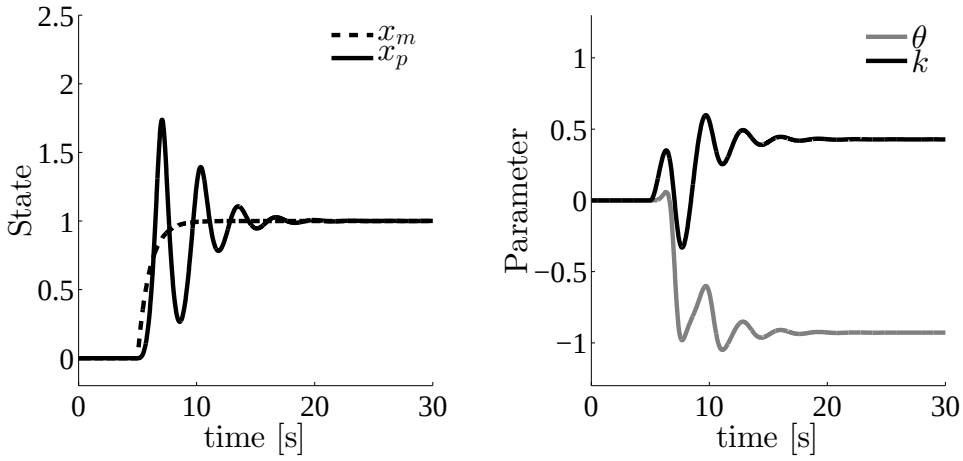

Figure 3-1: Trajectories of the ORM adaptive system $\gamma = 1$.

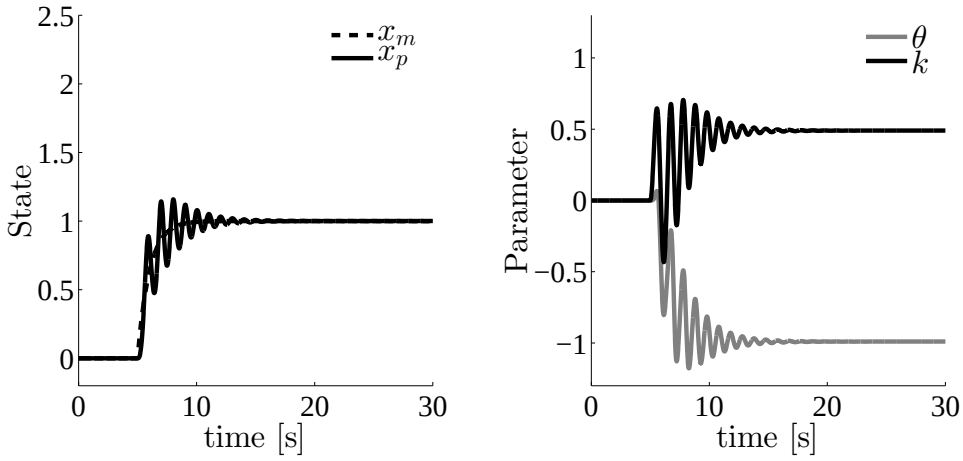

Figure 3-2: Trajectories of the ORM adaptive system $\gamma = 10$.

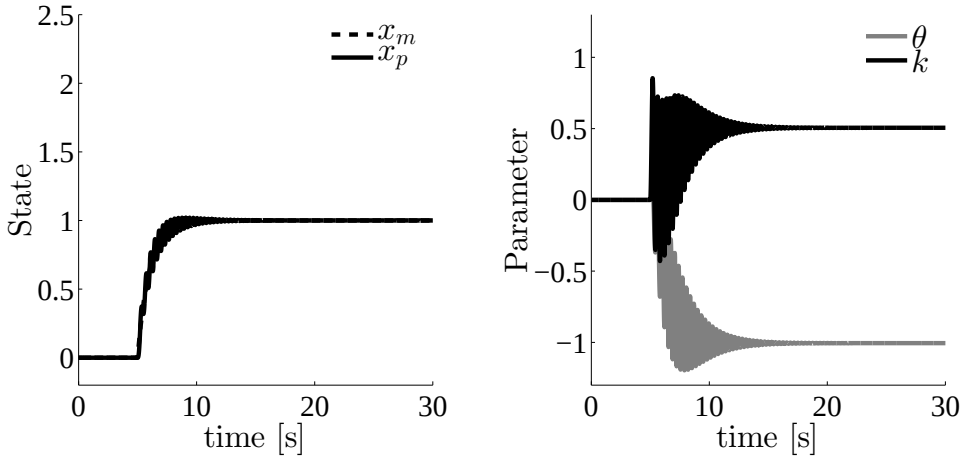

Figure 3-3: Trajectories of the ORM adaptive system $\gamma = 100$.

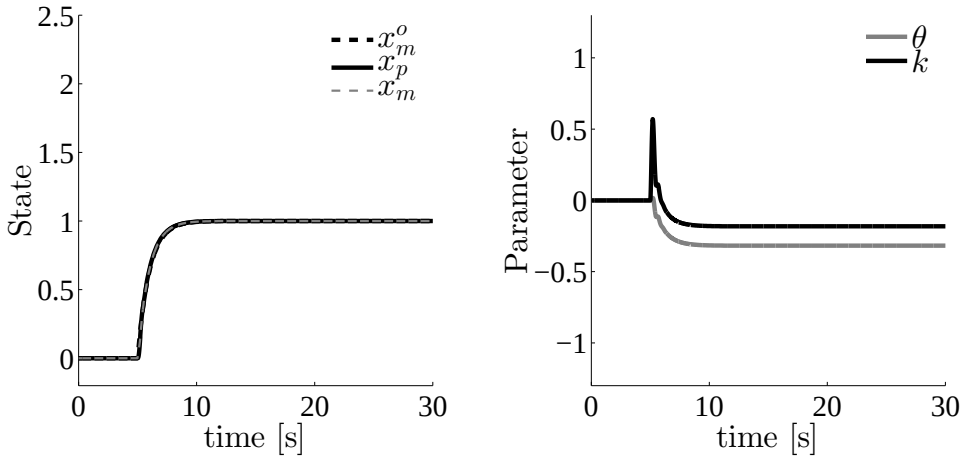

Figure 3-4: Trajectories of the CRM adaptive system $\gamma = 100$, $\ell = -10$.

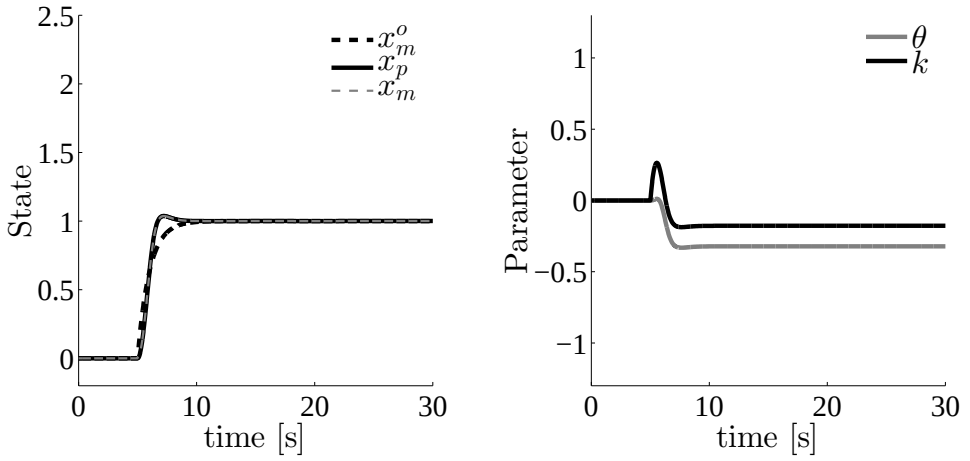

Figure 3-5: Trajectories of the CRM adaptive system $\gamma = 100$, $\ell = -100$.

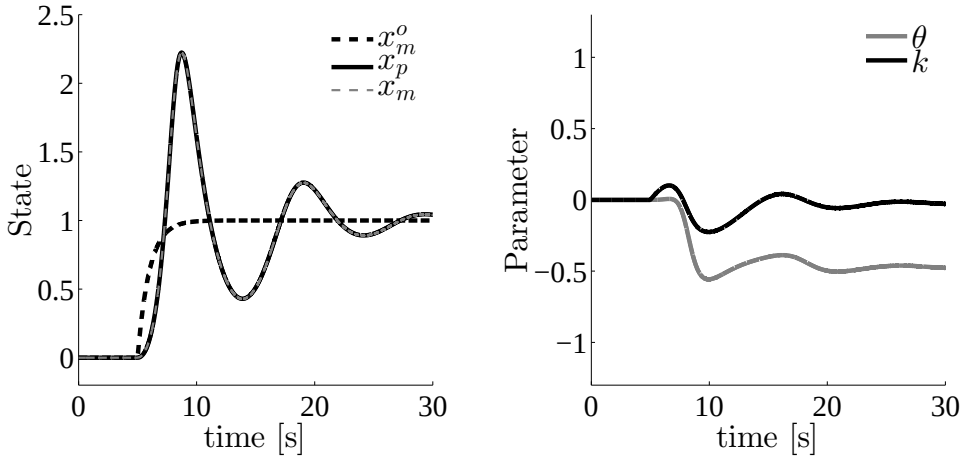

Figure 3-6: Trajectories of the CRM adaptive system $\gamma = 100$, $\ell = -1000$.

where λ_i denotes the i-th eigenvalue. The reference model is defined as

$$\dot{x}_m = A_m x_m + Br - Le. \tag{3.39}$$

The control input is defined as

$$u = \Theta x_p + Kr. \tag{3.40}$$

It is assumed that there exists Θ^* and K^* such that

$$\begin{aligned} A + B\Lambda\Theta^* &= A_m \\ \Lambda K^* &= I \end{aligned}$$

and the parameter errors are then defined as $\tilde{\Theta} = \Theta - \Theta^*$ and $\tilde{K} = K - K^*$. Defining the error as $e = x_p - x_m$, the update law for the adaptive parameters is then

$$\begin{aligned} \dot{\Theta} &= \mathrm{Proj}_{\Omega_1}(-\Gamma B^T P e x_p^T, \Theta) \\ \dot{K} &= \mathrm{Proj}_{\Omega_2}(-\Gamma B^T P e r^T, K) \end{aligned} \tag{3.41}$$

where $P = P^T > 0$ is the solution to the Lyapunov equation $(A_m + L)^T P + P(A_m + L) = -Q$ which exists for all $Q = Q^T > 0$. With a slight abuse of notation the following definition is reused from the previous section,

$$\sup_{\Theta, \Theta^* \in \Omega_1} \|\tilde{\Theta}\|_F \triangleq \Theta_{\max} \quad \text{and} \quad \sup_{K, K^* \in \Omega_2} \|\tilde{K}\|_F \triangleq K_{\max}, \tag{3.42}$$

where $\|\cdot\|_F$ denotes the Frobenius norm. The adaptive system can be shown to be stable by using the following Lyapunov candidate,

$$V(t) = e^T P e + \mathrm{Tr}(\Lambda \tilde{\Theta}^T \Gamma^{-1} \tilde{\Theta}) + \mathrm{Tr}(\Lambda \tilde{K}^T \Gamma^{-1} \tilde{K})$$

where after differentiating we have that $\dot{V} \leq -e^T Q e$. We choose L and Γ in a special form to ease the analysis in the following sections.

Assumption 3.1. The free design parameters are chosen as

$$\begin{aligned} \Gamma &= \gamma I_{n \times n} \\ L &= -A_m + g I_{n \times n} \end{aligned} \tag{3.43}$$

where $\gamma > 0$ and $g < 0$.

Assumption 1 allows us to choose a $P = 1/2 I_{n \times n}$ in the Lyapunov equation and therefore $Q = -g I_{n \times n}$. Using these simplification the Lyapunov candidate derivative can be bounded as

$$\dot{V}(t) \leq -|g| \, \|e(t)\|^2, \tag{3.44}$$

and by direct integration we have

$$\|e(t)\|^2 \leq \frac{V(0)}{|g|}. \tag{3.45}$$

Using the Gronwall-Bellman Lemma as was previously used in (3.25)-(3.28), we can deduce that

$$V(t) \leq \frac{1}{2}\|e(0)\|^2 \mathbf{e}^{-2|g|t} + \frac{\bar{\lambda}}{\gamma}\left(\Theta_{\max}^2 + K_{\max}^2\right). \tag{3.46}$$

Lemma 3.5. *For all $\epsilon > 0$ and $\delta > 1$ there exists a t_2 such that the plant and reference model in* (3.38) *and* (3.39) *respectively satisfy the bounds in* (3.29) *with t_2 replacing t_1.*

Lemma 3.6. *Consider the adaptive system with the plant in* (3.38)*, the controller in* (3.40)*, the update law in* (3.41)*, the reference model as in* (3.39) *and Γ and L parameterized as in Assumption 3.1. Given a time $t_2 \geq 0$, there exists a g^* s.t.*

$$\sqrt{\int_{t_2}^{\infty} \|e\|^2 d\tau} \leq \frac{\|e(0)\|}{\sqrt{2}\,|g|} + \sqrt{\frac{\bar{\lambda}(\Theta_{max}^2 + K_{max}^2)}{\gamma\,|g|}} \tag{3.47}$$

for all $g \leq g^*$.

Proof. From (3.46) we have that

$$V(t_2) \leq \frac{1}{2}\|e(0)\|^2 \mathbf{e}^{-2|g|t_2} + \frac{\bar{\lambda}}{\gamma}\left(\Theta_{\max}^2 + K_{\max}^2\right).$$

Using the above bound and integrating $-\dot{V}$ in (3.46) from t_2 to ∞ and dividing by $|g|$ leads to

$$\int_{t_2}^{\infty} \|e\|^2 d\tau \leq \frac{\|e(0)\|^2 \mathbf{e}^{-2|g|t_2}}{2\,|g|} + \frac{\bar{\lambda}}{\gamma\,|g|}\left(\Theta_{\max}^2 + K_{\max}^2\right) \tag{3.48}$$

Taking the square root, noting that $\sqrt{\mathbf{e}^{-2|g|t_2}} = \mathbf{e}^{-|g|t_2}$, and using the result from Lemma 3.3, we know that there exists an g^* such that for all $g < g^*$, $\mathbf{e}^{-|g|t_2} \leq |g|^{-1/2}$. □

Theorem 3.5. *Consider the adaptive system with the plant in* (3.38)*, the controller in* (3.40)*, the update law in* (3.41)*, the reference model as in* (3.39)*, Γ and L parameterized as in Assumption 3.1, with t_2 chosen as in Lemma 3.5 and $g \leq g^*$ where g^* is given in Lemma 3.6. It can be shown that*

$$\begin{aligned}\|x_m(t)\|_{t\geq t_2}^2 \leq\ & c_5(t) + 2\left(\frac{\|A_m\|^2}{|g|^2} + 1\right)\frac{a_1}{a_2}\|e(0)\|^2 \\ & + 4\bar{\lambda}\left(\frac{\|A_m\|^2}{\gamma\,|g|^2} + \frac{|g|}{\gamma}\right)\frac{a_1}{a_2}\left(\Theta_{max}^2 + K_{max}^2\right)\end{aligned} \tag{3.49}$$

where

$$c_5 \triangleq 2\left(\|x_m^o\|_{L_\infty} + \|x_m(t_2)\|a_1\mathbf{e}^{-a_2(t-t_2)}\right)^2$$
$$\mathbf{e}^{A_m t} \leq a_1\mathbf{e}^{a_2 t}$$

with $a_1, a_2 > 0$.

Proof. The existence of $a_1, a_2 > 0$ such that $\mathbf{e}^{A_m t} \leq a_1\mathbf{e}^{-a_2 t}$ follows from the fact that A_m is Hurwtiz [57]. Consider the dynamical system in (3.39) for $t \geq t_2$,

$$\begin{aligned}\|x_m(t)\|_{t\geq t_2} \leq &\|x_m^o\|_{L_\infty} + \|x_m(t_1)\|a_1\mathbf{e}^{-a_2(t-t_1)} \\ &+ \|L\|a_1\int_{t_2}^{\infty}\mathbf{e}^{-a_2(t-\tau)}\|e(\tau)\|d\tau.\end{aligned}$$

Using Cauchy Schwartz along with (3.47) in Lemma 3.6 we have that

$$\begin{aligned}\|x_m(t)\|_{t\geq t_2} \leq &\|x_m^o\|_{L_\infty} + \|\ x_m(t_2)\|\mathbf{e}^{-|a_m|(t-t_1)} \\ &+ \frac{\|L\|\sqrt{a_1}}{\sqrt{2a_2}}\left(\frac{\|e(0)\|}{\sqrt{2}\,|g|} + \sqrt{\frac{\bar{\lambda}(\Theta_{\max}^2 + K_{\max}^2)}{\gamma\,|g|}}\right).\end{aligned}$$

Squaring and using the fact that $L = -A_m + gI_{n\times n}$ and thus $\|L\| \leq \|A_m\| + g$ we have that

$$\begin{aligned}\|x_m(t)\|_{t\geq t_2}^2 \leq\ & c_5(t) + \frac{(\|A_m\| + g)^2}{|g|^2}\frac{a_1}{a_2}\|e(0)\|^2 \\ &+ \frac{2(\|A_m\| + g)^2\bar{\lambda}}{\gamma\,|g|}\frac{a_1}{a_2}\left(\Theta_{\max}^2 + K_{\max}^2\right).\end{aligned}$$

Inequality (3.49) follows since $(\|A_m\| + |g|)^2 \leq 2\|A_m\|^2 + 2\,|g|^2$. □

Remark 3.6. Just as in the scalar case, we have derived a bound for $\|x_m(t)\|_{t\geq t_2}^2$ which is once again a function of the initial condition of the plant and controller, but also dependent on a component which is proportional to $|g|/\gamma$. Therefore, by choosing $\frac{|g|}{\gamma} = 1$ with $\gamma > 0$ we can have bounded peaking in the reference model.

Theorem 3.6. *The adaptive system with the plant in* (3.38)*, the controller in* (3.40)*, the update law in* (3.41)*, the reference model as in* (3.39)*,* Γ *and* L *parameterized as in Assumption 3.1, with* t_2 *chosen as in Lemma 3.5,* $g \leq g^*$ *where* g^* *is given in Lemma 3.6 and* γ *chosen such that* $\gamma = |g|$ *the following bounds are satisfied for all*

$\gamma \geq 1$:

$$\begin{aligned}
\int_{t_2}^{\infty} \|\dot{K}\|^2 d\tau \leq & \|B\| \left(\|e(0)\|^2 + K_{max}^2 + \Theta_{max}^2 \right) \|r(t)\|_{L_\infty} \\
\int_{t_2}^{\infty} \|\dot{\Theta}\|^2 d\tau \leq & \|B\| \left(\|e(0)\|^2 + \Theta_{max}^2 + K_{max}^2 \right) \cdot \\
& \left(c_6 + \frac{c_7}{g^2} + \frac{c_8}{\sqrt{|g|}} + \frac{c_9}{\gamma} \right)
\end{aligned} \tag{3.50}$$

where c_6, c_7, c_8, c_9 are independent of γ and g, and are only a function of the initial conditions of the system and the fixed design parameters.

Proof. The proof follows the same steps as used to derive the bounds in Theorem 3.4. □

Remark 3.7. It should be noted that if γ and $|g|$ are increased while holding $\gamma = |g|$, the L-2 norms of the derivatives of the adaptive parameters can be decreased significantly.

Remark 3.8. The similarity of the bounds in Theorem 3.6 to those in Theorem 3.4 implies that the same bounds on frequencies and corresponding amplitudes of the overall adaptive systems as in Theorem 3.2 hold here in the higher-order plant as well.

We note that robustness issues have not been addressed with the CRM architecture in this work. However, recent results in [29, 30, 53, 54] have shown that adaptive systems do have a time-delay margin and robustness to unmodeled dynamics when projection is used in the update law. While we expect similar results to hold with CRM as well, a detailed investigation of the same as well as comparisons of their robustness properties to their ORM counterparts are topics for further research.

3.5 CRM Composite Control with Observer Feedback

In this section, we show that the tools introduced to demonstrate smooth transient in CRM-adaptive systems can be used to analyze CMRAC systems introduced in [16, 43, 72]. As mentioned in the introduction, these systems were observed to exhibit smooth transient response, and yet no analytical explanations have been provided until now for this behavior. Our focus is on first-order plants for the sake of simplicity. Similar to Section 3.4, all results derived here can be directly extended to higher order plants whose states are accessible.

The CMRAC system that we discuss in this paper differs from that in [16] and includes an observer whose state is fed back for control rather than the plant state. As mentioned in the introduction, we denote this class of systems as CMRAC-CO

and is described by the plant in (3.1), the reference model in (3.2), an observer as

$$\dot{x}_o(t) = \ell(x_o - x_p) + (a_m - k_p\hat{\theta})x_o(t) + k_p u(t), \tag{3.51}$$

and the control input is given by

$$u = \theta x_o + k^* r. \tag{3.52}$$

In the above k_p is assumed to be known for ease of exposition. The feedback gain ℓ is chosen so that

$$g_\theta \triangleq a_m + \ell + |k_p\theta^*| < 0. \tag{3.53}$$

Defining $e_m = x_p - x_m$ and $e_o = x_o - x_p$, the error dynamics are now given by

$$\begin{aligned} \dot{e}_m(t) &= (a_m + \ell)e_m + k_p\tilde{\theta}x_o + k_p\theta^* e_o \\ \dot{e}_o(t) &= (a_m + \ell)e_o - k_p\bar{\theta}x_o. \end{aligned} \tag{3.54}$$

where $\tilde{\theta} = \theta - \theta^*$ and $\bar{\theta} = \hat{\theta} - \theta^*$ with θ^* satisfying $a_p + k_p\theta^* = a_m$ and $k_p k^* = k_m$. The update laws for the adaptive parameters are then defined with the update law

$$\begin{aligned} \dot{\theta} &= \mathrm{Proj}_\Omega(-\gamma \mathrm{sgn}(k_p) e_m x_o, \theta) - \eta\epsilon_\theta \\ \dot{\hat{\theta}} &= \mathrm{Proj}_\Omega(\gamma \mathrm{sgn}(k_p) e_o x_o, \hat{\theta}) + \eta\epsilon_\theta \\ \epsilon_\theta &= \theta - \hat{\theta} \end{aligned} \tag{3.55}$$

where $\gamma, \eta > 0$ are free design parameters. As before we define the bounded set

$$\Theta_{\max} \triangleq \max\left\{ \sup_{\theta,\theta^*\in\Omega} \|\tilde{\theta}\|, \sup_{\hat{\theta},\theta^*\in\Omega} \|\bar{\theta}\| \right\}. \tag{3.56}$$

We first establish stability and then discuss the improved transient response.

3.5.1 Stability

The stability of the CMRAC-CO adaptive system given by (3.1), (3.2), (3.51)-(3.55) can be verified with the following Lyapunov candidate

$$V(t) = \frac{1}{2}\left(e_m^2 + e_o^2 + \frac{|k_p|}{\gamma}\tilde{\theta}^2 + \frac{|k_p|}{\gamma}\bar{\theta}^2 \right) \tag{3.57}$$

which has the following derivative

$$\dot{V} \leq g_\theta e_m^2 + g_\theta e_o^2 - \frac{\eta\,|k_p|}{\gamma}\epsilon_\theta^2. \tag{3.58}$$

Boundedness of all signals in the system follows since $g_\theta < 0$. From the integration of (3.58) we have $\{e_m, e_o, \epsilon_\theta\} \in \mathcal{L}_\infty \cap \mathcal{L}_2$ and thus $\lim_{t\to\infty}\{e_m, e_o, \epsilon_\theta\} = \{0, 0, 0\}$. Using

the Gronwall-Bellman Lemma as was previously used in (3.25)-(3.28), we can deduce that

$$V(t) \leq \frac{1}{2}\left(e_m(0)^2 + e_o(0)^2\right)\mathbf{e}^{-2|g_\theta|t} + \frac{|k_p|}{\gamma}\theta_{\max}^2. \tag{3.59}$$

It should be noted that the presence of a non-zero ℓ is crucial for stability, as g_θ cannot be guaranteed to be negative if $\ell = 0$.

3.5.2 Transient performance of CMRAC-CO

Similar to Sections II and III we divide the timeline into $[0, t_3]$ and $[t_3, \infty)$, where t_3 is arbitrarily small. We first derive bounds for the system states over the initial $[0, t_3]$ in Lemma 3.7, bounds for the tracking, observer, parameter estimation errors e_m, e_o and ϵ_θ over $[t_3, \infty)$ in Lemma 3.8, bounds for x_o over $[t_3, \infty)$ in Theorem 3.7, and finally bounds for the parameter derivatives $\dot{\theta}$ and $\dot{\hat{\theta}}$ in Theorem 3.8.

Lemma 3.7. *Consider the CMRAC-CO adaptive system with the plant in* (3.1)*, with the controller defined by* (3.52)*, the update law in* (3.55) *and with the reference model as in* (3.2)*. For all $\delta > 1$ and $\epsilon > 0$, there exists a time $t_3 \geq 0$ such that*

$$\begin{aligned} \|x_p(t)\| &\leq \delta\|x_p(0)\| + \epsilon\left(\|r(t)\|_{L_\infty} + \sqrt{2V(0)}\right) \\ \|x_o(t)\| &\leq \delta\|x_p(0)\| + \epsilon\|r(t)\|_{L_\infty} + (1+\epsilon)\sqrt{2V(0)} \end{aligned} \tag{3.60}$$

$\forall\ 0 \leq t \leq t_3$.

Proof. The plant in (3.2) with the controller in (3.52) can be represented as

$$\dot{x}_p = (a_p + k_p\theta)x_p + k_p\left(r + \theta e_o\right)$$

where we note that $(a_p + k_p\theta)$ can be positive. This leads to the inequality

$$\begin{aligned} \|x_p(t)\| \leq &\|x_p(0)\|\mathbf{e}^{(a_p+|k_p|\Theta_{\max})t} + \int_0^t \mathbf{e}^{(a_p+|k_p|\Theta_{\max})(t-\tau)}\cdot \\ &|k_p|\left(\Theta_{\max}\|r(\tau)\| + \Theta_{\max}\|e_o(\tau)\|\right)d\tau. \end{aligned}$$

For any $\delta > 1$ and any $\epsilon > 0$, it follows from the above inequality that a t_3 exists such that $\mathbf{e}^{(a_p+|k_p|\Theta_{\max})t} \leq \delta$ and $\int_0^t \mathbf{e}^{(a_p+|k_p|\Theta_{\max})(t-\tau)}\,|k_p|\,\Theta_{\max}d\tau \leq \epsilon$, $0 \leq t \leq t_3$ given $\delta > 0$ and $\epsilon > 0$. From the structure of the Lyapunov candidate in (3.57) and the fact that $\dot{V} \leq 0$ we have that $\|e_o(t)\|_{L_\infty} \leq \sqrt{2V(0)}$. The bound on $x_o(t)$ follows from the fact that $\|x_o\| \leq \|x_p\| + \|e_o\|$. □

Lemma 3.8. *Consider the adaptive system with the plant in* (3.1)*, the controller in* (3.52)*, the update law in* (3.55)*, and the reference model as in* (3.2)*. Given a time*

$t_2 \geq 0$, *there exists a* g_θ^* *s.t.*

$$\begin{aligned}
\sqrt{\int_{t_3}^{\infty} {e_m}^2 d\tau} &\leq \frac{\sqrt{e_m(0)^2 + e_o(0)^2}}{\sqrt{2}\,|g_\theta|} + \sqrt{\frac{|k_p|}{\gamma\,|g_\theta|}}\Theta_{max} \\
\sqrt{\int_{t_3}^{\infty} {e_o}^2 d\tau} &\leq \frac{\sqrt{e_m(0)^2 + e_o(0)^2}}{\sqrt{2}\,|g_\theta|} + \sqrt{\frac{|k_p|}{\gamma\,|g_\theta|}}\Theta_{max} \\
\sqrt{\int_{t_3}^{\infty} {\epsilon_\theta}^2 d\tau} &\leq \frac{\sqrt{\gamma}\sqrt{e_m(0)^2 + e_o(0)^2}}{\sqrt{2\eta\,|k_p|\,|g_\theta|}} + \sqrt{\frac{1}{\eta}}\Theta_{max}
\end{aligned} \tag{3.61}$$

for all $g_\theta \leq g_\theta^*$.

Theorem 3.7. *Consider the adaptive system with the plant in* (3.1)*, the controller in* (3.52)*, the update law in* (3.55)*, the reference model as in* (3.2)*, with* t_3 *chosen as in Lemma 3.7 and* $g_\theta \leq g_\theta^*$ *where* g_θ^* *is given in Lemma 3.8. It can be shown that*

$$\begin{aligned}
\|x_o(t)\|_{t\geq t_3}^2 \leq\, & c_{10}(t) + \frac{|\ell|^2}{|g_\theta|^2} 2\sqrt{a_4}\left(e_m(0)^2 + e_o(0)^2\right) \\
& + \frac{|\ell|^2\,|k_p|}{\gamma\,|g_\theta|} 4a_4\Theta_{max}^2
\end{aligned} \tag{3.62}$$

where

$$\begin{aligned}
c_{10} &\triangleq 2\left(a_3\,|k_p|\,\|r\|_{L_\infty} + \|x_o(t_3)\|\mathbf{e}^{a_\theta(t-t_3)}\right)^2 \\
a_\theta &\triangleq a_m + k_p\epsilon_\theta
\end{aligned}$$

and

$$\begin{aligned}
\int_{t_3}^{\infty} \mathbf{e}^{a_\theta(t-\tau)} d\tau &\leq a_3 \\
\int_{t_3}^{\infty} \mathbf{e}^{2a_\theta(t-\tau)} d\tau &\leq a_4
\end{aligned}$$

with $0 \leq a_i < \infty,\ i \in \{3, 4\}$.

Proof. Given that $\lim_{t\to\infty} \epsilon_\theta(t) = 0$ we have from (3.53) that $\lim_{t\to\infty} a_\theta = a_m$. Thus $\lim_{t\to\infty} \mathbf{e}^{a_\theta t} = 0$. Therefore, $a_3, a_4 < \infty$. Consider the dynamical system in (3.51) for $t \geq t_3$.

$$\|x_o(t)\|_{t\geq t_3} \leq \|x_o(t_3)\|\mathbf{e}^{a_\theta(t-t_3)} + \int_{t_3}^{\infty} \mathbf{e}^{a_\theta(t-\tau)}\left(|\ell|\,\|e_o(\tau)\| + |k_p|\,\|r(\tau)\|\right) d\tau.$$

Using Cauchy Schwartz and Lemma 3.8 as before we have

$$\|x_o(t)\|_{t\geq t_3} \leq a_3 |k_p| \|r\|_{L_\infty} + \| x_o(t_3)\| \mathbf{e}^{-|a_m|(t-t_3)} + |\ell| \sqrt{a_4} \frac{\sqrt{e_m(0)^2 + e_o(0)^2}}{\sqrt{2}\,|g_\theta|}$$
$$+ |\ell| \sqrt{a_4} a_4 \sqrt{\frac{|k_p|}{\gamma\,|g_\theta|}} \Theta_{\max}.$$

Squaring and using the inequality $(a+b)^2 \leq 2a^2 + 2b^2$ twice, we have our result. □

Corollary 3.2. *For the system presented in Theorem 3.7 setting $\gamma = |g_\theta|$ and taking the limit as $\ell \to -\infty$ the following bound holds for $x_o(t)$*

$$\lim_{\ell \to -\infty} \|x_o(t)\|^2_{t\geq t_3} \leq c_{10}(t) + 2\sqrt{a_4}\left(e_m(0)^2 + e_o(0)^2\right) + |k_p|\, 4a_4 \Theta^2_{max}. \tag{3.63}$$

Theorem 3.8. *The adaptive system with the plant in* (3.1)*, the controller defined by* (3.52)*, the update law in* (3.55) *with the reference model as in* (3.2)*, with t_3 chosen as in Lemma 3.7 and $g_\theta \leq g_\theta^*$ where g_θ^* is given in Lemma 3.8 and γ chosen such that $\gamma = |g_\theta|$ the following bounds are satisfied for all $\gamma \geq 1$:*

$$\int_{t_3}^{\infty} \|\dot{\theta}\|^2 d\tau \leq \alpha \text{ and } \int_{t_3}^{\infty} \|\dot{\hat{\theta}}\|^2 d\tau \leq \alpha \tag{3.64}$$

with

$$\alpha \triangleq \left(\frac{\ell^2}{g_\theta^2} + \frac{\eta}{|k_p|}\right)\left(e_m(0)^2 + e_o(0)^2 + |k_p|\,\Theta^2_{max}\right) c_{11}$$

where c_{11} is independent of γ and g_θ, and is only a function of the initial conditions of the system and the fixed design parameters.

Remark 3.9. Note that

$$\lim_{\ell \to -\infty} \frac{\ell^2}{g_\theta^2} = 1.$$

Thus for large $|\ell|$ the truncated L-2 norm of $\dot{\theta}$ is simply a function of the initial conditions of the system and the tuning parameter η.

Remark 3.10. The similarity of the bounds in Theorem 3.8 to those in Theorem 3.4 implies that the same bounds on frequencies and corresponding amplitudes of the overall adaptive systems as in Theorem 3.2 hold here in the CMRAC-CO case as well.

3.5.3 Robustness of CMRAC–CO to Noise

As mentioned earlier, the benefits of the CMRAC–CO is the use of the observer state x_o rather than the actual plant state x. This implies that the effect of any measurement noise on system performance can be reduced. This is explored in this section and Section 3.5.4.

Suppose that the actual plant dynamics is modified from (3.1) as

$$\dot{x}_a(t) = a_p x_a(t) + k_p u(t), \quad x_p(t) = x_a(t) + n(t) \tag{3.65}$$

where $n(t)$ represents measurement noise. For ease of exposition, we assume that $n(t) \in \mathcal{C}_1$.

This leads to a set of modified error equations

$$\begin{aligned} \dot{e}_m(t) =& (a_m + \ell)e_m + k_p\tilde{\theta}(t)x_o + k_p\theta^* e_o + \xi(t) \\ \dot{e}_o(t) =& (a_m + \ell - k_p\theta^*)e_o - k_p\bar{\theta}(t)x_o - \xi(t) \end{aligned} \tag{3.66}$$

where

$$\xi(t) \triangleq \dot{\eta}(t) - a_p\eta(t) \tag{3.67}$$

Theorem 3.9. *The adaptive system with the plant in* (3.65)*, the controller defined by* (3.52)*, the update law in* (3.55) *with the reference model as in* (3.2)*, and ℓ chosen such that $a_m + \ell + 2|k_p||\theta^*| < 0$, all trajectories are bounded and*

$$\begin{aligned} V(t) \leq& \frac{1}{2}\left(e_m(0)^2 + e_o(0)^2\right)\mathbf{e}^{-2|g_n|t} \\ &+ \frac{|k_p|}{\gamma}\Theta_{max}^2 + \frac{1}{4|g_n|^2}\|\xi(t)\|_{L_\infty}^2. \end{aligned} \tag{3.68}$$

where

$$g_n \triangleq a_m + \ell + 2|k_p||\theta^*|. \tag{3.69}$$

Proof. Taking the time derivative of V in (3.57) results in

$$\begin{aligned} \dot{V} \leq& g_n\left(\|e_m\|^2 + \|e_o\|^2\right) - |k_p|\frac{\eta}{\gamma}\epsilon_\theta^2 \\ &+ \|\xi(t)\|\|e_m(t)\| + \|\xi(t)\|\|e_o(t)\|. \end{aligned} \tag{3.70}$$

completing the square in $\|e_m\|\|n\|$ and $\|e_o\|\|n\|$

$$\begin{aligned} \dot{V} \leq& -|g_n|/2\left(\|e_m\|^2 + \|e_o\|^2\right) - |k_p|\frac{\eta}{\gamma}\epsilon_\theta^2 \\ &- |g_n|/2\left(\|e_m\| - 1/|g_n|\,\|\xi(t)\|\right)^2 \\ &- |g_n|/2\left(\|e_o\| - 1/|g_n|\,\|\xi(t)\|\right)^2 \\ &+ 1/(4|g_n|)\|\xi(t)\|^2. \end{aligned}$$

Neglecting the negative terms in lines 2 and 3 from above and the term involving ϵ_θ we have that

$$\dot{V} \leq -|g_n|/2\left(\|e_m\|^2 + \|e_o\|^2\right) + 1/(4|g_n|)\|\xi(t)\|^2,$$

and in terms of V gives us

$$\dot{V} \leq -|g_n|V + \frac{1}{2}\frac{|k_p||g_n|}{\gamma}\left(\tilde{\theta}^2 + \bar{\theta}^2\right) + \frac{1}{4|g_n|}\|\xi(t)\|^2.$$

Using the Gronwall-Bellman Lemma and substitution of $V(t)$ leads to the bound in (3.68). □

3.5.4 Simulation Study

For this study a scalar system in the presence of noise is to be controlled with dynamics as presented in (3.65), where $n(t)$ is a deterministic signal used to represent sensor noise. $n(t)$ is generated from a Gausian distribution with variance 1 and covariance 0.01, deterministically sampled using a fixed seed at 100 Hz, and then passed through a saturation function with upper and lower bounds of 0.1 and -0.1 respectively. For the CMRAC-CO systems the reference model is chosen as (3.2) with the rest of the controller described by (3.51)-(3.55).

The CMRAC system used for comparison is identical to that in [16]. For CMRAC the reference dynamics are now chosen as x_m^o in (3.3), the observer is the same as CMRAC-CO (3.51).

Further differences arise with the control law being chosen as

$$u = \theta x_p + k^* r$$

The open-loop error $e^o = x_p - x_m^o$ updates the direct adaptive component, with the regressor becoming x_p instead of x_o for both θ and $\hat{\theta}$ update laws:

$$\begin{aligned} \dot{\theta} &= \text{Proj}_\Omega(-\gamma \text{sgn}(k_p) e_m^o x_p, \theta) - \eta \epsilon_\theta \\ \dot{\hat{\theta}} &= \text{Proj}_\Omega(\gamma \text{sgn}(k_p) e_o x_p, \hat{\theta}) + \eta \epsilon_\theta. \end{aligned} \tag{3.71}$$

The complete CMRAC and CMRAC-CO systems are given in Table I with the design parameters given in Table II.

Table 3.1: Test Case Equations

Paramater	CMRAC	CMRAC-CO
Reference Dynamics	Equation (3.3)	Equation (3.2)
Observer Dynamics	Equation (3.51)	Equation (3.51)
Reference Error	$e_m^o = x_p - x_m^o$	$e_m = x_p - x_m$
Observer Error	$e_o = x_o - x_p$	$e_o = x_o - x_p$
Input	$u = \theta x_p + r$	$u = \theta x_o + r$
Update Laws	Equation (3.71)	Equation (3.55)

The simulations have two distinct regions of interest, with Region 1 denoting the first 4 seconds, Region 2 denoting the 4 sec to 15 sec range. In Region 1, the adaptive system is subjected to non–zero initial conditions in the state and the reference input is zero. At $t = 4$ sec, the beginning of Region 2, a filtered step input is introduced. Figures 3-7 and 3-8 illustrate the response of the CMRAC–CO adaptive system over

Table 3.2: Simulation Parameters

Paramater	Value
a_p	1
k_p	1
a_m	-1
k_m	1
ℓ	-10
γ	100
η	1

0 to 15 seconds, with x_m, x, and e_m indicated in Figure 3-7, and u, $\Delta u/\Delta t$, θ and $\hat{\theta}$ indicated in Figure 3-8. The addition of sensor noise makes the output x_p not differentiable and therefore we use the discrete difference function Δ to obtain the discrete time derivative of the control input, where

$$\frac{\Delta u}{\Delta t} \triangleq \frac{u(t_{i+1}) - u(t_i)}{t_{i+1} - t_i}, \qquad t_{i+1} - t_i = 0.01.$$

In both cases, the resulting performance is compared with the classical CMRAC system. The first point that should be noted is a satisfactory behavior in the steady-state of the CMRAC–CO adaptive controller. We note a significant difference between

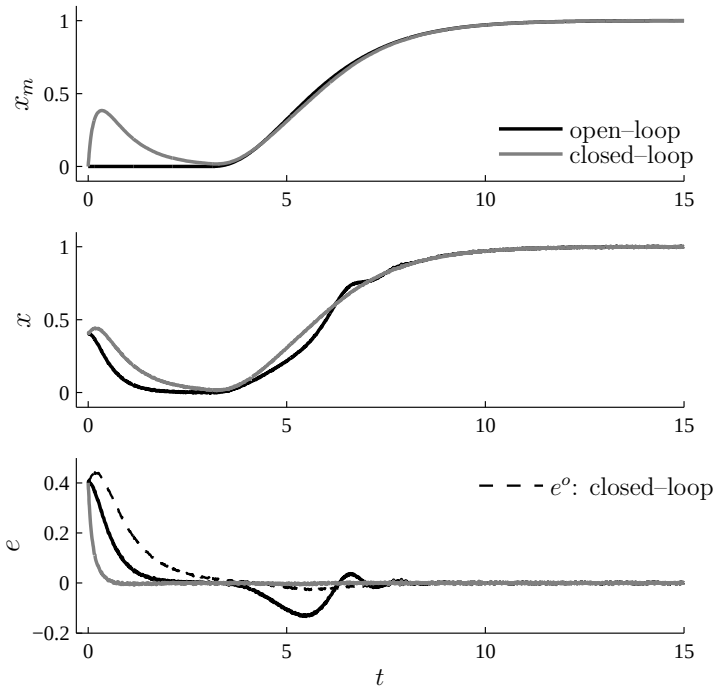

Figure 3-7: (top) reference model trajectories x_m, (middle) state x, and (bottom) model following e.

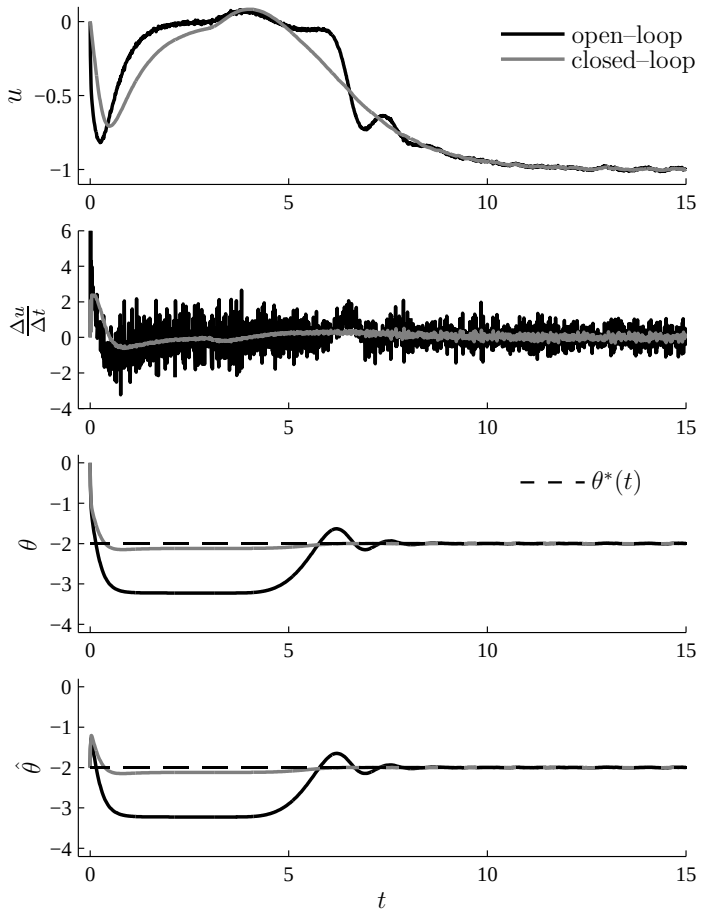

Figure 3-8: (top) Control input u, (middle–top) discrete rate of change of control input $\Delta u/\Delta t$, (middle–bottom) adaptive parameter $\theta(t)$ and (bottom) adaptive parameter $\hat{\theta}(t)$.

the responses of CMRAC–CO and CMRAC systems, which pertains to the use of filtered regressors in CMRAC–CO. An examination of $\Delta u/\Delta t$ in Figure 3-8 clearly illustrates the advantage of CMRAC–CO.

3.5.5 Comments on CMRAC and CMRAC–CO

As discussed in the Introduction, combining indirect and direct adaptive control has always been observed to produce desirable transient response in adaptive control. While the above analysis does not directly support the observed transient improvements with CMRAC, we provide a few speculations below: The free design parameter ℓ in the identifier is typically chosen to have eigenvalues faster than the plant that is being controlled. Therefore the identification model following error e_i converges rapidly and $\hat{\theta}(t)$ will have smooth transients. It can be argued that the desirable transient properties of the identifier pass on to the direct component through the tuning law, and in particular ϵ_θ.

3.6 CRMs in other Adaptive Systems

While CRMs can be traced to [49] in the context of direct model reference adaptive control, such a closed loop structure has always been present in, adaptive observers, tuning function designs, and in a similar fashion in adaptive control of robots. These are briefly described in the following sections.

3.6.1 Adaptive Backstepping with Tuning Functions

The control structure presented here is identical to that presented in [37, §4.3]. Consider the unknown system

$$\begin{aligned} \dot{x}_1 &= x_2 + \varphi_1(x_1)^T\theta^* \\ \dot{x}_1 &= x_3 + \varphi_2(x_1, x_2)^T\theta^* \\ &\vdots \\ \dot{x}_{n-1} &= x_n + \varphi_{n-1}(x_1, \ldots, x_{n-1})^T\theta^* \\ \dot{x}_n &= \beta(x)u + \varphi_n(x)^T\theta^* \end{aligned} \tag{3.72}$$

where θ^* is an unknown column vector, $\beta(x)$ is known and invertible, the φ_i are known, x is the state vector of the scalar x_i and the goal is to have $y = x_1$ follow a desired n times differentiable y_r. The control law propped in [37] is of the form

$$u = \frac{1}{\beta(x)}\left(\alpha_n + y_r^{(n)}\right) \tag{3.73}$$

with an update law

$$\dot{\theta} = \Gamma W z \tag{3.74}$$

where $\Gamma = \Gamma^T > 0$ is the adaptive tuning parameter, z is the transformed state error, and $W = \tau_n(z, \theta)$ with τ_i and the α_i, $1 \leq i \leq n$ defined in (3.76) in the Appendix along with the rest of the control design. The closed loop system reduces to

$$\dot{z} = A_z(z, \theta, t)z + W(z, \theta, t)\tilde{\theta} \tag{3.75}$$

where $\tilde{\theta} = \theta - \theta^*$ and

$$A_z = \begin{bmatrix} -c_1 & 1 & 0 & \cdots & 0 \\ -1 & -c_2 & 1+\sigma_{23} & \cdots & \sigma_{2n} \\ 0 & -1-\sigma_{23} & \ddots & \ddots & \vdots \\ \vdots & \vdots & \ddots & \ddots & 1+\sigma_{n-1,n} \\ 0 & -\sigma_{2n} & \cdots & -1-\sigma_{n-1,n} & -c_n \end{bmatrix}$$

where $\sigma_{ik} = -\frac{\partial \alpha_{i-1}}{\partial \theta}\Gamma w_k$. The c_i are free design parameters that arise in the definition of the α_i as defined below

$$\begin{aligned}
z_i =& x_i - y_r^{(i-1)} - \alpha_{i-1} \\
\alpha_i =& - z_{i-1} - c_i z_i - w_i^T \theta + \sum_{k=1}^{i-1} \left(\frac{\partial \alpha_{i-1}}{\partial x_k} + \frac{\partial \alpha_{i-1}}{\partial y_r^{(k-1)}} y_r^{(k)} \right) \\
& + \frac{\partial \alpha_{i-1}}{\partial \theta}\Gamma \tau_i + \sum_{k=2}^{i-1} \frac{\partial \alpha_{k-1}}{\partial \theta}\Gamma w_i z_k \\
\tau_i =& \tau_{i-1} + w_i z_i \\
w_i =& \varphi_i - \sum_{k=1}^{i-1} \frac{\partial \alpha_{i-1}}{\partial x_k}\varphi_k.
\end{aligned} \tag{3.76}$$

Notice that the $-c_i$ act in the same way as the ℓ in the simple adaptive system first presented in the reference model in (3.2). They act to close the reference trajectories with the plant state. The above system also results in similar L-2 norms for the z error state. Consider the Lyapunov candidate

$$V(z(t), \tilde{\theta}(t)) = \frac{1}{2} z^T z + \frac{1}{2} \tilde{\theta}^T \Gamma^{-1} \tilde{\theta} \tag{3.77}$$

which results in a negative semidefinite derivative $\dot{V} \leq -c_0 \|z\|^2$ where $c_0 = \min_{1 \leq i \leq n}(c_i)$. Thus we can integrate $-\dot{V}$ to obtain the following bound on the L-2 norm of z

$$\|z(t)\|_{L_2}^2 \leq \frac{V(0)}{c_0}. \tag{3.78}$$

It is addressed in [37, §4.4.1] that while it may appear that increasing c_0 uniformly decreases the L-2 norm of z, choosing c_i to be a large can result in large $z(0)$. The authors then provide a method for initializing the z dynamics so that $z(0) = 0$. We have already discussed why this may not be possible in a real system.

3.6.2 Adaptive Control in Robotics

The control structure presented here is taken directly from [73, §9.2]. Consider the dynamics of a rigid manipulator

$$H(q)\ddot{q} + C(q, \dot{q}) + g(q) = \tau \tag{3.79}$$

where q is the joint angle, and τ is the torque input. It is assumed that the system can be parameterized as

$$Y(q, \dot{q}, \dot{q}_r, \ddot{q}_r)a = H(q)\ddot{q}_r + C(q, \dot{q})\dot{q}_r + g(q) \tag{3.80}$$

where q_r is a twice differentiable reference signal, Y is known and a is an unknown vector. The control law is chosen as

$$\tau = Y\hat{a} - k_d s \quad \text{and} \quad \dot{\hat{a}} = -\Gamma Y^T s. \tag{3.81}$$

Then, defining the desired dynamics trajectory as q_d, the reference dynamics of the system are created by

$$\dot{q}_r = \dot{q}_d - \lambda \tilde{q} \tag{3.82}$$

where $\tilde{q} = q - q_d$ and

$$s = \dot{q} - \dot{q}_r = \dot{\tilde{q}} + \lambda \tilde{q}. \tag{3.83}$$

The stability of the above system can be verified with the following Lyapunov candidate,

$$V = \frac{1}{2}\left(s^T H s + \tilde{a}^T \Gamma^{-1} \tilde{a}\right).$$

Differentiating and using the property that $\dot{H} = C + C^T$ we have that

$$\dot{V} = -s^T k_d s. \tag{3.84}$$

We note that λ has a similar role in this control structure as the ℓ in the CRM. The desired trajectory is q_d (like x_m^o in our examples), however the adaptive parameter is updated by the composite variable s instead of directly adjusted by the true reference error.

We now conjecture as to why closed-loop reference models have not been studied in direct adaptive control until recently. In the two cases of nonlinear adaptive control, closed reference trajectory errors are used to update the adaptive controller. This is performed in the tuning function approach through the selection of the c_i and in the adaptive robot control example with λ and the creation of the composite variable s. In both cases the stability of the system necessitates the introduction of these variables. In contrast, in model reference adaptive control, stability is derived from the inherent stability of the reference model and hence any addition of new variables becomes superfluous. When no reference model is present, closing the loop on the reference trajectory becomes necessary. With the recent focus on improving transients in adaptive systems, CRM now has a role in MRAC. And as pointed out in this chapter improved transients can result with CRM without introducing peaking by choosing the ratio $|\ell|/\gamma$ carefully.

3.7 Conclusions

An increasingly oscillatory response with increasing adaptation gain is a transient characteristic that is ubiquitous in all adaptive systems. Recently, a class of adaptive systems has been investigated with closed-loop reference models where such oscillatory response can be curtailed. In this paper, a detailed analysis of such adaptive systems is carried out. It is shown through the derivation of analytical bounds on both states of the adaptive system and on parameter derivatives that a phenomenon of peaking can

occur with CRMs and that this phenomenon can be curtailed through a combination of design and analysis, with the peaking exponent reduced from 0.5 to zero. In particular, it is shown that bounds on the parameter derivatives can be related to bounds on frequencies and corresponding amplitudes, thereby providing an analytical basis for the transient performance. This guarantees that the resulting adaptive systems have improved transient characteristics with reduced or no oscillations even as the adaptation gains are increased. CRMs are shown to be implicitly present in other problems including adaptive nonlinear control and a class of problems in robotics.

Chapter 4

Closed-loop Reference Models in SISO Adaptive Control

4.1 Introduction

Recently a class of adaptive controllers with *Closed–loop Reference Models* (CRM) for states accessible control has been proposed [21, 22, 24, 46]. The main feature of this class is the inclusion of a Luenberger gain which feeds back the tracking error into the reference model. Without the Luenberger gain the CRM reduces to the *Open–loop Reference Model* (ORM) which is used in classical adaptive control [32,61]. Reference [46] introduces the concept of the CRM. In references [21,22,24] the stability and robustness properties of the CRM based adaptive system, and more importantly, an improved transient response were established for the case when state variables are accessible. The transient response was quantified through the use of $\mathcal{L}_2$ norms of the model following error as well as the rate of control input. In [21, 22, 24], it was shown that the extra design freedom in the adaptive system in the form of the Luenberger gain allowed this improvement. Others recent works on states accessible CRM adaptive control can be found in [74, 75].

This chapter addresses the next step in the design of adaptive systems, which is the case when only outputs are available for measurement rather than the entire state. It is shown that even with output feedback, the resulting CRM–based adaptive systems are first and foremost stable, and exhibit an improved transient response. As in the case when states are accessible, it is shown that this improvement is possible due to the suitable choice of the Luenberger gain. Unlike the approach in [45], the classical model reference adaptive control structure is used here. Also, our focus here is only on single-input single-output systems.

Using CRMs has two advantages over ORMs: 1) The reference model need not be *Strictly Positive Real* (SPR) for CRM systems, and need only have the same number of poles and zeros as its ORM counter part; 2) In CRM systems the reference model, filters and Luenberger gain can be chosen so that the error transfer function used in the update law is SPR and has arbitrarily fast poles and zeros. While the stability and performance bounds are given for arbitrary reference models, we show in Examples 1

and 2 how one can explicitly obtain error transfer functions of the form

$$k\frac{s^{m-1}+b_1s^{m-2}+\cdots b_{m-1}}{s^m+a_1s^{m-1}+\cdots+a_m}\triangleq k\mathcal{W}'(s) \tag{4.1}$$

where m is the relative degree of the plant to be controlled, s is the differential operator, k is the high–frequency gain which is unknown but with known sign, and the a_i, b_i are free to be choose so long as $\mathcal{W}'(s)$ is SPR.

Another contribution of this work comes by way of the performance analysis technique used. When studying the stability of output feedback adaptive systems non–minimal state space representations of the model following error are constructed so that it can be shown that *all* signals in the system are bounded. After stability is obtained, the performance analysis comes by way of studying the behavior of a minimal representation of the adaptive system. The analysis is no longer hindered by the unknown eigenvalues of the non–observable states in the error equation. It is precisely this technique that allows us to extend the results of transient response analysis from the states accessible case to the output feedback case, where we will show that we have complete control over the location of the eigenvalues of the minimal system.

This chapter is organized as follows. Section II contains the notation. In Section III the control problem is defined. Section IV contains the analysis of the ORM (classical) relative degree 1 case. Section V and VI contain the analysis of the CRM relative degree 1 and 2 cases respectively. Section VII analysis the arbitrary relative degree case, and Section VIII closes with our conclusions.

4.2 Notation

All norms unless otherwise stated are the Euclidean norm and enduced Euclidean norm. Let $\mathcal{PC}_{[0,\infty)}$ denote the set of all bounded piecewiese continuous signal.

Definition 4.1. Let $x, y \in \mathcal{PC}_{[0,\infty)}$. The big O–notation, $y(t) = O[x(t)]$ is equivalent to the existence of constants $M_1, M_2 > 0$ and $t_0 \in \mathbb{R}^+$ such that $|y(t)| \leq M_1 |x(t)| + M_1 \ \forall t \geq t_0$.

Definition 4.2. Let $x, y \in \mathcal{PC}_{[0,\infty)}$. The small o–notaion, $y(t) = o[x(t)]$ is equivalent to the existence of constants $\beta(t) \in \mathcal{PC}_{[0,\infty)}$ and $t_0 \in \mathbb{R}^+$ such that $|y(t)| = \beta(t)x(t) \ \forall t \geq t_0$ and $\lim_{t\to\infty} \beta(t) = 0$.

Definition 4.3. Let $x, y \in \mathcal{PC}_{[0,\infty)}$. If $y(t) = O[x(t)]$ and $x(t) = O[y(t)]$. Then x and y are said to be equivalent and denoted as $x(t) \sim y(t)$.

Definition 4.4. Let $x, y \in \mathcal{PC}_{[0,\infty)}$. x and y are said to grow at the same rate if $\sup_{t\leq\tau} |x(\tau)| \sim \sup_{t\leq\tau} |y(\tau)|$.

Definition 4.5. The prime notation is an operator that removes the high frequency gain from a transfer function

$$\mathcal{W}(s) \triangleq k\frac{s^{m-1}+b_1s^{m-2}+\cdots b_{m-1}}{s^m+a_1s^{m-1}+\cdots+a_m}.$$

so that

$$\mathcal{W}'(s) \triangleq \frac{\mathcal{W}(s)}{k},$$

Just as was done in (4.1).

4.3 The Control Problem

Consider the *Single Input Single Output* (SISO) system of equations

$$y(t) = W(s)u(t) \tag{4.2}$$

where $u \in \mathbb{R}$ is the input, $y \in \mathbb{R}$ is the measurable output, and s the differential operator. The transfer function of the plant is parameterized as

$$W(s) \triangleq k_p \frac{Z(s)}{P(s)} \triangleq k_p W'(s) \tag{4.3}$$

where k_p is a scalar, and $Z(s)$ and $P(s)$ are monic polynomials with $\deg(Z(s)) < \deg(P(s))$. The following assumptions will be made throughout.

Assumption 4.1. $W(s)$ is minimum phase.

Assumption 4.2. The sign of k_p is known.

Assumption 4.3. The relative degree of $W(s)$ is known.

4.4 Classical $n^* = 1$ case (ORM $n^* = 1$)

The goal is to design a control input u so that the output y in (4.2) tracks the output y_m of the reference system

$$y_m(t) = W_m(s)r(t) \triangleq k_m \frac{Z_m(s)}{P_m(s)} r(t) \tag{4.4}$$

where k_m is a scalar and $Z_m(s)$ and $P_m(s)$ are monic polynomials with $W_m(s)$ relative degree 1. Just as before we use the prime notation from Definition 4.5

$$k_m W'_m(s) = W_m(s). \tag{4.5}$$

Assumption 4.4. $W'_m(s)$ is *Strictly Positive Real* (SPR).

The previous assumption can be relaxed by using pre–filters in the adaptive law, similar to what will be done in the relative degree 2 controller. This increased generalization though is not necessary for our discussion.

The structure of the adaptive controller is now presented:

$$\dot{\omega}_1(t) = \Lambda\omega_1 + b_\lambda u(t) \tag{4.6}$$
$$\dot{\omega}_2(t) = \Lambda\omega_2 + b_\lambda y(t) \tag{4.7}$$
$$\omega(t) \triangleq [r(t),\ \omega_1^T(t),\ y(t),\ \omega_2^T(t)]^T \tag{4.8}$$
$$\theta(t) \triangleq [k(t),\ \theta_1^T(t),\ \theta_0(t),\ \theta_2^T(t)]^T \tag{4.9}$$
$$u = \theta^T(t)\omega \tag{4.10}$$

where $\Lambda \in \mathbb{R}^{(n-1)\times(n-1)}$ is Hurwitzx, $b_\lambda \in \mathbb{R}^{n-1}$, $\hat{k} \in \mathbb{R}$, $\omega_1, \omega_2 \in \mathbb{R}^{n-1}$, and $\theta \in \mathbb{R}^{2n}$ is adaptive gain vector with $k(t) \in \mathbb{R}$, $\theta_1(t) \in \mathbb{R}^{n-1}$, $\theta_2(t) \in \mathbb{R}^{n-1}$ and $\theta_0(t) \in \mathbb{R}$. The update law for the adaptive parameter is then defined as

$$\dot{\theta}(t) = -\gamma \text{sign}(k_p) e_y \omega, \tag{4.11}$$

where $e_y = y - y_m$.

Before stability is proved, a discussion on parameter matching is needed. Let $\theta_c \triangleq [k_c,\ \theta_{1c}^T,\ \theta_{0c},\ \theta_{2c}^T]^T$ be a constant vector. When $\theta(t) = \theta_c$ the forward loop and feedback loop take the form

$$\frac{\lambda(s)}{\lambda(s) - C(\theta_c; s)} \quad \text{and} \quad \frac{D(\theta_c; s)}{\lambda(s)}.$$

For simplicity we choose $\lambda(s) = Z_m(s)$, but note that this is not necessary and the stability of the adaptive system will still hold. The closed loop system is now of the form

$$y(t) = W_{cl}(\theta_c; s) r(t)$$

with

$$W_{cl}(\theta_c; s) \triangleq \frac{k_c k_p Z(s) Z_m(s)}{(Z_m(s) - C(\theta_c; s))P(s) - k_p Z(s) D(\theta_c; s)}.$$

From the Bezout Identity, a $\theta^{*T} \triangleq [k^*,\ \theta_1^{*T},\ \theta_0^*,\ \theta_2^{*T}]^T$ exists such that $W_{cl}(\theta^*; s) = W_m(s)$.

Therefore,

$$y(t) = k_p W'_m(s)(\phi^T(t)\omega(t) + k^* r(t)) \tag{4.12}$$

and

$$e_y(t) = k_p W'_m(s)\phi(t)\omega(t), \tag{4.13}$$

where $\phi(t) = \theta(t) - \theta^*(t)$ and $k^* = k_m/k_p$.

4.4.1 Stability for $n^* = 1$

The plant in (4.3) can be represented by the unknown quadruple, (A_p, b_p, c_p, k_p)

$$\dot{x} = A_p x + b_p u; \quad y = k_p c_p^T x \tag{4.14}$$

where

$$k_p c_p^T (sI - A_p) b_p = W(s).$$

In general one does not need to keep the high frequency gain as a separate variable when writing the transfer function dynamics in state space form. In the context of adaptive control however, the sign of k_p is important in proving stability and is therefore always singled out from the rest of the dynamics. Using (4.14), the dynamics in (4.12) can be represented as

$$\dot{x} = A_{mn} x + b_{mn}(\phi^T(t)\omega + k^* r); \quad y = k_p c_{mn}^T x \tag{4.15}$$

where

$$A_{mn} = \begin{bmatrix} A_p + b_p \theta_0^* k_p c_p^T & b_p \theta_1^{*T} & b_p \theta_2^{*T} \\ b_\lambda \theta_0^* k_p c_p^T & \Lambda + b_\lambda \theta_1^{*T} & b_\lambda \theta_2^{*T} \\ b_\lambda k_p c_p^T & 0 & \Lambda \end{bmatrix}$$

$$b_{mn} = \begin{bmatrix} b_p \\ b_\lambda \\ 0 \end{bmatrix}, \quad c_{mn} = \begin{bmatrix} c_p \\ 0 \\ 0 \end{bmatrix} \text{ and } x \triangleq \begin{bmatrix} x_p \\ \omega_1 \\ \omega_2 \end{bmatrix}$$

with the reference model having an equivalent non–minimal representation

$$\dot{x}_{mn} = A_{mn} x_{mn} + b_{mn} k^* r; \quad y_m = k_p c_{mn}^T x_{mn}$$

with the property that

$$k_p c_{mn}^T (sI - A_{mn}) b_{mn} = k_p W_m'(s).$$

The non–minimal error vector is defined as $e_{mn} = x - x_{mn}$ and satisfies the following dynamics

$$\dot{e}_{mn} = A_{mn} e_{mn} + b_{mn} \phi^T \omega; \quad e_y = k_p c_{mn}^T e_{mn}. \tag{4.16}$$

Theorem 4.1. *Following Assumptions 4.1-4.4, the plant in* (4.2) *with the reference model in* (4.4)*, controller in* (4.10) *and the update law in* (4.11) *are globally stable with the model following error asymptotically converging to zero.*

Proof. See [61, §5.3]. □

4.5 CRM $n^* = 1$

In the case of ORM adaptive control, the reference model only receives one input and is unaffected by the plant state trajectory. In order to facilitate the use of a Luenbereger feedback gain ℓ into the reference model, the reference model is chosen as

$$\dot{x}_m = A_m x_m + b_m k_m r + \ell(y - y_m), \quad y_m = c_m^T x_m \tag{4.17}$$

where (A_m, b_m, c_m^T) is an m dimensional system in observer canonical form with $c_m^T = [0 \ \dots \ 0 \ 1]$ and satisfying

$$c_m^T(sI - A_m)b_m k_m = W_m(s).$$

$y_m(t)$ is now related to the reference command $r(t)$ and model following error $e_y(t)$ as

$$y_m(t) = W_m(s)r(t) + W_\ell(s)(y(t) - y_m(t)) \tag{4.18}$$

where

$$W_\ell(s) \triangleq k_\ell \frac{Z_\ell(s)}{P_m(s)}, \tag{4.19}$$

and $k_\ell \in \mathbb{R}$ along with the $m-1$ order monic polynomial $Z_\ell(s)$ are a function of ℓ and free to choose. Subtracting (4.18) from (4.12) results in the following differential relation

$$e_y = k_p W_e'(s)\phi^T\omega \tag{4.20}$$

where

$$W_e'(s) \triangleq \frac{Z_m(s)}{P_m(s) - k_\ell Z_\ell(s)}. \tag{4.21}$$

Lemma 4.1. *An ℓ can be chosen such that $W_e'(s)$ is SPR for any $n^* = 1$ and minimum phase transfer function $W_m'(s)$.*

Proof. The product $k_\ell Z_\ell(s)$ a polynomial of order $n-1$ with $n-1$ degrees of freedom through ℓ. $P_m(s)$ is a monic polynomial of degree n. Therefore, $P_m(s) - k_\ell Z_\ell(s)$ is a monic polynomial of order n with $n-1$ degrees of freedom determined by ℓ. Thus for any $Z_m(s)$ the roots of $W_e'(s)$ can be placed freely in the closed left–half plane such that $W_e'(s)$ is SPR. □

Let

$$A_e = A_{mn} + G\ell k_p c_{mn}^T \tag{4.22}$$

where G transforms x_m to the controllable subspace in x_{mn}, which always exist [34]. The non–minimal error dynamics therefore take the form

$$\dot{e}_{mn}(t) = A_e e_{mn}(t) + b_{mn}\phi(t)\omega(t). \tag{4.23}$$

Remark 4.1. It is worth noting that in the construction of the minimal and non–minimal systems the location of the gains k_p and k_m switch from being located at the input to the output. The non–minimal systems is never created and thus need not be realized. Therefore, the influence of k_p whether it be on the input or output matrix of the state space does not matter. For the case of the minimal reference model in (4.17) it is critical however that k_m appears at the input of the system. This is done on purpose so that given the canonical form of c_m the ℓ in (4.17) completely determines the zeros and high frequency gain of $W_\ell(s)$ in (4.19).

Theorem 4.2. *Following Assumptions 4.1-4.3 and ℓ chosen as in Lemma 4.1, the plant in* (4.2) *with the reference model in* (4.17)*, controller in* (4.10) *and the up-*

date law in (4.11) *are globally stable with the model following error asymptotically converging to zero.*

Proof. Given that $W'_e(s)$ is SPR, there exists a $P_e = P_e^T > 0$ such that

$$A_e^T P_e + P_e A_e = -Q_e \text{ and } P_e b_{mn} = c_{mn}. \tag{4.24}$$

where $Q_e = Q_e^T > 0$. Thus

$$V = e_{mn}^T P_e e_{mn} + \frac{\phi^T \phi}{\gamma \left| k_p \right|} \tag{4.25}$$

is a Lyapunov function with derivative $\dot{V} = -e_{mn}^T Q_e e_{mn}$. Barbalat Lemma ensures the asymptotic convergence of e_{mn} to zero. □

4.5.1 Performance

Now that we have proved stability we can return to a minimal representation of the error dynamics in (4.20) which is

$$\dot{e}_m = A_\ell e_m + b_m k_p \phi^T \omega, \quad e_y = c_m^T e_m; \tag{4.26}$$

where the all the eigen–values of A_ℓ are the roots to $P_m(s) - k_\ell Z_\ell(s)$, as can be seen from (4.21). Recall the Anderson version of KY Lemma;

$$A_\ell^T P + P A_\ell = -g g^T - 2\mu P; \quad P b_m = c_m \tag{4.27}$$

where

$$\mu \triangleq \min_i \left| \lambda_i(A_\ell) \right|, \quad i = 1 \text{ to } m. \tag{4.28}$$

The following performance function

$$V_p = e_m^T P e_m + \frac{\phi^T \phi}{\gamma \left| k_p \right|} \tag{4.29}$$

has a time derivative

$$\dot{V}_p \leq -2\mu e_m^T P e_m. \tag{4.30}$$

From (4.30) it directly follows that

$$\| e_y(t) \|_{L_2}^2 \leq \frac{1}{2\mu} \left(\frac{\lambda_{\max}(P)}{\lambda_{\min}(P)} \| e(0) \|^2 + \frac{1}{\gamma \left| k_p \right|} \frac{\| \phi(0) \|^2}{\lambda_{\min}(P)} \right). \tag{4.31}$$

Example 4.1. The transfer function $W'_e(s)$ must be SPR, therefore, the poles of $W'_e(s)$ are limited by the location of its zeros. The order of A_m however is free to choose so long as $m \geq 1$, thus we can choose $m = 1$. Therefore making

$$W_m(s) = k_m \frac{1}{s + a_m}$$

where $b_m = k_m$ and $A_m = -a_m$. The closed loop reference model transfer function therefore is

$$W_e(s) = k_m \frac{1}{s + a_m + l} \tag{4.32}$$

where $\ell = -l$, $l > 0$. From (4.32), it is clear that there are no zeros limiting the location of the closed loop pole.

Further more, the Anderson Lemma reduces to the trivial solution of $P = 1$, $g = 0$, and $\mu = a_m + l$. Since there are no zeros to worry about $W_e'(s)$ is SPR for all l. Therefore, μ can can be chosen arbitrarily. The bound in (4.31) for this example simplifies to

$$\|e_y(t)\|_{L_2} \leq \frac{1}{2(a_m + \ell)} \left(\|e(0)\|^2 + \frac{\|\phi(0)\|^2}{\gamma |k_p|} \right). \tag{4.33}$$

Remark 4.2. The use of CRMs has two advantages compared to the use of ORMs. The first is that the reference model need not be SPR a priori, but only needs to be of appropriate relative degree. There are several methods of dealing with non–SPR reference models for $n^* = 1$, but these methods require the use of pre–filters [39], or augmented error approaches (see [61], and Section 4.7).

The second advantage is illustrated in Example 4.1. Using this approach, a reference model can be chosen such that it has no zeros. When this is done and a CRM is used, the location of the slowest pole of the error model dynamics is free to choose. When using ORMs, the location of the slowest eigenvalue of the closed–loop error model is not free to choose, as speeding up the reference model eigenvalues without the use of CRMs will require the use of high–gain feedback which is equivalent to $\|\theta^*\|$ being large if the open–loop plant has slow eigenvalues.

4.6 CRM SISO $n^* = 2$

Consider the dynamics in (4.2) where the relative degree of the transfer function in (4.3) is now 2 instead of 1 and the reference to be followed is the CRM in (4.17). The control input in (4.10) will no longer lead to stable adaptation and must be adjusted as

$$u(t) = \dot{\theta}^T(t)\zeta(t) + \theta^T(t)\omega(t) \tag{4.34}$$

$$\dot{\theta}(t) = -\operatorname{sign}(k_p) e_y(t)\zeta(t)^T \tag{4.35}$$

where $\zeta(t)$ is a filtered version of the regressor vector ω and defined as

$$\zeta(t) = A^{-1}(s)\omega(t) \text{ where } A(s) = s + a. \tag{4.36}$$

Using the same reference model as in (4.17), the error $e_y(t)$ now takes the form

$$e_y(t) = k_p W_e'(s) A(s) \phi^T(t)\zeta(t). \tag{4.37}$$

With ℓ and $A(s)$ chosen such that the transfer function $W_e'(s)A(s)$ is SPR the CRM adaptive controller for $n^* = 2$ is stable.

4.6.1 Performance

The same analysis performed in the previous section can be used to analyze the $n^* = 2$ case. The minimum eigenvalue of $W'_e(s)A(s)$ in (4.37) along with γ control the $\mathcal{L}_2$ norm of e_y. As in the previous example, a reference model with no zeros that is relative degree 2 can be chosen. Then, the zeros of $W'_e(s)A(s)$ are completely determined by $A(s)$ and the poles are freely placed with ℓ. Thus any SPR transfer function of order 2 can be created with an arbitrarily fast slowest eigenvalue.

4.7 CRM Arbitrary n^*

The adaptive controller for $n^* = 2$ is special given that we have access to $\dot{\theta}(t)$. Instead, for higher relative degrees it is common to use an augmented error approach, where by the original model following error e_y is not used to adjust the adaptive parameter, but an augmented error signal which does satisfy the SPR conditions needed for stability. The augmented error method used in this result is Error Model 2 as presented in [61, §5.4], with some changes to the notation.

For ease of exposition and clarity in presentation we present the k_p known and k_p unknown presentation in two sections.

4.7.1 Stability for known high frequency gain

We begin by replacing Assumption 2 with:
Assumption 4.2′. k_p is known.

Without loss of generality we choose $k_m = k_p = 1$ and the control input for the generic relative degree case reduces to

$$u(t) = r(t) + \overline{\theta}^T(t)\bar{\omega}(t) \tag{4.38}$$

where $\overline{(\cdot)}$ denotes the vectors,

$$\bar{\omega}(t) \triangleq [\omega_1^T(t),\ y(t),\ \omega_2^T(t)]^T \tag{4.39}$$

$$\overline{\theta}(t) \triangleq [\theta_1^T(t),\ \theta_0(t),\ \theta_2^T(t)]^T. \tag{4.40}$$

A feedforward time varying adaptive gain $k(t)$ is no longer needed and thus $r(t)$ has been removed from the regressor vector do to the fact that $k_p = k_m = 1$. The model following error then, satisfies the following differential relation

$$e_y = W'_e(s)\overline{\phi}^T\bar{\omega} \tag{4.41}$$

where the reader is reminded that the prime notation removes the high frequency gain from transfer functions, and since $k_m = k_p = 1$, $W'_e(s) = W_e(s)$. Similar to the use of $A(s)$ in (4.36) for the relative degree 2 case, a stable minimally realized filter

$F(s)$ with no zeros is used to generate the filtered regressor

$$\bar{\zeta} = F(s)I\bar{\omega} \tag{4.42}$$

where I is the $2n-1$ by $2n-1$ identity matrix, $F(s)$ designed with unity high frequency gain, and $F(s)$ and ℓ chosen so that

$$W_f'(s) \triangleq W_e'(s)F^{-1}(s) \tag{4.43}$$

is SPR.

Lemma 4.2. *For any stable $F(s)$ an ℓ can be chosen such that $W_f'(s)$ is SPR.*

Proof. The proof follows the same arguments as in Lemma 4.1. □

The tuning law for the arbitrary relative degree case uses an augmented error e_a, which is generated from the model following error e_y and an auxiliary error e_χ. Using the CRM in (4.17), the augmented and auxiliary error are defined as:

$$e_a \triangleq e_y + W_f'(s)\left(e_\chi - e_a\bar{\zeta}^T\bar{\zeta}\right) \tag{4.44}$$

$$e_\chi \triangleq \bar{\theta}^T\bar{\zeta} - F(s)\bar{\theta}^T\bar{\omega}. \tag{4.45}$$

A stable tuning law for the system is then defined as

$$\dot{\bar{\theta}} = -\gamma e_a\bar{\zeta}. \tag{4.46}$$

Theorem 4.3. *Following Assumptions 4.1, 4.2′ and 4.13, with ℓ chosen such that $W_f'(s)$ is SPR, the plant in* (4.2) *with the reference model in* (4.17)*, controller in* (4.38) *and update law in* (4.46) *are globally stable with the model following error e_y asymptotically converging to zero.*

Proof. The proof proceeds in 4 steps. First it is shown that $\bar{\theta}(t)$ and e_a are bounded and that $e_a, \dot{\bar{\theta}} \in \mathcal{L}_2$. Second, treating $\bar{\theta}(t)$ as a bounded time–varying signal, then all signals in the adaptive system can grow at most exponentially. Third, if it is assumed that the signals grow in an unbounded fashion, then it can be shown that y, ω_1 ω_2, $\bar{\omega}$, $\bar{\zeta}$ and u grow at the same rate. Finally, from the fact that $\dot{\bar{\theta}} \in \mathcal{L}_2$ it is shown that ω_2 and $\bar{\omega}$ do not grow at the same rate. This results in a contradiction and therefore, all signals are bounded and furthermore, $e_y(t)$ asymptotically converges to zero. Steps 1 and 4 are detailed below. Steps 1-3 follow directly from [61, §5.5] with little changes. Step 4 does involve a modification to the analysis which is addressed in detail next.

Step 1

Expanding the error dynamics in (4.44) and canceling like terms of $W_e'(s)\bar{\theta}^T\omega$ we have

$$e_a = -W_e'(s)\bar{\theta}^{*T}\bar{\omega} + W_f'(s)\left(\bar{\theta}^T\bar{\zeta} - e_a\bar{\zeta}^T\bar{\zeta}\right).$$

Adding and subtracting $W_f'(s)\bar{\theta}^{*T}\bar{\zeta}$ the equation becomes

$$e_a = W_f'(s)\left(\bar{\phi}^T\bar{\zeta} - e_a\bar{\zeta}^T\bar{\zeta}\right) + \delta(t) \tag{4.47}$$

where $\delta(t)$ is an exponentially decaying term do to initial conditions and defined as

$$\delta(t) = W_f'(s)\left(\bar{\theta}^{*T}\bar{\zeta}(t) - F(s)\bar{\theta}^{*T}\bar{\omega}(t)\right). \tag{4.48}$$

Breaking apart $\bar{\zeta}$ from its definition in (4.42) and noting that $\bar{\theta}^*$ now commutes with $F(s)$ we have that

$$\delta(t) = W_f'(s)\left(\bar{\theta}^{*T}\left(F(s) - F(s)\right)I\bar{\omega}\right). \tag{4.49}$$

Therefore, if the filter $F(s)$ is chosen to have the same initial conditions when constructing $\bar{\zeta}$ and e_χ then, $\delta = 0$ for all time. For this reason we ignore the affect of choosing different filter initial conditions. The interested reader can see how one can prove stability in augmented error approaches where $\delta(0) \neq 0$ [61, pg. 213], with the addition of an extra term in the Lyapunov function.

A non–minimal representation of e_a is given as

$$\dot{e}_{an} = A_e e_{an} + b_{an}\left(\bar{\phi}^T\bar{\zeta} - e_a\bar{\zeta}^T\bar{\zeta}\right), \quad e_a = c_{an}^T e_{an} \tag{4.50}$$

where

$$c_{an}^T(sI - A_e)^{-1}b_{an} \triangleq W_f'(s). \tag{4.51}$$

Given that $W_f(s)$ is SPR, there exists a $P_a = P_a^T > 0$ such that

$$A_e^T P_a + P_a A_e = -Q_a \text{ and } P_a b_{an} = c_{an}. \tag{4.52}$$

where $Q_a = Q_a^T > 0$.

Consider the Lyapunov candidate

$$V = e_{an}^T P_a e_{an} + \frac{\phi^T\phi}{\gamma} \tag{4.53}$$

Differentiating along the system dynamics in (4.50) and substitution of the tuning law from (4.46) results in

$$\dot{V} \leq -e_{an}^T Q_a e_{an} - 2e_a^2\bar{\zeta}^T\bar{\zeta}. \tag{4.54}$$

Therefore, $e_{an}, \bar{\theta} \in \mathcal{L}_\infty$ and $e_{an}, \dot{\bar{\theta}} \in \mathcal{L}_2$

Step 2

The plant dynamics can be expressed as

$$\dot{x} = A_{mn}x + b_{mn}(\bar{\phi}^T(t)\omega + r); \quad y = c_{mn}^T x \tag{4.55}$$

where with an appropriate choice of a C can be expressed as

$$\dot{x} = \left(A_{mn} + b_{mn}\bar{\phi}^T(t)C\right)x + b_{mn}r \tag{4.56}$$

From Step 1 it is known that $\bar{\phi}$ is bounded, and therefore x grows at most exponentially. Futhermore, for r piecewise continuous, x and $\bar{\zeta}$ are both piecewise continuous as well.

Step 3

If it is assumed that all signals grow in an unbounded fashion then it can be shown that

$$\sup_{\tau\leq t}|y(\tau)| \sim \sup_{\tau\leq t}\|\omega_1(\tau)\| \sim \sup_{\tau\leq t}\|\omega_2(\tau)\| \sim \sup_{\tau\leq t}\|\bar{\omega}\| \sim \sup_{\tau\leq t}\|\bar{\zeta}\| \sim \sup_{\tau\leq t}|u(\tau)| \tag{4.57}$$

[61, §5.5]

Step 4

Rewinting (4.45) in terms of $\bar{\omega}$ we have that

$$e_\chi \triangleq \bar{\theta}^T F(s) I\bar{\omega} - F(s)\bar{\theta}^T\bar{\omega} \tag{4.58}$$

and given that $\dot{\bar{\theta}} \in \mathcal{L}_2$ and $F(s)$ is stable the following holds

$$e_\chi(t) = o\left[\sup_{\tau\leq t}\|\bar{\omega}(\tau)\|\right]. \tag{4.59}$$

The above bound follows from the *Swapping Lemma* [61, Lemma 2.11]. From (4.46) and the fact that $\dot{\bar{\theta}} \in \mathcal{L}_2$ we have that $e_a\bar{\zeta} \in \mathcal{L}_2$. Given that $W_f'(s)$ is asymptotically stable, [61, Lemma 2.9] can be applied and it follows that

$$W_f'(s)\left((e_a\bar{\zeta})^T\bar{\zeta}\right) = o\left[\sup_{\tau\leq t}\|\bar{\zeta}(\tau)\|\right] \tag{4.60}$$

The plant output can be written in terms of the reference model and model following error as

$$\begin{aligned} y(t) =& y_m(t) + e_y(t) \\ =& W_m'(s)r(t) + \left(1 + W_\ell'(s)\right)e_y(t). \end{aligned}$$

Using (4.44), $e_y(t) = e_a - W_f'(s)\left(e_\chi - e_a\bar{\zeta}^T\bar{\zeta}\right)$ and the above equation expands as

$$y(t) = W_m'(s)r(t) + \left(1 + W_\ell'(s)\right)e_a - \left(1 + W_\ell'(s)\right)W_f'(s)\left(e_\chi - e_a\bar{\zeta}^T\bar{\zeta}\right).$$

Using (4.59) (4.60) and noting that $1 + W'_\ell(s)$ is asymptotically stable [61, Lemma 2.9] can be applied again and

$$y(t) = W'_m(s)r(t) + (1 + W'_\ell(s))\, e_a + o\left[\sup_{\tau\leq t}\|\bar{\zeta}(\tau)\|\right] + o\left[\sup_{\tau\leq t}\|\bar{\omega}(\tau)\|\right].$$

Given that r and e_a are piecewise continuous and bounded we finally have that

$$y(t) = o\left[\sup_{\tau\leq t}\|\bar{\omega}(\tau)\|\right]. \tag{4.61}$$

This contradicts (4.57) and therefore all signals are bounded. Furthermore, from (4.50) it now follows that $\dot{e}_{an}$ is bounded and given that $e_{an} \in \mathcal{L}_2$, from Step 1, it follows that e_{an} asymptotically converges to zero and therefore $\lim_{t\to\infty} e_a(t) = 0$. From (4.59) it follows that e_χ asymptotically converges to zero. Therefore, $\lim_{t\to\infty} e_y(t) = 0$. The above analysis differs from the analysis for the ORM output feedback adaptive control do to the fact that one can not a priori assume that $y_m(t)$ is bounded, do to the feedback of e_y into the reference model. □

4.7.2 Performance when k_p known

Just as in the $n^* = 1$ case, with stability proved a Lyapunov performance function can be studied that uses a minimal representation of the dynamics. That being said, consider the minimal representation of the dynamics in (4.47)

$$\dot{e}_{am} = A_\ell e_{am} + b_{am}\left(\bar{\phi}^T\bar{\zeta} - e_a\bar{\zeta}^T\bar{\zeta}\right), \quad e_y = c_{am}^T e_{am} \tag{4.62}$$

in observer canonical form so that $c_{am}^T = [0\ \ldots\ 0\ 1]$ and

$$c_{am}^T(sI - A_\ell)^{-1}b_{am} \triangleq W'_f(s)$$

Recall the Anderson version of KY Lemma;

$$A_\ell^T P_p + P_p A_\ell = -gg^T - 2\mu P_p; \quad P_p b_{am} = c_{am} \tag{4.63}$$

where μ is defined in (4.28). The following performance function

$$V_p = e_{am}^T P_p e_{am} + \frac{\bar{\phi}^T\bar{\phi}}{\gamma} \tag{4.64}$$

has a time derivative

$$\dot{V}_p \leq -2\mu e_{am}^T P_p e_{am} - 2e_a^2\bar{\zeta}^T\bar{\zeta}. \tag{4.65}$$

From (4.65) it directly follows that

$$\|e_a(t)\|_{L_2}^2 \leq \frac{1}{2\mu}\left(\frac{\lambda_{\max}(P_p)}{\lambda_{\min}(P_p)}\|e(0)\|^2 + \frac{1}{\gamma}\frac{\|\bar{\phi}(0)\|^2}{\lambda_{\min}(P_p)}\right) \tag{4.66}$$

and

$$\|\dot{\bar{\theta}}(t)\|_{L_2}^2 \leq \frac{1}{2}\left(\gamma^2\lambda_{\max}(P_p)\|e(0)\|^2 + \gamma\|\bar{\phi}(0)\|^2\right). \tag{4.67}$$

Ultimately we would like to compute the $\mathcal{L}_2$ norm of e_χ and e_y. Given that these norms will depend explicitly on the specific values of the filter and reference model, we perform that analysis in the following example.

Example 4.2. In this example we consider a relative degree 2 plant. The reference model is chosen as

$$W_m(s) = \frac{1}{s^2 + b_1 s + b_2} \tag{4.68}$$

and the filter is chosen as

$$F(s) = \frac{1}{s + f_1}. \tag{4.69}$$

The reference model gain is expanded as

$$\ell = \begin{bmatrix} -l_1 & -l_2 \end{bmatrix}^T. \tag{4.70}$$

Then

$$W_e(s) = \frac{1}{s^2 + (b_1 + l_1)s + (b_2 + l_2)} \tag{4.71}$$

and

$$W_f(s) = \frac{s + f_1}{s^2 + (b_1 + l_1)s + (b_2 + l_2)}. \tag{4.72}$$

Since, $k_p = k_m = 1$, then $W_m(s) = W'_m(s)$, $W_e(s) = W'_e(s)$ and $W_f(s) = W'_f(s)$. For stability to hold $W'_f(s)$ must be SPR and from (4.72) it is clear that the SPR condition can be satisfied by choosing ℓ and f_1 appropriately. More importantly though, we see that the slowest eignvalue of $W_f(s)$ can be arbitrarily placed and thus the μ in (4.28) can be arbitrarily increased.

$$\|e_\chi(t)\|_{\mathcal{L}_2}^2 \leq 3\left(\frac{e_\chi^2(0)}{2f_1} + \left(\frac{e_\chi^2(0)}{4f_1^2} + \frac{\|\bar{\omega}(t)\|_\infty^2}{f_1^3}\right)\|\dot{\bar{\theta}}(t)\|_{\mathcal{L}_2}^2\right) \tag{4.73}$$

A detailed proof of this expression is given in Appendix B.1. Furthermore, we have the following bound for the model following error

$$\|e_y(t)\|_{\mathcal{L}_2}^2 \leq 2\|e_a(t)\|_{\mathcal{L}_2}^2 + 2\|e_\zeta(t)\|_{\mathcal{L}_2}^2 \tag{4.74}$$

where

$$e_\zeta(t) \triangleq W_f(s)e_\chi(t) \tag{4.75}$$

can be bounded as

$$\|e_\zeta\|_{\mathcal{L}_2}^2 \leq 3m^2\left(\frac{e_\zeta^2(0)}{2\mu} + \left(\frac{e_\chi(0)^2}{4\mu f_1} + \frac{\|\bar{\omega}(t)\|_\infty^2}{\mu f_1^2}\right)\|\dot{\bar{\theta}}(t)\|_{\mathcal{L}_2}^2\right). \tag{4.76}$$

The bound in (4.76) is given in Appendix B.2.

Remark 4.3. Now we compare the norms in (4.73) and (4.76) for an ORM and CRM system and note that increasing both f_1 and μ decreases the two norms. For the ORM system $\ell = 0$, therefore μ is solely a function of b_1 and b_2 in (4.72). The coefficients b_1 and b_2 can not be arbitrarily changed without affecting the matching parameter vector $\bar{\theta}^*$. In the presence of persistence of excitation, $\bar{\theta}(t) \to \bar{\theta}^*$ and large $\bar{\theta}^*$ will directly imply a large control input. Furthermore, one can not arbitrarily change the reference model poles, as the reference model is a target behavior for the plant, in which case the control engineer may not want to track a reference system with arbitrarily fast poles. Therefore, given that b_1 and b_2 are not completely free to choose this also limits the value of f_1 as $W_f(s)$ must always be SPR. In the CRM case b_1 and b_2 can be held fixed and l_1, l_2 and f_1 can be adjusted so that the poles of $W_f(s)$ are arbitrarily fast and $W_f(s)$ is still SPR.Therefore, the added degree of freedom through ℓ in the CRM adaptive systems allows more flexibility in decreasing the $\mathcal{L}_2$ norm of e_y.

Remark 4.4. In the above, we have derived bounds on the $\mathcal{L}_2$ norm of the tracking error. That the same error has finite $\mathcal{L}_\infty$ bounds is easily shown using Lyapunov function arguments and the fact that projection algorithms ensure exponential convergence of the error to a compact set, similar to the analysis in [21, 22, 24].

4.7.3 Stability in the case of unknown high frequency gain

When k_p is unknown but with known sign as in Assumption 2, the control structure must include $k(t)$ into the adaptive vector as well as including $r(t)$ back into the regressor vector. Therefore, the controller take the form of (4.10), repeated here in for clarity,

$$u(t) = \theta^T(t)\omega(t).$$

The reference model is chosen as in (4.17) where $W_m(s)$ has the same relative degree as the plant to be controlled and thus the output error is

$$e_y(t) = k_p W'_e(s)\phi^T(t)\omega(t)$$

where $W_e(s)$ is of the same relative degree as the plant. A complete filtered regressor vector then is defined as

$$\zeta = F(s)I\omega \tag{4.77}$$

where I is the $2n$ by $2n$ identity matrix, the high frequency gain of $F(s)$ is unity, and $F(s)$ and ℓ chosen so that

$$W'_f(s) \triangleq W'_e(s)F(s)^{-1} \tag{4.78}$$

is SPR and $W_f(s) = k_m W'_f(s)$. In addition to the adaptive parameters in the control law however another adaptive parameter $k_\chi(t)$ is included whose parameter error is defined as

$$\psi \triangleq k_\chi(t) - k_p \tag{4.79}$$

with an update law shortly to be defined. The error equations for this system then are constructed as

$$e_a \triangleq e_y + W_f'(s)\left(k_\chi e_\chi - e_a\zeta^T\zeta\right) \tag{4.80}$$

$$e_\chi \triangleq \theta^T\zeta - F(s)\theta^T\omega. \tag{4.81}$$

The update law for the adaptive parameters is then chosen as

$$\dot{\theta}(t) = -\gamma \text{sign}(k_p) e_a \zeta \tag{4.82}$$

$$\dot{k}_\chi(t) = -\gamma e_a e_\chi. \tag{4.83}$$

Theorem 4.4. *Following Assumptions 1, 2 and 3, with ℓ chosen such that $W_f'(s)$ is SPR, the plant in (4.2) with the reference model in (4.17), controller in (4.10) and update law in (4.82)–(4.83) are globally stable with the model following error e_y asymptotically converging to zero.*

Proof. The entire proof would come in 4 parts just as in the proof of Theorem 5. We however only present a detailed proof of step 1 and then briefly present the other 3 steps.

Step 1

The boundedness of e_a, ϕ and ψ are now addressed. First consider the representation of (4.80)

$$e_a = W_e'(s)k_p\phi^T\omega + W_f'(s)\left(k_\chi e_\chi - e_a\zeta^T\zeta\right) + W_f'(s)(k_p e_\chi - k_p e_\chi)$$

where $k_p e_\chi$ has been added and subtracted from. Expanding $k_p e_\chi$, $W_f'(s)$ and ϕ we have

$$e_a = W_e'(s)k_p(\theta - \theta^*)^T\omega + W_f'(s)\left(\psi e_\chi - e_a\zeta^T\zeta\right) + W_e'(s)k_p F(s)^{-1}\left(\theta^T\zeta - F(s)\theta^T\omega\right).$$

Canceling like terms in $\theta^T\omega$, and adding and subtracting the term $W_f'(s)\theta^{*T}\zeta$ the expression reduces to

$$e_a = W_f'(s)\left(k_p\phi^T\zeta + \psi e_\chi - e_a\zeta^T\zeta\right) + \delta(t) \tag{4.84}$$

where δ is an exponentially decaying term defined as

$$\delta(t) = W_f'(s)k_p\left(\bar{\theta}^{*T}\left(F(s) - F(s)\right)I\bar{\omega}\right).$$

Therefore, if the filter $F(s)$ is chosen to have the same initial conditions when constructing ζ and e_χ, then $\delta = 0$ for all time. For this reason we ignore the affect of choosing different filter initial conditions. The interested reader can see how one can prove stability in augmented error approaches where $\delta(0) \neq 0$ [61, pg. 213], with the addition of an extra term in the Lyapunov function. Given that θ^* is constant and

the following holds. Now consider a non–minimal representation of e_a from (4.84) as

$$\begin{aligned} \dot{e}_{an} &= A_e e_{an} + b_{an}\left(k_p \phi^T \zeta + \psi e_\chi - e_a \zeta^T \zeta\right) \\ e_a &= c_{an}^T e_{an} \end{aligned} \tag{4.85}$$

where

$$c_{an}^T (sI - A_e)^{-1} b_{an} \triangleq W_f'(s). \tag{4.86}$$

Given that $W_f'(s)$ is SPR, there exists a $P_a = P_a^T > 0$ such that

$$A_e^T P_a + P_a A_e = -Q_a \text{ and } P_a b_{an} = c_{an}. \tag{4.87}$$

where $Q_a = Q_a^T > 0$.

Consider the Lyapunov candidate

$$V = e_{an}^T P_a e_{an} + \frac{\phi^T \phi}{\gamma \left|k_p\right|} + \frac{\psi^2}{\gamma} \tag{4.88}$$

Differentiating along the system dynamics in (4.50) and substitution of the tuning law from (4.46) results in

$$\dot{V} \leq -e_{an}^T Q_a e_{an} - 2 e_a^2 \zeta^T \zeta. \tag{4.89}$$

Therefore, $e_{an}, \theta, k_\chi \in \mathcal{L}_\infty$ and $e_{an}, \dot{\theta} \in \mathcal{L}_2$.

Step 2

Given that ϕ is bounded, then (4.15) can grow at most exponentially.

Step 3

The only difference between the k_p known and unknown case is the addition of $k(t)$ in the feedforward loop and $k_\chi(t)$ in the augmented error. Then, if we assume that signals in the system grow in an unbounded fashion and using the results from (4.57) it immediately follows that

$$\begin{aligned} \sup_{\tau \leq t} |y(\tau)| \sim \sup_{\tau \leq t} \|\omega_1(\tau)\| \sim \sup_{\tau \leq t} \|\omega_2(\tau)\| \sim \sup_{\tau \leq t} \|\bar{\omega}\| \sim \sup_{\tau \leq t} \|\bar{\zeta}\| \sim \sup_{\tau \leq t} \|\omega\| \ldots \\ \sim \sup_{\tau \leq t} \|\zeta\| \sim \sup_{\tau \leq t} |u(\tau)| \end{aligned} \tag{4.90}$$

where $\bar{\zeta}$ and $\bar{\omega}$ are defined in (4.42) and (4.39) respectively.

Step 4

Given that $\dot{\bar{\theta}} \in \mathcal{L}_2$ and $F(s)$ is stable the following holds

$$e_\chi(t) = o\left[\sup_{\tau \leq t} \|\omega(\tau)\|\right]. \tag{4.91}$$

Then, following the same steps as in Step 4 from the proof of Theorem 5 we can conclude that

$$y(t) = o\left[\sup_{\tau \leq t} \|\omega(\tau)\|\right]. \tag{4.92}$$

This contradicts (4.90) and therefore all signals are bounded. Furthermore, from (4.85) it now follows that $\dot{e}_{an}$ is bounded and given that $e_{an} \in \mathcal{L}_2$, from Step 1, it follows that e_{an} asymptotically converges to zero and therefore $\lim_{t\to\infty} e_a(t) = 0$. From (4.91) it follows that e_χ asymptotically converges to zero. Therefore, $\lim_{t\to\infty} e_y(t) = 0$. □

4.8 Conclusion

This work shows that with the introduction of CRMs the adaptive system can have improved transient performance in terms of reduction of the $\mathcal{L}_2$ norm of the model following error. Similar to previous work in [24], bounds on derivatives of key signals in the system, and trade–off between transients and learning remain to be addressed and is the subject of on–going investigation.

Chapter 5

Control Oriented Modeling of Very Flexible Aircraft

5.1 Introduction

The first investigations into the dynamics of a highly flexible aircraft came from the Daedalus Project, initiated in 1984 [13, 42]. The goal of this project was to push the limits of human powered flight while promoting engineering, science and education. Prior to the Daedalus Project the longest distance traveled by a human powered plane was 23 miles, a record set in 1979 with a flight across the English Channel [2]. Over the course of the project the distance record was broken several times and in 1988 *Daedalus 88* flew 73 miles over the Aegean Sea from Iraklion Air Force Base on Crete to Santorini.

Key results from the project were: an attempt to identify stability derivatives for a flexible aircraft using flight data [82], modeling the aeroelastic characteristics of a highly flexible aircraft [78], and tools for analyzing aerodynamic and structural loads on flexible–high–aspect–ratio wings under large deformation [15]. Van Schoor et al. [78] identified the importance of including the flexible states in the stability analysis as the flexible model predicted an unstable phugoid mode with the rigid model predicting a stable phugoid. Building on his work in [15] Drela designed ASWING [14], a software package used for the study and simulation of flexible aircraft undergoing arbitrarily large deformations.

The Daedalus Project, by design, was a segue to High Altitude Long Endurance (HALE) vehicles. The Helios aircraft, depicted in Figure 5-1, was developed under the *Environmental Research Aircraft and Sensor Technology* (ERAST) as a HALE class vehicle. The aircraft had two configurations specifically tailored to: 1) high altitude flight and 2) long endurance flight. On August 13^{th} 2001 Helios configuration–1 climbed to a record breaking altitude of 96,863 feet [65]. The second configuration did not have the same success however, and on June 26^{th} 2003 broke apart mid–flight during testing. Throughout the flight the aircraft encountered turbulence. After approximately 30 minutes of flight time a larger than expected wing dihedral formed and the aircraft began a slowly diverging pitch oscillation. The oscillations never

subsided and led to flight speeds beyond the design specifications for Helios. The loading on the aircraft compromised the structure of the aircraft and the skin of the aircraft pulled apart. One of the key recommendations that came from the flight mishap investigation was to, "Develop more advanced, multidisciplinary (structures, aeroelastic, aerodynamics, atmospheric, materials, propulsion, controls, etc) "time-domain" analysis methods appropriate to highly flexible, "morphing" vehicles" [65].

A large body of work on VFA modeling has come since the Helios flight mishap. Patil et al. [66] studied the open loop dynamics of a flying wing structure similar to that of Helios and found that flap positions used to trim the flexible aircraft differ greatly from those used to trim the rigid aircraft. The authors also captured instability in the phugoid mode which is present during large dihedral angles. Similar studies by Raghavan et al. [68] and Su et al. [76] confirmed this result. In order to validate the modeling approach presented by the authors in [76] the same authors have built an unmanned very flexible UAV called X–HALE with flight tests coming in the future [8, 9]. For a more comprehensive literature review see [71].

It is important to distinguish between VFA that can sustain large deviations from trim dihedral (or mode shape) and those aircraft that cannot sustain a morphed geometry and simply have structural dynamics on the order of the rigid body dynamics. To remove such ambiguities, in this paper, we refer to the former class as VFA and the latter as simply *Flexible Aircraft* (FA). The former class includes the Helios aircraft and the aircraft geometry of interest for this work.

The instability associated with VFA and large dihedral configurations has been thoroughly studied [19,66]. However, the mechanism which initiated the dihedral drift observed in the Helios accident remains unknown. This work explores the dynamics of VFA, with particular focus on large dihedral angles. We construct the longitudinal dynamics of a VFA model containing three rigid wing sections with elastic joint connections, using which we demonstrate that dihedral drift can occur in the presence of turbulence. We also carry out further analysis and link the observed instability to a drift in the phugoid mode as the dihedral angle increases. Finally, we demonstrate the link between controllability (observability) and different choices of control inputs (measured outputs), and speculate that the reason for the Helios crash may be due to weak controllability. An alternate set of inputs and outputs is proposed that can

Figure 5-1: NASA Helios in flight.

ensure stabilization and therefore a viable, control-configured, VFA design. Modeling, trim analysis and instability at large dihedral angles, controllability/observability and turbulence induced dihedral drift are treated in Sections II through V respectively.

5.2 Modeling

5.2.1 Vector Notation

Vectors are defined in bold font as

$$\mathbf{U} = U_x\hat{\mathbf{x}} + U_y\hat{\mathbf{y}} + U_z\hat{\mathbf{z}} \tag{5.1}$$

where $\hat{\cdot}$ denotes a unit vector with the triple, $(\hat{\mathbf{x}}, \hat{\mathbf{y}}, \hat{\mathbf{z}})$ orthogonal. The same vector can be defined in two different reference frames using the following notation:

$$\begin{aligned} \mathbf{U}^{\{1\}} &= U_{x_1}\hat{\mathbf{x}}_1 + U_{y_1}\hat{\mathbf{y}}_1 + U_{z_1}\hat{\mathbf{z}}_1 \\ \mathbf{U}^{\{2\}} &= U_{x_2}\hat{\mathbf{x}}_2 + U_{y_2}\hat{\mathbf{y}}_2 + U_{z_2}\hat{\mathbf{z}}_2 \end{aligned} \tag{5.2}$$

and in column vector representation,

$$\mathbf{U} = \begin{bmatrix} U_x \\ U_y \\ U_z \end{bmatrix} \quad \text{or} \quad \mathbf{U}^{\{1\}} = \begin{bmatrix} U_x \\ U_y \\ U_z \end{bmatrix}^{\{1\}} = \begin{bmatrix} U_{x_1} \\ U_{y_1} \\ U_{z_1} \end{bmatrix} \tag{5.3}$$

if the specific frame of reference is important.

Tensors are defined in bold font with an over bar as

$$\bar{\mathbf{I}} = \begin{bmatrix} I_{xx} & I_{xy} & I_{xz} \\ I_{yx} & I_{yy} & I_{yz} \\ I_{zx} & I_{zy} & I_{zz} \end{bmatrix} \tag{5.4}$$

and with the reference frame of the unit vectors included as

$$\bar{\mathbf{I}}^{\{1\}} = \begin{bmatrix} I_{x_1x_1} & I_{x_1y_1} & I_{x_1z_1} \\ I_{y_1x_1} & I_{y_1y_1} & I_{y_1z_1} \\ I_{z_1x_1} & I_{z_1y_1} & I_{z_1z_1} \end{bmatrix}. \tag{5.5}$$

5.2.2 Forces and Frames for Aircraft Dynamics

Consider the reference frame relations depicted in Figure 5-2. Let $(\hat{\mathbf{X}}, \hat{\mathbf{Y}}, \hat{\mathbf{Z}})$ be an inertial frame and let the Euler angles (ϕ, θ, ψ) carry the inertial frame into the body fixed frame $(\hat{\mathbf{x}}, \hat{\mathbf{y}}, \hat{\mathbf{z}})$ via the successive rotations $\psi \to \theta \to \phi$. Letting the aerodynamic force vector from pressure differentials on an aircraft be denoted as $\mathbf{P}$, the transformation from the wind axis forces $\mathcal{L},\ \mathcal{Y},\ \mathcal{D}$ (Lift, Sideforce, and Drag) to

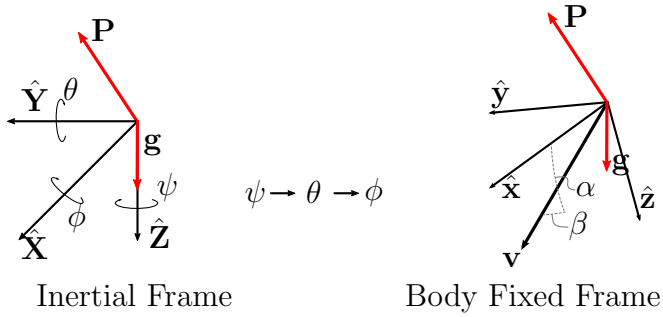

Figure 5-2: Reference frames important for describing aircraft motion.

the body fixed frame $(\hat{\mathbf{x}},\ \hat{\mathbf{y}},\ \hat{\mathbf{z}})$ is realized through

$$\begin{bmatrix} P_x \\ P_y \\ P_z \end{bmatrix} = H_W^B(\alpha, \beta) \begin{bmatrix} -\mathcal{D} \\ \mathcal{Y} \\ -\mathcal{L} \end{bmatrix} \tag{5.6}$$

with the wind to body axis transformation matrix formally defined as

$$H_W^B(\alpha, \beta) \triangleq \begin{bmatrix} \cos(\alpha)\cos(\beta) & -\cos(\alpha)\sin(\beta) & -\sin(\alpha) \\ \sin(\beta) & \cos(\beta) & 0 \\ \sin(\alpha)\cos(\beta) & -\sin(\alpha)\sin(\beta) & \cos(\alpha) \end{bmatrix} \tag{5.7}$$

where α is the angle of attack and β is the side slip angle, both of which are defined with respect to the velocity vector $\mathbf{v}$,

$$\begin{aligned} V &= \|\mathbf{v}\| \\ \beta &= \arcsin\left(v_y / V\right) \\ \alpha &= \arctan\left(v_z / v_x\right), \end{aligned} \tag{5.8}$$

and for completeness we include the reverse transformation:

$$\begin{bmatrix} v_x \\ v_y \\ v_z \end{bmatrix} = \begin{bmatrix} V\cos(\alpha)cos(\beta) \\ V\sin(\beta) \\ V\sin(\alpha)\sin(\beta) \end{bmatrix}. \tag{5.9}$$

Similarly, the body axis forces can be transformed to the wind axis forces via:

$$H_B^W(\alpha, \beta) \triangleq \left(H_W^B(\alpha, \beta)\right)^{-1}. \tag{5.10}$$

The gravity vector $\mathbf{g}$ always points in the inertial $\hat{\mathbf{Z}}$ direction, therefore the effect of gravity is realized in the body axis as

$$\mathbf{g} = \begin{bmatrix} g_x \\ g_y \\ g_z \end{bmatrix} = g \begin{bmatrix} -\sin(\theta) \\ \sin(\phi)\cos(\theta) \\ \cos(\phi)\cos(\theta) \end{bmatrix} \tag{5.11}$$

where g is the gravitational constant.

5.2.3 Linear and Angular Momentum for Very Flexible Aircraft

The aircraft of interest is shown in Figure 5-3. It is comprised of 3 rigid wings with elastic connections adjoining them. Each rigid panel has a propeller for thrust production, an aileron that runs along the aft of the main wing, and an elevator attached at the end of the boom. A schematic of the aircraft with appropriate axes and points of interest labeled is shown in Figure 5-4.

We are only interested the longitudinal dynamics of this aircraft. Therefore, denoting the angular momentum of the center of mass fixed frame (axes–g at point d) as $\boldsymbol{\omega}_d$, it is assumed that

$$\boldsymbol{\omega}_d^{\{g\}} = \begin{bmatrix} 0 \\ \omega_{d,y_g} \\ 0 \end{bmatrix} \tag{5.12}$$

and the velocity of the center of mass in frame–g is assumed to be of the form:

$$\mathbf{v}_d^{\{g\}} = \begin{bmatrix} v_{d,x_g} \\ 0 \\ v_{d,z_g} \end{bmatrix}. \tag{5.13}$$

Letting $\mathbf{F}$ be the total force acting on the system of 3 wings, the linear momentum of the system changes as:

$$\begin{aligned} \mathbf{F} =& \frac{d}{dt}\boldsymbol{\rho}_d \\ =& \quad m\left(\dot{v}_{d,x_g} + v_{d,z_g}\omega_{d,y_g}\right)\hat{\mathbf{x}}_g \\ &+ m\left(\dot{v}_{d,z_g} - v_{d,x_g}\omega_{d,y_g}\right)\hat{\mathbf{z}}_g \end{aligned} \tag{5.14}$$

where m is the total mass of the system given as $m = 3m^*$ with m^* denoting the mass of one of the three identical panels making up the flying wing.

The total Moment acting on the system of three wings about point d is defined

Figure 5-3: Artistic rendering of VFA.

as $\mathbf{M}$ and the time rate of change of the angular momentum about d is governed by

$$\begin{aligned}\mathbf{M} =& \frac{d}{dt}\mathbf{H}_d \\ =& \frac{d}{dt}\bar{\mathbf{I}}_d\boldsymbol{\omega}_d + \bar{\mathbf{I}}_d\frac{d}{dt}\boldsymbol{\omega}_d\end{aligned} \tag{5.15}$$

where $\bar{\mathbf{I}}_d$ is the moment of inertia for the entire wing about the center of mass at point d. Time rate of change of angular velocity reduces as

$$\begin{aligned}\frac{d}{dt}\boldsymbol{\omega}_d =& \dot{\omega}_{d,y_g}\hat{\mathbf{y}}_g + \omega_{d,y_g}\left(\omega_{d,y_g}\hat{\mathbf{y}}_g \times \hat{\mathbf{y}}_g\right) \\ =& \dot{\omega}_{d,y_g}\hat{\mathbf{y}}_g.\end{aligned} \tag{5.16}$$

Next we investigate the moment of inertia. The total moment of inertia has been defined as $\bar{\mathbf{I}}$. Now let the moment of inertia for each individual wing about its respective center of mass be defined as $\bar{\mathbf{I}}^*$. The moment of inertia then for the wing in frame–3 about point d is then:

$$\bar{\mathbf{I}}^*_{d,\text{wing–3}} = \bar{\mathbf{I}}^* + m^*\left(\langle \mathbf{c}_d, \mathbf{c}_d\rangle\, I - \mathbf{c}_d \otimes \mathbf{c}_d\right) \tag{5.17}$$

where $\mathbf{c}_d$ is the vector from point c to point d, $\langle\cdot,\cdot\rangle$ is the inner product operator, I is a 3×3 identity matrix carrying the inner product into the tensor space and $\otimes$ is the outer product. The moment of inertia for wings 1 and 2 can be calculated and hence forth denoted as $\bar{\mathbf{I}}^*_{d,\text{wing–1}}$ and $\bar{\mathbf{I}}^*_{d,\text{wing–2}}$. Then the total moment of inertia for the entire system becomes

$$\bar{\mathbf{I}} = \bar{\mathbf{I}}^*_{d,\text{wing–1}} + \bar{\mathbf{I}}^*_{d,\text{wing–2}} + \bar{\mathbf{I}}^*_{d,\text{wing–3}}. \tag{5.18}$$

Given that the angular velocity only has a non–zero component in the y_g axis, the only component from the moment of inertia that is important is $I_{y_gy_g}$ where

$$I_{y_gy_g} = c_1 + c_2\sin^2(\eta) \tag{5.19}$$

with $c_1 = 3I^*_{yy}$ and $c_2 = 2I^*_{zz} - 2I^*_{yy} + m^*\frac{s^2}{6}$. The only unknown quantity is the time varying nature of the dihedral angle. Up until this point the equations of motion have all been calculated from the center of mass of the entire system. In what follows we derive the dynamics of the dihedral angle from point j. The angular momentum of

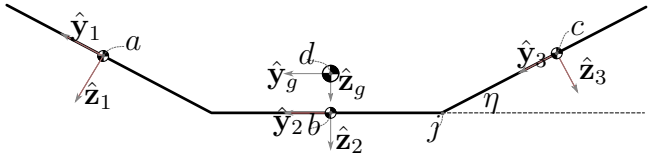

Figure 5-4: Schematic of VFA.

wing–3 about point j is

$$\mathbf{H}_j^* = \mathbf{j}_c \times \boldsymbol{\rho}^* + \mathbf{H}_c^* \tag{5.20}$$

where

$$\begin{aligned} \mathbf{j}_c \times \boldsymbol{\rho}^* &= -\tfrac{s}{2}\hat{\mathbf{y}}_3 \times m^* \begin{bmatrix} v_{c,x3} \\ v_{c,y3} \\ v_{c,z3} \end{bmatrix} \\ \mathbf{H}_c^* &= \begin{bmatrix} I^*_{x_3x_3} & 0 & 0 \\ 0 & I^*_{y_3y_3} & 0 \\ 0 & 0 & I^*_{z_3z_3} \end{bmatrix} \begin{bmatrix} \omega_{c,x_3} \\ \omega_{c,y_3} \\ \omega_{c,z_3} \end{bmatrix} \end{aligned} \tag{5.21}$$

where the angular momentum of frame–3, denoted as $\boldsymbol{\omega}_c$ is related to the angular momentum in frame–2, $\boldsymbol{\omega}_b = \boldsymbol{\omega}_d$ by the following:

$$\begin{bmatrix} \omega_{c,x_3} \\ \omega_{c,y_3} \\ \omega_{c,z_3} \end{bmatrix} = \begin{bmatrix} 1 & 0 & 0 \\ 0 & \cos(\eta) & \sin(\eta) \\ 0 & -\sin(\eta) & \cos(\eta) \end{bmatrix} \begin{bmatrix} \omega_{d,x_2} \\ \omega_{d,y_2} \\ \omega_{d,z_2} \end{bmatrix} + \begin{bmatrix} \dot{\eta} \\ 0 \\ 0 \end{bmatrix} \tag{5.22}$$

and noting that $\omega_{d,x_3} = \omega_{d,z_3} = 0$, the angular momentum of frame–3 about point j becomes

$$\mathbf{H}_j^* = \begin{bmatrix} -\frac{s}{2}m^* v_{c,z3} \\ 0 \\ \frac{s}{2}m^* v_{c,x3} \end{bmatrix} + \begin{bmatrix} I^*_{x_3x_3}\dot{\eta} \\ I^*_{y_3y_3}\cos(\eta)\omega_{d,y2} \\ -I^*_{z_3z_3}\sin(\eta)\omega_{d,y2} \end{bmatrix}. \tag{5.23}$$

The angular momentum $\mathbf{H}_j^*$ is then expanded so that all of the velocity components are with respect to frame–2,

$$\begin{aligned} \mathbf{H}_j^* = &\left(-\tfrac{s}{2}m^*\left(\left(v_{d,z} + \tfrac{s}{3}\eta_{\mathbf{c}}\dot{\eta}\right)\eta_{\mathbf{c}} - \dot{\eta}\tfrac{s}{2}\right) + I^*_{xx}\dot{\eta}\right)\hat{\mathbf{x}}_3 \\ &+ \left(I^*_{yy}\eta_{\mathbf{c}}\omega_{d,y}\right)\hat{\mathbf{y}}_3 \\ &+ \left(\tfrac{s}{2}m^*\left(v_{d,x} - \frac{s}{6}\eta_{\mathbf{s}}\omega_{d,y}\right) - I^*_{zz}\eta_{\mathbf{s}}\omega_{d,y}\right)\hat{\mathbf{z}}_3 \end{aligned} \tag{5.24}$$

where the subscript 2 has been removed to save space, and the following definitions have been used:

$$\begin{aligned} \eta_{\mathbf{c}} &\triangleq \cos(\eta) \\ \eta_{\mathbf{s}} &\triangleq \sin(\eta) \\ \eta_{\mathbf{sc}} &\triangleq \sin(\eta)\cos(\eta). \end{aligned} \tag{5.25}$$

Taking the time derivative $\mathbf{H}_j^*$ and relating only the x–axis external and internal moments

$$\begin{aligned} M^*_{j,x_3} - 2\omega_\kappa\zeta_\kappa\dot{\eta} - \omega_\kappa^2\eta = &-\tfrac{s}{2}m^*\left(\dot{v}_{d,z}\eta_{\mathbf{c}} - v_{d,z}\eta_{\mathbf{s}}\dot{\eta} - \tfrac{s}{3}\eta_{\mathbf{c}}^2\ddot{\eta} + 2\tfrac{s}{3}\eta_{\mathbf{sc}}\dot{\eta}^2\right) \\ &+ \left(I^*_{xx} + m^*\tfrac{s^2}{4}\right)\ddot{\eta} + \left(I^*_{yy}\eta_{\mathbf{c}}\omega_{d,y}\right)\eta_{\mathbf{s}}\omega_{d,y} \\ &+ \left(\tfrac{s}{2}m^*\left(v_{d,x} - \tfrac{s}{6}\eta_{\mathbf{s}}\omega_{d,y}\right) - I^*_{zz}\eta_{\mathbf{s}}\omega_{d,y}\right)\eta_{\mathbf{c}}\omega_{d,y}. \end{aligned} \tag{5.26}$$

where M^*_{j,x_3} is the total external moment acting on joint–j through wing–3, ζ_κ is the damping ratio for the joint and ω_κ is the undamped natural frequency of the joint.

5.2.4 Forces and Moments acting on VFA in Stability Axis Frame

The loads on an airfoil are defined in the wind axis frame. Using the relations illustrated in Figure 5-2, we denote the magnitude of the velocity at the center of mass as V and the angle of attack as α, note that $\beta = 0$. The three panels each have their own local (V_i, α_i, β_i) $i = 1, 2, 3$. For ease of exposition and to conform with historical notation the pitch rate of the center of mass frame is redefined as $q \triangleq \omega_{d,y_g}$.

The total wind axis forces defined with respect to the center of mass of the vehicle are denoted

$$\mathbf{W} = \begin{bmatrix} -\mathcal{D} \\ 0 \\ -\mathcal{L} \end{bmatrix} \tag{5.27}$$

which are defined relative to the body axis forces through the center of gravity body fixed frame g as:

$$\mathbf{W} = H^W_B(\alpha, \beta)\left(\mathbf{P}^{\{g\}}_w + \mathbf{P}^{\{g\}}_t\right) \tag{5.28}$$

where $\mathbf{P}_w$ is the resultant pressure driven force from the three wing sections

$$\begin{aligned} \mathbf{P}^{\{g\}}_w = &\underbrace{R_x(\eta)H^B_W(\alpha_1, \beta_1)\mathbf{W}^*_{w,1}}_{\mathbf{P}^*_{w,1}} \\ &+ \underbrace{H^B_W(\alpha_2, \beta_2)\mathbf{W}^*_{w,2}}_{\mathbf{P}^*_{w,2}} \\ &+ \underbrace{R_x(-\eta)H^B_W(\alpha_3, \beta_3)\mathbf{W}^*_{w,3}}_{\mathbf{P}^*_{w,3}} \end{aligned} \tag{5.29}$$

and where $\mathbf{P}_t$ is the resultant pressure driven force from the three tail sections

$$\begin{aligned} \mathbf{P}^{\{g\}}_t = &\underbrace{R_x(\eta)H^B_W(\alpha_1, \beta_1)\mathbf{W}^*_{t,1}}_{\mathbf{P}^*_{t,1}} \\ &+ \underbrace{H^B_W(\alpha_2, \beta_2)\mathbf{W}^*_{t,2}}_{\mathbf{P}^*_{t,2}} \\ &+ \underbrace{R_x(-\eta)H^B_W(\alpha_3, \beta_3)\mathbf{W}^*_{t,3}}_{\mathbf{P}^*_{t,3}}. \end{aligned} \tag{5.30}$$

Both of which are part of the total force acting on the body:

$$\mathbf{F}^{\{g\}} = \mathbf{P}^{\{g\}}_w + \mathbf{P}^{\{g\}}_t + \mathbf{T}^{\{g\}} + \mathbf{g}^{\{g\}}. \tag{5.31}$$

The local pressure driven forces defined in the local stability axes are given by

$$\mathbf{W}^*_{w,i} = \begin{bmatrix} -\mathcal{D}^*_{w,i} \\ 0 \\ -\mathcal{L}^*_{w,i} \end{bmatrix} \quad \mathbf{W}^*_{t,i} = \begin{bmatrix} -\mathcal{D}^*_{t,i} \\ 0 \\ -\mathcal{L}^*_{t,i} \end{bmatrix} \quad i = 1, 2, 3 \tag{5.32}$$

and the total thrust as

$$\mathbf{T} = \begin{bmatrix} \mathcal{T} \\ 0 \\ 0 \end{bmatrix} = \sum_{i=1}^{3} \underbrace{\begin{bmatrix} \mathcal{T}^*_i \\ 0 \\ 0 \end{bmatrix}}_{\mathbf{T}^*_i} \tag{5.33}$$

where $\mathcal{T}^*_i$ are the thrust force vectors applied on each wing by a propeller engine. The local lift and drag on the wing and tail sections are defined as:

$$\begin{aligned} \mathcal{L}^*_{w,i} &= \bar{\rho}^*_i C_{L_{w,i}} S^*_w & C_{L_{w,i}} &= C_{L_0} + C_{L_\alpha}\alpha_i + C_{L_\delta}\delta_{a,i} \\ \mathcal{L}^*_{t,i} &= \bar{\rho}^*_i C_{L_{t,i}} S^*_t & C_{L_{t,i}} &= C_{L_\alpha}(\alpha_i + \delta_{e,i}) \\ \mathcal{D}^*_{w,i} &= \bar{\rho}^*_i C_{D_{w,i}} S^*_w & C_{D_{w,i}} &= C_{D_0} + \kappa_D C^2_{L_{w,i}} \\ \mathcal{D}^*_{t,i} &= \bar{\rho}^*_i C_{D_{t,i}} S^*_t & C_{D_{t,i}} &= C_{D_0} + \kappa_D C^2_{L_{t,i}} \end{aligned}$$

where $\bar{\rho}^*_i$ is the local dynamic pressure at the center of each wing, S^*_w is the area of the wing and S^*_t is the area of the tail, $\delta_{a,i}$ are the aileron deflection angles and $\delta_{e,i}$ are the elevator deflection angles with $i = 1, 2, 3$.

The total moment on the aircraft is parameterized as

$$\begin{bmatrix} 0 \\ \mathcal{M} \\ 0 \end{bmatrix} = \mathbf{M}^{\{g\}} = \sum_{i=1}^{3} \left(\mathbf{M}^*_i + \mathbf{l}_{w,i} \times \mathbf{P}^*_{w,i} + \mathbf{l}_{t,i} \times \mathbf{P}^*_{t,i} \right), \tag{5.34}$$

where $\mathbf{M}^*_i = \begin{bmatrix} 0 & \mathcal{M}^*_i & 0 \end{bmatrix}^T$ and

$$\mathcal{M}^*_i = \bar{\rho}^*_i C_{M_i} c_w S^*_w \qquad C_{M_i} = C_{M_0} + C_{M_\delta}\delta_{a,i} \tag{5.35}$$

where c_w is the cord length of the wing, and $\mathbf{l}_{w,i}$ and $\mathbf{l}_{t,i}$ are the vectors that point from the quarter cord of the wing to the center of mass and the vectors that point from the quarter chord of the tail to center of mass, respectively. The length of the boom connecting from the quarter chord of the wing to the quarter chord of the tail is denoted l_b. Finally, the hinge moment at j acting on wing–3 in the x–direction is redefined as

$$\mathcal{H} \triangleq M^*_{j,x_3} = -(P^*_{w,1_z} + P^*_{t,1_z}) - m^* g \cos(\eta)\cos(\theta) \tag{5.36}$$

The dynamics for the VFA can now be be compactly expressed in the wind axis

as:

$$\begin{aligned}
\dot{V} =& \left(\mathcal{T}\cos\alpha - \mathcal{D}\right)/m - g\sin\gamma \\
\dot{\alpha} =& -\left(\mathcal{T}\sin\alpha + \mathcal{L}\right)/(mV) + q + g\cos(\gamma)/V \\
\dot{h} =& V\sin\gamma \\
\dot{\theta} =& q \\
\dot{q} =& \frac{\mathcal{M} - 2c_2\sin(\eta)\cos(\eta)\dot{\eta}q}{c_1 + c_2\sin^2(\eta)} \\
\ddot{\eta} =& \frac{\mathcal{H} - 2\omega_\kappa\zeta_\kappa\dot{\eta} - \omega_\kappa^2\eta + d_1 - d_2}{d_3}
\end{aligned} \tag{5.37}$$

where h is the height, $\gamma = \theta - \alpha$, and

$$\begin{aligned}
c_1 =& 3I_{yy}^* \\
c_2 =& 2I_{zz}^* - 2I_{yy}^* + m^*\tfrac{s^2}{6} \\
d_1 =& m^*\tfrac{s}{2}\left(\left(\dot{V}\sin(\alpha) + V\cos(\alpha)\dot{\alpha}\right)\eta_{\mathbf{c}}\right) \\
& - m^*\tfrac{s}{2}\left(V\sin(\alpha)\eta_{\mathbf{s}}\dot{\eta} + 2\tfrac{s}{3}\eta_{\mathbf{sc}}\dot{\eta}^2\right) \\
d_2 =& \left(I_{yy}^* - I_{zz}^* - m^*\tfrac{s^2}{12}\right)\eta_{\mathbf{sc}}q^2 - \tfrac{s}{2}m^*\eta_{\mathbf{c}}V\cos(\alpha)q \\
d_3 =& I_{xx}^* + m^*\left(\tfrac{s^2}{4} + \tfrac{s^2}{6}\eta_{\mathbf{c}}^2\right).
\end{aligned} \tag{5.38}$$

The geometric parameters and aerodynamic coefficients for the VFA are listed in Table 5.1.

5.3 Effect of Large Dihedral Angles

5.3.1 Trim Analysis

A trim analysis is now carried out to ensure that the VFA model presented captures the unstable phugoid mode that was observed in the higher fidelity models [66,68,76]. It should be noted that the model presented differs from the authors' previous work in [19] as the amount of structural damping has been significantly reduced.

The nonlinear dynamics in (5.37) can be compactly expressed as

$$\dot{X} = f(X, U) \tag{5.39}$$

where X is the state vector and U is the control input:

$$\begin{aligned}
X &= \begin{bmatrix} V & \alpha & h & \theta & q & \eta & \dot{\eta} \end{bmatrix}^T \\
U &= \begin{bmatrix} \delta_{a_c} & \delta_{a_o} & \delta_{e_c} & \delta_{e_o} & \delta_{\mathcal{T}} \end{bmatrix}^T.
\end{aligned} \tag{5.40}$$

The subscript a_c and a_o signify aileron center and aileron outer respectively so that

Table 5.1: Constants.

Variable	Value	Units
m^*	11	[slugs]
I^*_{xx}	54	[slugs ft^2]
I^*_{yy}	5.4	[slugs ft^2]
I^*_{zz}	48	[slugs ft^2]
s	60	[ft]
c_w	8	[ft]
c_t	2	[ft]
l_b	36	[ft]
S^*_w	480	[ft^2]
S^*_t	40	[ft^2]
C_{L_0}	$4\pi^2/180$	[-]
C_{L_α}	2π	[-]
C_{L_δ}	2	[-]
C_{M_0}	0.025	[-]
C_{M_δ}	-0.25	[-]
C_{D_0}	0.007	[-]
κ_D	0.07	[-]
ζ_κ	0.1	[-]
ω_κ	80	[-]

$\delta_{a_c} = \delta_{a_2}$ and $\delta_{a_o} = \delta_{a_i}$ where $i \in \{1, 3\}$. The subscripts e_c and e_o signify elevator center and elevator outer respectively. The control input $\delta_{\mathcal{T}} = \mathcal{T}_i,\ i \in \{1, 2, 3\}$. The linear dynamics are then defined as:

$$\dot{x} = Ax + Bu + \epsilon(X, U) \tag{5.41}$$

where $x = X - X_0$, $u = U - U_0$ with X_0 the trim state and U_0 the trim input satisfying $0 = f(X_0, U_0)$,

$$A = \left.\frac{\partial f(X,U)}{\partial X}\right|_{\substack{X=X_0\\U=U_0}} \quad B = \left.\frac{\partial f(X,U)}{\partial U}\right|_{\substack{X=X_0\\U=U_0}} \tag{5.42}$$

and ϵ is the linearization error.

The nonlinear VFA dynamics in (5.39) was linearized at a velocity of 30 ft/s and a height of 40,000 ft with the dihedral angle varied from 0 to 45 degrees. The eigenvalues from the study are shown in Figure 5-5. At zero dihedral angle the short period mode is lightly damped and the phugoid mode is stable. As the dihedral angle increases the pitch moment of inertia increases, leading to increased damping in the short period mode and instability in the phugoid mode. The transition to instability occurs at a dihedral angle of 15 degrees. These results agree with the findings from Ref. [66].

For the next study the aircraft was trimmed at a dihedral angle of 5 degrees. The trim inputs were held fixed while the initial condition of the dihedral angle was varied

from 10 to 30 degrees in 10 degree increments so as to observe the open–loop behavior of the aircraft. These results are shown in Figure 5-6. For initial conditions of 10 and 20 degrees in dihedral angle the aircraft exhibits steady motion as the dihedral slowly approaches the trim condition. For large perturbation from trim the dihedral angle diverges, and thus warranting active dihedral control.

The above discussions clearly reveal that the open loop system is unstable when linearized around sufficiently large dihedral angles. This directly corroborates the Helios mishap, which was accompanied by large excursions in dihedral angles and other state variables (see Figure 5-7 which shows the flight data). As can be seen in this figure, the dihedral (measured in feet) behaves erratically drifting up and down. This occurs for several minutes until eventually the dihedral exceeds 35 ft leading to a diverging oscillation and the ultimate demise of the aircraft.

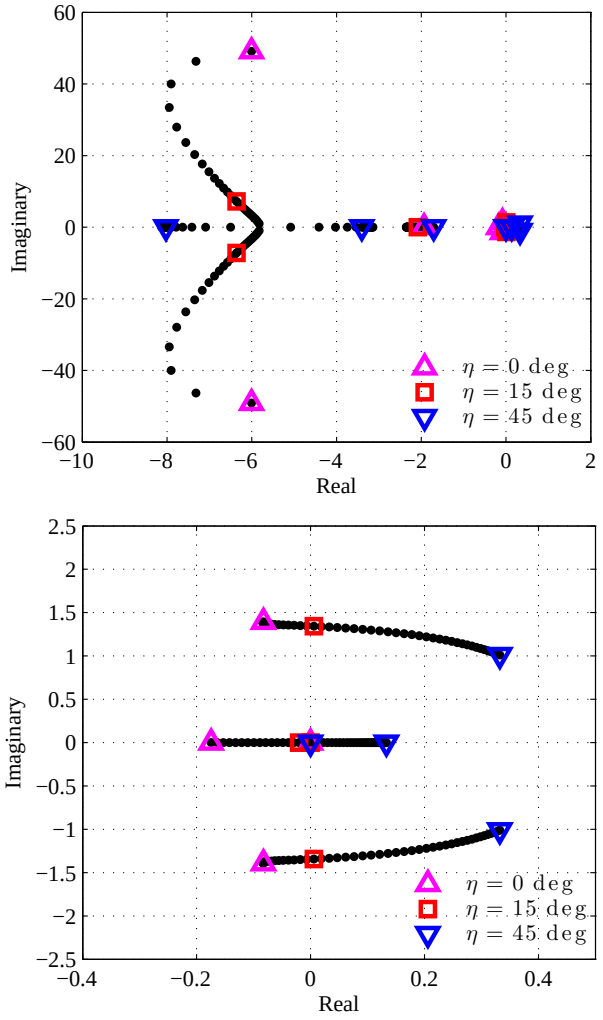

Figure 5-5: Eigenvalues for trim points. At zero dihedral angle the short period mode is lightly damped and the phugoid mode is stable. As the dihedral angle increases the short period mode damping increases and the phugoid mode becomes unstable.

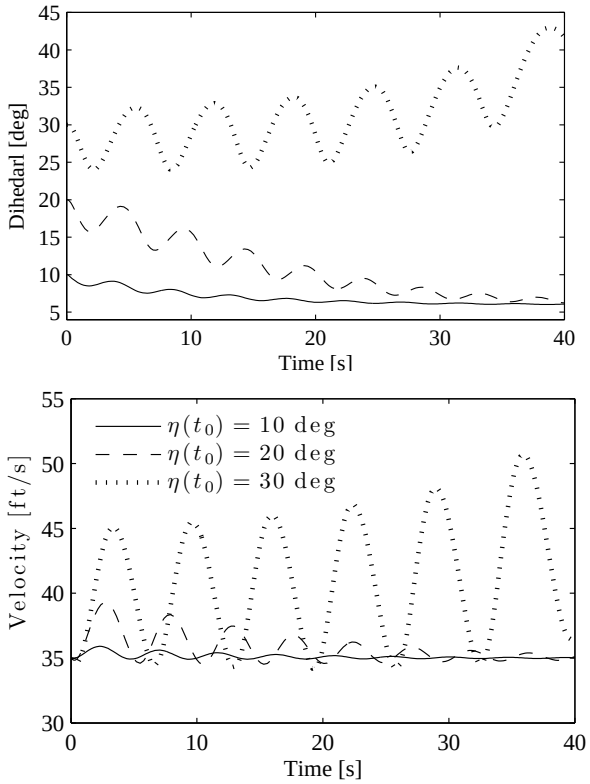

Figure 5-6: Initial condition perturbation from trim input for dihedral angle of 5 degrees.

The interesting point to note is that this instability cannot always be controlled satisfactorily. In fact, as observed in the Helios, the resident controller was in fact ineffective in overcoming the destabilization. As will be shown in the next section using the model proposed above, the effect of control is a direct function of the specific control inputs and measured outputs that are used. We analyze this effect by using the model proposed in this section, a control design, and metrics of controllability and observability.

5.4 Control of Dihedral Angles

5.4.1 Control Design

The goal of the controller is to design u, from (5.40), such that the control input $U = U_0 + u$ returns the system of equations back to trim in the presence of turbulence. The control input is defined as

$$u = -K\hat{x} \tag{5.43}$$

where the observer state $\hat{x}$ is defined as

$$\dot{\hat{x}} = (A - LC)\hat{x} + Bu + Ly \tag{5.44}$$

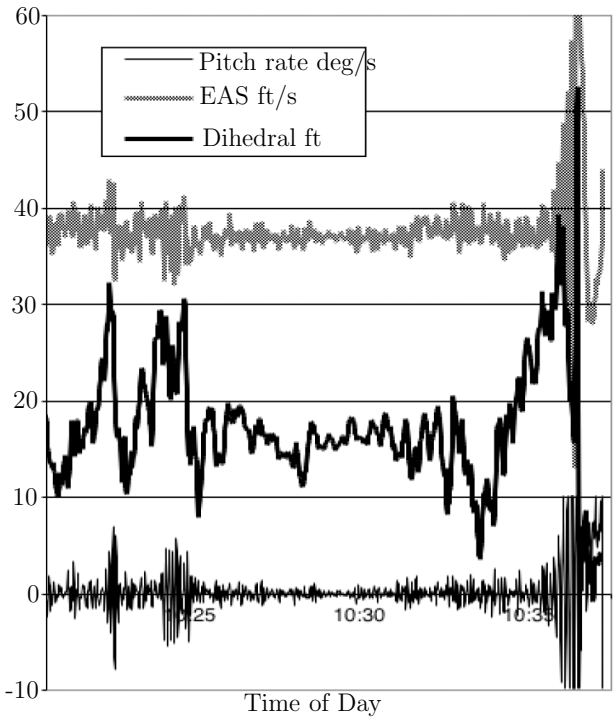

Figure 5-7: Helios flight mishap data (adapted from [65]).

with

$$L = P_o C^T R_o^{-1} \tag{5.45}$$

and $P_o = P_o^T > 0$ the solution to the *Observer Algebraic Riccati Equation* (OARE)

$$P_o A^T + A P_o - P_o C^T R_o^{-1} C P_o + Q_o = 0. \tag{5.46}$$

Q_o and R_o are symmetric positive definite free design parameters.

The control input for the baseline controller is then defined as

$$K = P_c B R_c^{-1} \tag{5.47}$$

with $P_c = P_c^T > 0$ the solution to the *Control Algebraic Riccati Equation* (CARE)

$$P_c A + A^T P_c - P_c B R_c^{-1} B^T P_c + Q_c = 0. \tag{5.48}$$

The free design weights (Q_c, R_c), are both symmetric and positive definite. The baseline control input can be compactly expressed as:

$$u = -K\hat{x}, \quad \dot{\hat{x}} = (A - LC - BK)\hat{x} + Ly, \tag{5.49}$$

where the free design parameters for the observer and control design are (Q_o, R_o, Q_c, R_c). The overall feedback loop is shown in Figure 6-2.

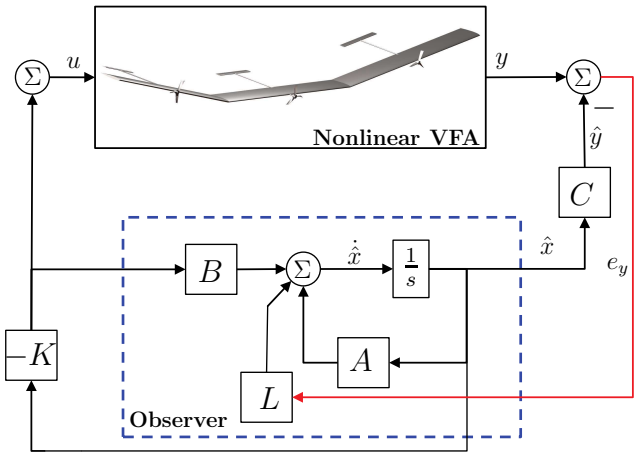

Figure 5-8: LQG Control Structure.

5.4.2 Controllability and Observability

Recall that a linear system with the pair (A, B), (5.41), is controllable if and only if the controllability matrix $\mathcal{C}$ is full rank, where

$$\mathcal{C} \triangleq \begin{bmatrix} B & AB & A^2B & \cdots & A^{n-1}B \end{bmatrix}. \tag{5.50}$$

Similarly, given output measurements y, where

$$y = Cx, \tag{5.51}$$

the pair (A, C), is fully observable if and only if the observability matrix $\mathcal{O}$ is full rank, with

$$\mathcal{O} \triangleq \begin{bmatrix} C \\ CA \\ CA^2 \\ \vdots \\ CA^{n-1} \end{bmatrix}. \tag{5.52}$$

The *controllability measure* is defined as

$$\mu(\mathcal{O}) \triangleq \kappa^{-1}(\mathcal{O}) \triangleq \frac{\sigma_{\min}(\mathcal{O})}{\sigma_{\max}(\mathcal{O})} \tag{5.53}$$

where κ is commonly referred to as the condition number of a matrix and σ signifies the singular value of a matrix. The *observability measure* is similarly defined as

$$\mu(\mathcal{C}) \triangleq \kappa^{-1}(\mathcal{C}) \triangleq \frac{\sigma_{\min}(\mathcal{C})}{\sigma_{\max}(\mathcal{C})}. \tag{5.54}$$

Table 5.2: Controllability/Observability Study.

Input Jacobian / Output Selection	Inputs/Outputs
B_1	$\mathcal{T},\ \delta_{a_c}$
B_2	$\mathcal{T},\ \delta_{a_c},\ \delta_{e_c}$
B_3	$\mathcal{T},\ \delta_{a_c},\ \delta_{e_c},\ \delta_{a_o}$
B_4	$\mathcal{T},\ \delta_{a_c},\ \delta_{e_c},\ \delta_{a_o},\ \delta_{e_o}$
C_1	$V,\ q,\ h$
C_2	$V,\ q,\ h,\ \eta$

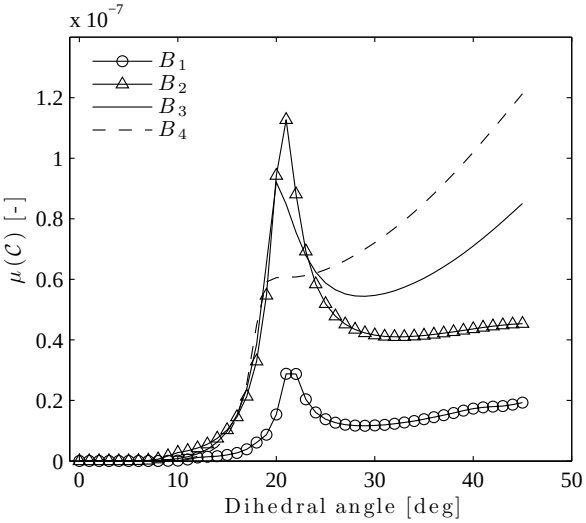

Figure 5-9: Measure of controllability as a function of input selection and dihedral angle.

5.4.3 Controllability and Observability Measures applied to VFA Model

Table 5.2 contains different control input and measured output definitions. These definitions will be used in this section, as well as the simulation section that follows. Figures 5-9 and 5-10 shows different control inputs with their respective controllability measure as a function of trim dihedral, the only difference between the two figures is the y axis in Figure 5-10 is in log scale. The general trend observed is that as the dihedral angle increases so does the the Controllability. It can furthermore be observed that B_1 results in the least controllable configuration and that as more inputs become available for control the Controllability of the VFA increases. The observability measures for C_1 and C_2 are not shown as they both result in a highly observable configuration. In what follows, we attempt to recreate the Helios crash using the model and, control inputs and outputs discussed above. Deterministic disturbances are added to the local velocity vectors so as to simulate turbulence.

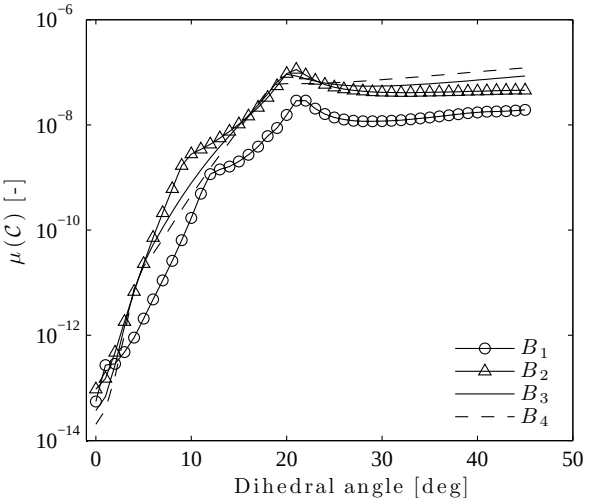

Figure 5-10: Measure of controllability as a function of input selection and dihedral angle, semilog plot.

5.5 Analysis of Helios Crash

We now carry out a detailed study of the Helios crash using the model presented in Section II and III and the control design in Section IV. This study consists of four parts that include: (I) the effect of different input and output configurations in the presence of turbulence, (II) the effect of variations in the frequency of the turbulence, (III) the effect of variations in the amplitude of the turbulence, and (IV) a direct comparison of our model to the Helios crash data. We will show that for a specific selection of control inputs and measured outputs dihedral drift in the presence of turbulence occurs regardless of the frequency or amplitude of the turbulence. In all cases, the nonlinear VFA model in (5.39) with the LQG controller in (6.39) are used.

The turbulence is introduced into the model in (5.39) by adding disturbances to the local velocity vectors of the three wings. In order to keep the aircraft symmetric about the $\hat{\mathbf{x}}_g$, $\hat{\mathbf{z}}_g$ plane, there are only local $\hat{\mathbf{x}}_i$ and $\hat{\mathbf{z}}_i$ disturbances affecting the three wings. Furthermore, the disturbances on wing–1 and wing–3 are identical. The disturbance are generated from a gaussian distribution with mean 0 ft/s and standard deviation of 1 ft/s sampled at an adjustable interval Δ_t with adjustable multiplicative output gain D.

5.5.1 Part I:

The controller is chosen as in (6.39), with the input matrix B and output matrix C chosen according to three different cases which are defined in Tables 5.2 and 5.3. The cost function design parameters for the choice of K and L are chosen as in Table 5.4. The wind disturbances for this study occur with a $\Delta_t = 0.1$ and $D = 1$. In Case (i), the control inputs available for stabilization are the thrust and center aileron, with the measured outputs selected to be the velocity, pitch rate and height of the VFA. Progressing to Case (ii), the center elevator and outboard ailerons are added as

Table 5.3: Simulation Cases.

Test Case	Control Design Triple
(i)	(A, B_1, C_1)
(ii)	(A, B_3, C_1)
(iii)	(A, B_3, C_2)

Table 5.4: Simulation Cases.

Param.	Case (i)	Case (ii)	Case (iii)
Q_c	$\leftarrow$ diag([0.01 1 0.001 1 1 10 100]) $\rightarrow$		
Q_o	$\leftarrow$ diag([1 10 1 10 100 10 0.1]) $\rightarrow$		
R_c	diag([100 10])	diag([100 10 10])	diag([100 10 10])
R_o	diag([.1 .1 .1])	diag([.1 .1 .1])	diag([.1 .1 .1 .1])

control inputs, which increases the controllability of the aircraft. For the third case the dihedral angle is added as a measurable output. Each of the simulations begin with the VFA trimmed at 40,000 ft with a velocity of 30 ft/s and dihedral angle of 12 deg. The results from the simulations are shown in Figure 5-11.

For test Case (i) the VFA model exhibits a similar dihedral trajectory to that of the Helios aircraft accident shown in Figure 5-7. The dihedral angle can be seen to drift upwards until instability is encountered where the dihedral begins to oscillate until it quickly diverges. Test Case (ii) exhibits a bounded behavior. Case (iii) results in satisfactory performance in the presence of turbulence as the vehicle is more stable when the dihedral angle is directly measured.

The results from test Case (i) are to be expected given that the control inputs selected resulted in a weakly controllable system. In test Case (ii) the vehicle exhibits stable behavior, however without measuring the dihedral angle directly the vehicle oscillations are further from the trim dihedral as compared to Case (iii). That is, the dihedral dynamics are not observable with only the velocity, height and pitch rate as measured outputs. The linear observability analysis suggests that even without direct measurement of the dihedral angle the system is fully observable, thus illustrating that the dihedral dynamics are in fact highly nonlinear. Therefore, in order to stabilize the Very Flexible Aircraft it is important to select control inputs such that the underlying linear system is controllable and select measured outputs so that the dominant nonlinear dynamics of the dihedral are captured. Our speculation is that in the case of the Helios aircraft the control design did not take into account the lack of controllability when the outside control surfaces are not used and the inherent nonlinear relationship between the dihedral angle and the pitch rate of the center wing section was not accounted for either.

5.5.2 Part II:

The second simulation study analysis the affect of varying the frequency of the turbulence. For this study the same control configuration as test Case (i) is used with

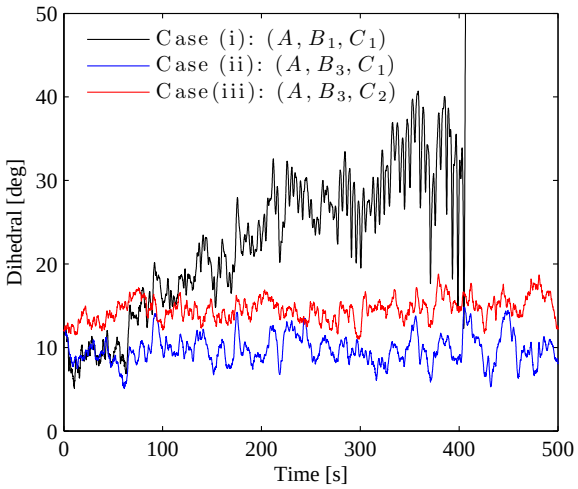

Figure 5-11: Simulation in the presence of turbulence with $\Delta_t = 0.1$ and $D = 1$ for the three test case scenarios in Table 5.3.

$D = 1$ and $\Delta_t \in \{0.1, 0.05, 0.01\}$ varied over three values. The results from this study are presented in Figure 5-12. For case when $\Delta_t = 0.1$ the results from this study are identical to test Case (i) in the previous study. So the unsteady behavior is expected. This confirms that the instability is invariant to the frequency characteristics of the turbulence and that the VFA is not able to stabilize around its trim condition when the controller in Case (i) is chosen. Increasing the frequency of the turbulence in fact leads to a quicker departure of the dihedral angle. It is interesting to note that Cases (ii) and (iii) once again show a stable behavior (not included in Figure 5-12).

5.5.3 Part III:

We now study the effect of varying the magnitude of the turbulence. For this study the same control configuration as test Case (i) is used with $D \in \{1, \sqrt{.5}, \sqrt{.1}\}$ and $\Delta_t = 0.1$. The results from this study are presented in Figure 5-13. Once again, a divergent behavior can be seen with reduction in the amplitude only resulting in the increase in the amount of time it takes for the dihedral angle to depart. The simulation scenario with $D = \sqrt{0.1}$ also departs even though this is not captured over the time window chosen to present the results. At such a low amplitude the departure is very slow, but the dihedral does eventually surpass 50 deg. Thus from the two previous studies it is clear that regardless of the frequency or the amplitude of the disturbance, the VFA is not stable in the presence of turbulence when control Case (i) is used. One again, Cases (ii) and (iii) led to a stable behavior in this study as well (not included in Figure 5-13).

5.5.4 Part IV:

The simulation section is closed by directly comparing control Case (i) in the presence of turbulence, $D = 1$ and $\Delta_t = 0.05$, to the Helios flight data. This comparison is

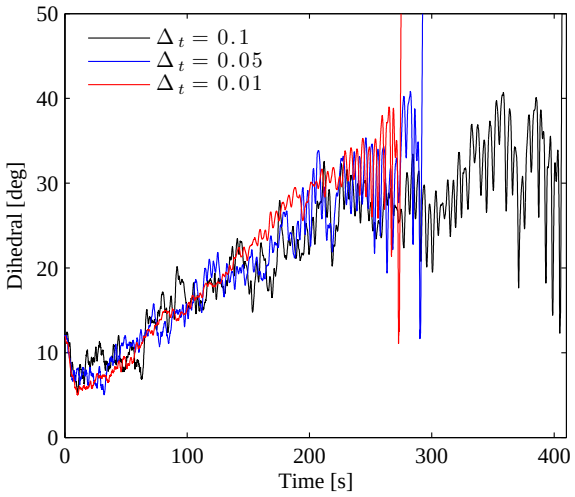

Figure 5-12: Comparison of dihedral measured in ft for Helios mishap and VFA sim Case (i), $D = 1$, and $\Delta_t \in \{0.1, 0.05, 0.01\}$.

shown in Figure 5-14. The simulation data shown in red is matched to the Helios data in black at the excursion point on the right hand side of the plot, just after the 10:35 mark. This overlay illustrates that the Helios crash can be mimicked with; a simple first principles model of a three panel VFA, a classical LQG controller in the presence of disturbances, and an improper selection of control inputs and measurement.

5.6 Conclusions

A model sufficient for control design and analysis of VFA has been presented. Controllability studies suggest that the dihedral dynamics are weakly controllable and when the outer control surfaces are not used in the control design the VFA is in the most weakly controllable configuration. While the observability studies were inconclusive in the linear setting, it is clear that the dynamics of the dihedral in relation to the other states are highly nonlinear, and thus direct measurement of the dihedral is necessary for satisfactory dihedral stabilization. Finally, it was shown that when a controller is designed without taking these lessons into account VFA can be susceptible to turbulence induced dihedral drift, as was the case in the Helios flight mishap. This result ultimately suggests that the conclusions from the flight mishap investigation are not necessarily correct. More sophisticated multidisciplinary analysis techniques are not needed to understand what caused the Helios crash. A simple control oriented model with classical control analysis suffices.

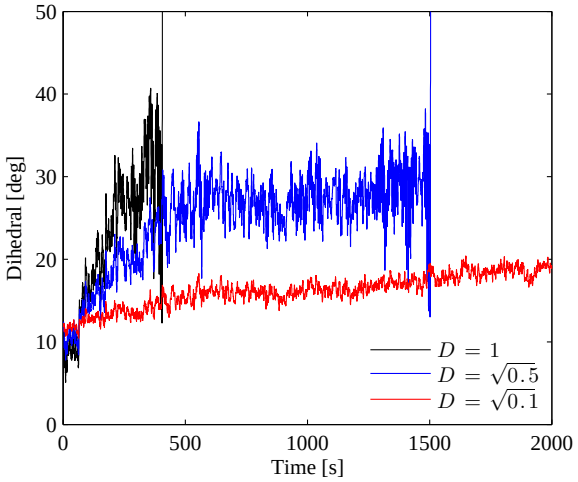

Figure 5-13: Comparison of dihedral measured in ft for Helios mishap and VFA sim Case (i), $\Delta_t = 0.1$, and $D \in \{1, \sqrt{0.5}, \sqrt{0.1}\}$.

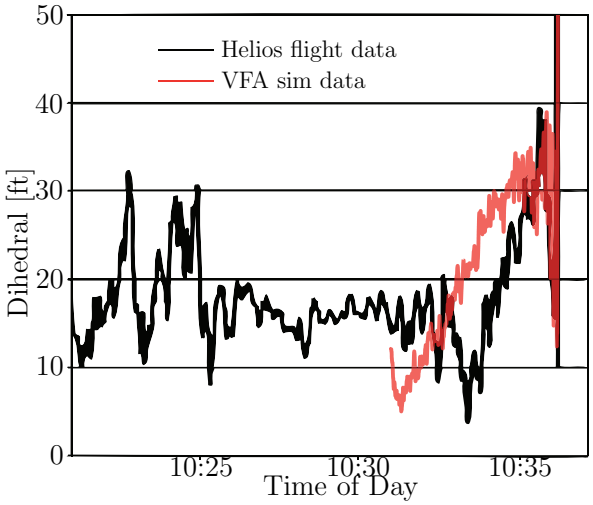

Figure 5-14: Comparison of dihedral measured in ft for Helios mishap and VFA sim Case (i).

Chapter 6

Modern Output Feedback Adaptive Control

In the following sections we are concerned with systems of the following form:

$$\dot{x} = Ax + B\Lambda u, \qquad y = C^T x \tag{6.1}$$

where $x \in \mathbb{R}^n$, $u \in \mathbb{R}^m$, and $y \in \mathbb{R}^m$. The only known quantities are B and C, $\Lambda > 0$ is diagonal with known sign only and A is unknown. The goal is to design a control input u so that x tracks the reference model state x_m

$$\dot{x}_m = A_m x_m + Br - Le, \qquad y_m = C^T x_m \tag{6.2}$$

where $r \in \mathbb{R}^m$ is the reference input and y alone is available for measurement.

We are only presenting results for square systems, i.e. the same number of outputs as inputs, in this paper. Note however that squaring-up and squaring-down procedures do exists that allow for the adaptive control of non-square systems, similar to what is done in [47, §13]

The following assumptions are made throughout.

Assumption 6.1. The product $C^T B$ is full rank.

Assumption 6.2. The system in (6.1) is observable.

Assumption 6.3. There exists a $\Theta^* \in \mathbb{R}^{n\times m}$ such that $A + B\Lambda\Theta^{*T} = A_m$. Note that in general this condition is stronger than (A, B) controllable.

The uncertain parameters live in bounded sets.

$$\sup_{\Theta,\Theta^*\in\Omega_1} \|\tilde{\Theta}\|_F \triangleq \Theta_{\max} \qquad \sup_{K,K^*\in\Omega_2} \|\tilde{K}\|_F \triangleq K_{\max}, \tag{6.3}$$

It will be shown that the control input

$$u = \Theta^T(t)x_m + K^T(t)r \tag{6.4}$$

has stable update laws which lead to $\lim_{t\to\infty} e_y(t) = 0$ where $e_y = y - y_m$. The model following error satisfies the following dynamical relation:

$$\begin{aligned} \dot{e} &= (A_m + LC^T)e + B\Lambda\left(\tilde{\Theta}^T x_m + \tilde{K}^T r + \tilde{\Theta}^{*T} e\right) \\ e_y &= C^T e \end{aligned} \tag{6.5}$$

6.1 SISO: Zero Annihilation

We begin with the selection of the observer gain.

Lemma 6.1. *For the system in* (6.1) *satisfying Assumptions 6.1-6.3 and SISO* ($m = 1$) *there exists an* L *such that*

$$C^T(sI - A_m - LC^T)^{-1}B = \frac{a}{s+\mu}$$

where $\mu > 0$ *is completely free to choose and* $a = C^T B$.

Proof. Given that $C^T B$ is non-zero $C^T(sI - A_m - LC^T)^{-1}B$ is a relative degree 1 transfer function. Furtheremore, given that the system is observable all of the eigenvalues of $A_m + LC^T$ are free to choose. Therefore, one can place $n-1$ of the Eigen values of $A_m + LC^T$ at the $n-1$ zeros of $C^T(sI - A_m)^{-1}B$ and the n-th Eigen value value of $A_m + LC^T$ at $-\mu$. □

Corollary 6.1. *As a direct consequence of the above Lemma, the SISO transfer function* $(C^T B)C^T(sI - A_m - LC^T)^{-1}B$ *is SPR. Therefore, there exists* $P = P^T > 0$ *and* $Q = Q^T > 0$ *such that*

$$\begin{aligned} (A_m + LC^T)^T P + P(A_m + LC^T) &= -Q \\ PB &= C(B^T C). \end{aligned} \tag{6.6}$$

The error dynamics for e_y are now presented in their minimal form when L is chosen as in Lemma 6.1.

$$\dot{e}_y = -\mu e_y + C^T B\Lambda\left(\tilde{\Theta}^T x_m + \tilde{K}^T r + \Theta^{*T} e\right) \tag{6.7}$$

The update laws for the adaptive parameters are given as

$$\begin{aligned} \dot{\Theta} =& \text{Proj}_{\Omega_1}(-\Gamma_\theta x_m e_y B^T C, \Theta) \\ \dot{K} =& \text{Proj}_{\Omega_2}(-\Gamma_k r e_y B^T C, K) \end{aligned} \tag{6.8}$$

Theorem 6.1. *The Adaptive system given in* (6.1), (6.2), (6.18), *following Assumptions 6.1-6.3 and with* L *chosen as in Lemma 6.1 is stable, and* $\lim_{t\to\infty} e(t) = 0$ *for all* $\mu > \mu^*$ *where*

$$\mu^* = 4(C^T B)^2 \Lambda^2 \Theta^{*T} \lambda_{min}(Q)^{-1} \Theta_{max}^2. \tag{6.9}$$

Proof. Consider the Lyapunov candidate function

$$V = e^T P e + e_y^2 + 2\mathrm{Tr}(\Lambda \tilde{\Theta}^T \Gamma^{-1} \tilde{\Theta}) + 2\mathrm{Tr}(\Lambda \tilde{K}^T \Gamma^{-1} \tilde{K}) \tag{6.10}$$

For simplicity of exposition we will derive the result for when the projection algorithm is not active. Then using the fundamental properties of the projection algorithm the same result trivially holds. Taking the time derivative of (6.10) along the system trajectories in (6.5) and (6.7) , along with the substitution of the update laws in (6.18) and (6.6), the following holds:

$$\begin{aligned}
\dot{V} = &- e^T Q e + 2e^T P B \Lambda \Theta^{*T} e \\
&+ 2e^T P B \Lambda \tilde{\Theta}^T x_m + 2\mathrm{Tr}(\Lambda \tilde{\Theta}^T x_m e_y B^T C) \\
&+ 2e^T P B \Lambda \tilde{K}^T r + 2\mathrm{Tr}(\Lambda \tilde{K}^T r e_y B^T C) \\
&- 2\mu e_y^2 + 2e_y C^T B \Lambda \Theta^{*T} e \\
&+ 2e_y C^T B \Lambda \tilde{\Theta}^T x_m + 2\mathrm{Tr}(\Lambda \tilde{\Theta}^T x_m e_y B^T C) \\
&+ 2e_y C^T B \Lambda \tilde{K}^T r + 2\mathrm{Tr}(\Lambda \tilde{K}^T r e_y B^T C)
\end{aligned} \tag{6.11}$$

Using the fact that $PB = C(B^T C)$ from (6.6) and the fact the Trace operator is invariant under cyclic permutations the inequality in (6.11) can be rewritten as

$$\begin{aligned}
\dot{V} = &- e^T Q e + 2e^T P B \Lambda \Theta^{*T} e \\
&+ 2e^T C(B^T C) \Lambda \tilde{\Theta}^T x_m - 2e_y B^T C \Lambda \tilde{\Theta}^T x_m \\
&+ 2e^T C(B^T C) \Lambda \tilde{K}^T r - 2e_y B^T C \Lambda \tilde{K}^T r \\
&- 2\mu e_y^2 + 2e_y C^T B \Lambda \Theta^{*T} e \\
&+ 2e_y C^T B \Lambda \tilde{\Theta}^T x_m - 2e_y B^T C \Lambda \tilde{\Theta}^T x_m \\
&+ 2e_y C^T B \Lambda \tilde{K}^T r - 2e_y B^T C \Lambda \tilde{K}^T r
\end{aligned} \tag{6.12}$$

Using the fact that $e_y = C^T e$ and for a SISO system $C^T B = B^T C$ the 2nd, 3rd, 5th and 6th lines in the above equation equal zero. Therefore, (6.12) can be written as

$$\dot{V} = -\mathcal{E}^T M(\mu) \mathcal{E} \tag{6.13}$$

where

$$M(\mu) = \begin{bmatrix} 2\mu & -2C^T B \Lambda \Theta^{*T} \\ -2\Theta^* \Lambda B^T C & Q \end{bmatrix} \quad \mathcal{E} = \begin{bmatrix} e_y \\ e \end{bmatrix}$$

Given that $\mu > \mu^*$, μ is necessarily positive and $2\mu - 4(C^T B)^2 \Lambda^2 \Theta^{*T} Q^{-1} \Theta^* > 0$. By Lemma 2.2, $M(\mu)$ is positive definite. Therefore $\dot{V} \leq 0$ and thus $e_y, e, \tilde{\Theta}, \tilde{K} \in \mathcal{L}_\infty$. Furthermore, given that M is positive definite $e_y, e \in \mathcal{L}_2$. Using Barbalat Lemma it follows that $\lim_{t\to\infty} e(t) \to 0$. □

6.2 MIMO Square: Zero Annihilation

Lemma 6.2. *For the system in* (6.1) *satisfying Assumptions there exists an* L *such that* $C^T(sI - A_m - LC^T)^{-1}B$ *has* $n-m$ *poles at the transmission zeros and the other* m *poles with real component less than* $\mu > 0$.

Proof. Given that the system is observable all of the eigenvalues of $A_m + LC^T$ are free to choose. Therefore, one can place $n - m$ of the Eigen values of $A_m + LC^T$ at the $n - m$ transmission zeros of $C^T(sI - A_m)^{-1}B$ and m Eigenvalues to the left of $-\mu$ on the real line. See Figure 6-1. □

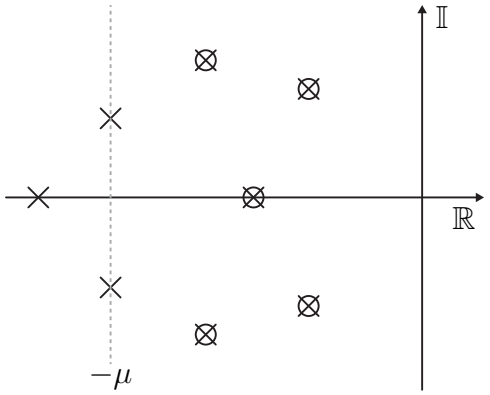

Figure 6-1: PZ Map for MIMO system with feedback gain L chosen as in Lemma 6.2.

A minimal representation for the system in (6.5) with L chosen as in Lemma 7, is now given

$$\dot{e}_y = \bar{A}e_y + \bar{B}\Lambda\left(\tilde{\Theta}^T x_m + \tilde{K}^T r + \tilde{\Theta}^{*T} e\right) \tag{6.14}$$

Given that $\bar{A}$ is Hurwitz, the following relation holds,

$$\bar{A}^T\bar{P} + \bar{P}\bar{A} = -\bar{Q}. \tag{6.15}$$

Furthermore, from the AKY Lemma, defining

$$\bar{C} \triangleq \bar{P}\bar{B} \tag{6.16}$$

the transfer function $\bar{C}^T(sI - \bar{A})^{-1}\bar{B}$ is SPR. This also implies that the transfer function $\bar{C}^T C^T(sI - A_m - LC^T)^{-1}B$ is SPR. Therefore, there exists $P = P^T > 0$ and $Q = Q^T > 0$ such that the following relation holds

$$\begin{aligned}(A_m + LC^T)^T P + P(A_m + LC^T) &= -Q \\ PB &= C\bar{C}.\end{aligned} \tag{6.17}$$

The update law for the adaptive system is then chose as

$$\begin{aligned}\dot{\Theta} &= \text{Proj}_{\Omega_1}(-\Gamma_\theta x_m e_y^T \bar{C}, \Theta) \\ \dot{K} &= \text{Proj}_{\Omega_2}(-\Gamma_k r e_y^T \bar{C}, K)\end{aligned} \tag{6.18}$$

Theorem 6.2. *The Adaptive system given in* (6.1), (6.2), (6.18), *following Assumptions 6.1-6.3 and with L chosen as in Lemma 6.2 is stable, and* $\lim_{t\to\infty} e(t) = 0$ *for all* $\mu > \mu^*$ *where*

$$\mu^* = 4\frac{\lambda_{max}(\Lambda)^2\|\bar{C}\|^2\Theta_{max}}{\lambda_{min}(\bar{P})\lambda_{min}(Q)}. \tag{6.19}$$

Proof. Consider the Lyapunov candidate function

$$\begin{aligned} V =& e^T P e + e_y^T \bar{P} e + 2\mathrm{Tr}(\Lambda\tilde{\Theta}^T\Gamma^{-1}\tilde{\Theta}) \\ &+ 2\mathrm{Tr}(\Lambda\tilde{K}^T\Gamma^{-1}\tilde{K}) \end{aligned} \tag{6.20}$$

where $\bar{P}$ and P are defined in (6.15) and (6.17) respectively. For simplicity of exposition we will derive the result for when the projection algorithm is not active. Then using the fundamental properties of the projection algorithm the same result trivially holds. Taking the time derivative of (6.10) along the system trajectories in (6.5) and (6.7) , along with the substitution of the update laws in (6.18) and (6.6), the following holds:

$$\begin{aligned} \dot{V} =& - e^T Q e + 2e^T P B \Lambda \Theta^{*T} e \\ &+ 2e^T P B \Lambda \tilde{\Theta}^T x_m + 2\mathrm{Tr}(\Lambda\tilde{\Theta}^T x_m e_y^T \bar{C}) \\ &+ 2e^T P B \Lambda \tilde{K}^T r + 2\mathrm{Tr}(\Lambda\tilde{K}^T r e_y^T \bar{C}) \\ &- e_y^T \bar{Q} e_y + 2e_y^T \bar{P}\bar{B}\Lambda\Theta^{*T} e \\ &+ 2e_y^T \bar{P}\bar{B}\Lambda \tilde{\Theta}^T x_m + 2\mathrm{Tr}(\Lambda\tilde{\Theta}^T x_m e_y^T \bar{C}) \\ &+ 2e_y^T \bar{P}\bar{B}\Lambda \tilde{K}^T r + 2\mathrm{Tr}(\Lambda\tilde{K}^T r e_y^T \bar{C}) \end{aligned} \tag{6.21}$$

Using the fact that $\bar{P}\bar{B} = \bar{C}$, $PB = C\bar{C}$, $e_y = C^T e$ and the fact the Trace operator is invariant under cyclic permutations the inequality in (6.21) can be rewritten as

$$\begin{aligned} \dot{V} =& - e^T Q e + 2e_y^T \bar{C}\Lambda\Theta^{*T} e \\ &+ 2e_y^T \bar{C}\Lambda\tilde{\Theta}^T x_m - 2e_y^T \bar{C}\Lambda\tilde{\Theta}^T x_m \\ &+ 2e_y^T \bar{C}\Lambda\tilde{K}^T r - 2e_y^T \bar{C}\Lambda\tilde{K}^T r \\ &- e_y^T \bar{Q} e_y + 2e_y^T \bar{C}\Lambda\Theta^{*T} e \\ &+ 2e_y^T \bar{C}\Lambda\tilde{\Theta}^T x_m - 2e_y^T \bar{C}\Lambda\tilde{\Theta}^T x_m \\ &+ 2e_y^T \bar{C}\Lambda\tilde{K}^T r - 2e_y^T \bar{C}\Lambda\tilde{K}^T r \end{aligned} \tag{6.22}$$

Note that the 2nd, 3rd, 5th and 6th lines in the above equation equal zero. Therefore, (6.22) can be written as

$$\dot{V} = -\mathcal{E}^T M(\mu)\mathcal{E}$$

where

$$M(\mu) = \begin{bmatrix} \bar{Q} & -2\bar{C}\Lambda\Theta^{*T} \\ -2\Theta^*\Lambda\bar{C}^T & Q \end{bmatrix} \quad \mathcal{E} = \begin{bmatrix} e_y \\ e \end{bmatrix}$$

$\bar{Q} \geq \mu \bar{P}$ and therefore

$$M(\mu) \geq \begin{bmatrix} \bar{\mu}\bar{P} & -2\bar{C}\Lambda\Theta^{*T} \\ -2\Theta^*\Lambda\bar{C}^T & Q \end{bmatrix} \quad \mathcal{E} = \begin{bmatrix} e_y \\ e \end{bmatrix}$$

Given that $\mu > \mu^*$, μ is necessarily positive and $\mu\bar{P} - 4\bar{C}\Lambda\Theta^{*T}Q^{-1}\Theta^*\Lambda\bar{C}^T > 0$. By Lemma 2.2, $M(\mu)$ is positive definite. Therefore $\dot{V} \leq 0$ and thus $e_y, e, \tilde{\Theta}, \tilde{K} \in \mathcal{L}_\infty$. Furthermore, given that M is positive definite $e_y, e \in \mathcal{L}_2$. Using Barbalat Lemma it follows that $\lim_{t\to\infty} e(t) \to 0$. □

6.3 MIMO LQG/LTR

Let L in (6.2) be chosen as

$$L_\nu = -P_\nu C R_\nu^{-1}. \tag{6.23}$$

where P_ν is the solution to the Riccati Equation

$$P_\nu A_m^T + A_m P_\nu - P_\nu C R_\nu^{-1} C^T P_\nu + Q_\nu = 0 \tag{6.24}$$

where $Q_0 = Q_0^T > 0$ in $\mathbb{R}^n$ and $R_0 = R_0^T > 0$ in $\mathbb{R}^m$ and $\nu > 0$, with

$$Q_\nu = Q_0 + \left(1 + \frac{1}{\nu}\right) BB^T, \quad R_\nu = \frac{\nu}{\nu+1} R_0.$$

Note that (6.24) can also be represented as

$$P_\nu (A_m + LC^T)^T + (A_m + LC^T) P_\nu = -P_\nu C R_\nu^{-1} C^T P_\nu - Q_\nu \tag{6.25}$$

which is also equivalent to

$$(A_m + LC^T)^T \tilde{P}_\nu + \tilde{P}_\nu (A_m + LC^T) = -C R_\nu^{-1} C^T - \tilde{Q}_\nu \tag{6.26}$$

where

$$\tilde{P}_\nu = P_\nu^{-1} \text{ and } \tilde{Q}_\nu = \tilde{P}_\nu Q_\nu \tilde{P}_\nu.$$

The update law for the adaptive parameters is then given as

$$\begin{aligned} \dot{\Theta} =& \text{Proj}_{\Omega_1}(-\Gamma_\theta x_m e_y^T R_0^{-1/2} W, \Theta) \\ \dot{K} =& \text{Proj}_{\Omega_2}(-\Gamma_k r e_y^T R_0^{-1/2} W, K) \end{aligned} \tag{6.27}$$

$B^T C R_0^{-1/2} = U\Sigma V$ and $W = (UV)^T$.

Remark 6.1. The stability analysis of this method was first presented in [47]. This remark illustrates one issue with this techniques. Consider the Lyapunov candidate

$$V = e^T \tilde{P}_\nu e + \text{Tr}(\Lambda \tilde{\Theta}^T \Gamma^{-1} \tilde{\Theta}) + \text{Tr}(\Lambda \tilde{K}^T \Gamma^{-1} \tilde{K}).$$

Taking the time derivative

$$\begin{aligned}\dot{V} =& -e^T\tilde{Q}_\nu e - e^T C R_\nu^{-1} C^T e + 2e^T\tilde{P}_\nu B\Lambda\Theta^{*T} e \\ &+ 2e^T\tilde{P}_\nu B\Lambda\tilde{\Theta}^T x_m + 2\mathrm{Tr}(\Lambda\tilde{\Theta}^T x_m e_y^T R_0^{-1/2} W) \\ &+ 2e^T\tilde{P}_\nu B\Lambda\tilde{K}^T r + 2\mathrm{Tr}(\Lambda\tilde{K}^T r e_y^T R_o^{-1/2} W)\end{aligned}$$

which can simplify as

$$\begin{aligned}\dot{V} \leq& -e^T\tilde{Q}_\nu e - e^T C R_\nu^{-1} C^T e + 2e^T\tilde{P}_\nu B\Lambda\Theta^{*T} e \\ &+ O(\nu)\|e\|\|x_m\| + O(\nu)\|e\|\|r\|\end{aligned}$$

as $\nu \to 0$. This leads to a problem however, as x_m is a function of e and therefore, it is difficult to bound x_m before the boundedness of e is obtained.

Theorem 6.3. *The Adaptive system given in* (6.1), (6.2), (6.18), *following Assumptions 6.1-6.3 and with L chosen as in* (6.23) *is stable, and* $\lim_{t\to\infty} e(t) = 0$ *for all ν sufficiently small.*

Proof. Consider the Lyapunov candidate

$$V = e^T\tilde{P}_0 e + \mathrm{Tr}(\Lambda\tilde{\Theta}^T\Gamma^{-1}\tilde{\Theta}) + \mathrm{Tr}(\Lambda\tilde{K}^T\Gamma^{-1}\tilde{K}) \tag{6.28}$$

Taking the derivative along the system trajectories results in

$$\begin{aligned}\dot{V} =& -e^T\tilde{Q}_\nu e - e^T C R_\nu^{-1} C^T e + 2e^T\tilde{P}_0 B\Lambda\Theta^{*T} e \\ &- e^T(A_m + L_\nu C^T)^T \sum_{i=1}^{\infty} \nu^i \tilde{P}_i e \\ &- e^T \sum_{i=1}^{\infty} \nu^i \tilde{P}_i (A_m + L_\nu C^T) e \\ &+ 2e^T\tilde{P}_0 B\Lambda\tilde{\Theta}^T x_m + 2\mathrm{Tr}(\Lambda\tilde{\Theta}^T x_m e_y^T R_0^{-1/2} W) \\ &+ 2e^T\tilde{P}_0 B\Lambda\tilde{K}^T r + 2\mathrm{Tr}(\Lambda\tilde{K}^T r e_y^T R_o^{-1/2} W)\end{aligned} \tag{6.29}$$

Expanding R_ν and L_ν and using the fact that $\tilde{P}_0 B = C R_0^{-1/2} W$

$$\begin{aligned}\dot{V} =& -e^T\tilde{Q}_\nu e - e^T C\frac{\nu+1}{\nu} R_0^{-1} C^T e \\ &- e^T(A_m - \tilde{P}_\nu C\frac{\nu+1}{\nu} R_0^{-1} C^T)^T \sum_{i=1}^{\infty} \nu^i \tilde{P}_i e \\ &- e^T \sum_{i=1}^{\infty} \nu^i \tilde{P}_i (A_m - \tilde{P}_\nu C\frac{\nu+1}{\nu} R_0^{-1} C^T) e \\ &+ 2e^T C R_0^{-1/2} W\Lambda\Theta^{*T} e.\end{aligned} \tag{6.30}$$

Collecting the $O(\nu)$ terms

$$\begin{aligned}\dot{V} \leq & -e^T\tilde{Q}_0 e - \frac{1}{\nu}e_y^T R_0^{-1} e_y + O(\nu)e^T e \\ & - e^T(\tilde{P}_\nu C\frac{\nu+1}{\nu}R_0^{-1}C^T)^T\nu\tilde{P}_1 e \\ & - e^T\nu\tilde{P}_1\tilde{P}_\nu C\frac{\nu+1}{\nu}R_0^{-1}C^T e \\ & + 2e^T C R_0^{-1/2}W\Lambda\Theta^{*T}e\end{aligned} \tag{6.31}$$

Collecting more $O(\nu)$ terms from the 2nd and 3rd lines above results in

$$\begin{aligned}\dot{V} \leq & -e^T\tilde{Q}_0 e - \frac{1}{\nu}e_y^T R_0^{-1} e_y + O(\nu)e^T e \\ & - e^T C R_0^{-1}C^T P_\nu\tilde{P}_1 e - e^T\tilde{P}_1\tilde{P}_\nu C R_0^{-1}C^T e \\ & + 2e^T C R_0^{-1/2}W\Lambda\Theta^{*T}e.\end{aligned} \tag{6.32}$$

Using the fact that $e_y = C^T e$

$$\begin{aligned}\dot{V} \leq & -e^T\tilde{Q}_0 e - \frac{1}{\nu}e_y^T R_0^{-1} e_y + O(\nu)e^T e \\ & - e_y^T R_0^{-1}C^T P_\nu\tilde{P}_1 e - e^T\tilde{P}_1\tilde{P}_\nu C R_0^{-1}e_y \\ & + 2e_y^T R_0^{-1/2}W\Theta^{*T}e\end{aligned} \tag{6.33}$$

□

Let $P_\Theta = R_0^{-1}C^T P_\nu\tilde{P}_1 - R_0^{-1/2}W\Theta^{*T}$. Then the above can be simplified as

$$\dot{V} \leq -\mathcal{E}^T M(\nu)\mathcal{E} + O(\nu)e^T e. \tag{6.34}$$

where

$$M(\nu) = \begin{bmatrix}\frac{1}{\nu}R_0^{-1} & P_\Theta \\ P_\Theta^T & \tilde{Q}_0\end{bmatrix} \text{ and } \mathcal{E} = \begin{bmatrix}e_y \\ e\end{bmatrix} \tag{6.35}$$

Given that Q_0 is positive definite, $\frac{1}{\nu}R_0^{-1} > 0$ and for ν sufficiently small $\frac{1}{\nu}R_0^{-1} - P_\Theta\tilde{Q}_0^{-1}P_\Theta^T > 0$. It follows that the $M(\nu)$ is positive definite and thus adaptive system is bounded for sufficiently small ν. Furtheremore, given that e is a subset of $\mathcal{E}$, it follows that $e \in \mathcal{L}_2$. Thus, by Barbalat Lemma, $\lim_{t\to\infty} e(t) = 0$.

6.4 Adaptive Control for Very Flexible Aircraft

This section illustrates how the LQG/LTR adaptive controller is ideal for the stabilization of Very Flexible Aircraft. The model that will be used to validate the controller is that presented in Chapter 5. The inputs available for control are Thrust $\mathcal{T}$, center elevator δ_{e_c} and the outer ailerons δ_{a_o}, the other inputs, δ_{e_c} and δ_{o_c} are fixed at trim values. It is assumed that the states available for measurement are the

Velocity V, the dihedral angle η, and the pitch rate q. The control problem then is equivalent to the design of a stabilizing controller for the system

$$\dot{x} = Ax + B\Lambda u, \quad y = C^T x \tag{6.36}$$

where $x \in \mathbb{R}^n$, $u, y \in \mathbb{R}^m$. The system Jacobian A is unknown, and Λ is a positive unknown diagonal matrix representing uncertain input effectiveness in an aircraft.

The following assumptions are made:

- (A, B) is controllable and (A, C^T) is observable.
- $\det\,(C^T B) \neq 0$.
- $C^T(sI - A)^{-1}B$ is minimum phase.

The control design incorporates two components

$$u = u_{\text{nom}} + u_{\text{ad}} \tag{6.37}$$

a nominal and adaptive component. The nominal and adaptive components are defined as

$$u_{\text{nom}} = K^T x_m \quad \text{and} \quad u_{\text{ad}} = \Theta^T(t) x_m \tag{6.38}$$

where K is the baseline fixed gain, $\Theta(t)$ is the adaptive gain, and x_m is the state of the reference model. The reference model dynamics are defined as

$$\dot{x}_m = (A_{\text{nom}} + L_\nu C^T)x_m + Bu_{\text{nom}} + L_\nu y, \quad y_m = C^T x_m \tag{6.39}$$

where A_{nom} is a nominal value for the state Jacobian matrix, and L_ν is the closed loop reference model gain chosen as,

$$L_\nu = P_o C R_o^{-1}$$

with $P_o = P_o^T > 0$ the solution to the *Observer Algebraic Riccati Equation* (OARE)

$$P_o(A_{\text{nom}} + BK^T)^T + (A_{\text{nom}} + BK^T)P_o - P_o C R_o^{-1} C^T P_o + Q_o = 0.$$

The weighting parameters (Q_o, R_o), both symmetric and positive definite, are defined as

$$Q_o = Q_0 + \frac{\nu + 1}{\nu} BB^T, \quad R_o = \frac{\nu}{\nu + 1} R_0$$

where Q_0 and R_0 are symmetric positive definite free design parameters and ν is a small gain parameter.

The control input for the baseline controller is chosen as

$$K^T = -R_c^{-1} B^T P_c$$

with $P_c = P_c^T > 0$ the solution to the *Control Algebraic Riccati Equation* (CARE)

$$P_c A_{\text{nom}} + A_{\text{nom}}^T P_c - P_c B R_c^{-1} B^T P_c + Q_c = 0.$$

The free design weights (Q_c, R_c), are both symmetric and positive definite. The reference model Jacobian is defined as

$$A_m \triangleq A_{\text{nom}} + BK^T$$

and using this definition the reference model dynamics can be simplified as

$$\dot{x}_m = A_m x_m - L_o C^T e$$

where $e = x - x_m$. The adaptive gain is adjusted as

$$\dot{\Theta} = \text{Proj}\left(\Theta, -\Gamma x_m e_y^T R_0^{-1} W, F(\Theta; \vartheta, \varepsilon)\right) \tag{6.40}$$

where

$$\begin{aligned} e_y &= y - y_m \\ W &= VU^T \\ B^T C R_0^{-\frac{1}{2}} &= U\Lambda V^T. \end{aligned}$$

The convex function $F = [f_1 \ \dots \ f_m]^T \in \mathbb{R}^{m\times 1}$ where

$$f_i(\theta_i) = f(\theta_i; \vartheta, \varepsilon)$$

with

$$f(\theta; \vartheta, \varepsilon) \triangleq \frac{\|\theta\|^2 - \vartheta^2}{2\varepsilon\vartheta + \varepsilon^2}.$$

In addition to the reference model and baseline control free design parameters, the adaptive controller is uniquely defined by the choice of $(\Gamma, \vartheta, \varepsilon)$. Schematic representations for the two controllers can be found in Figure 6-2

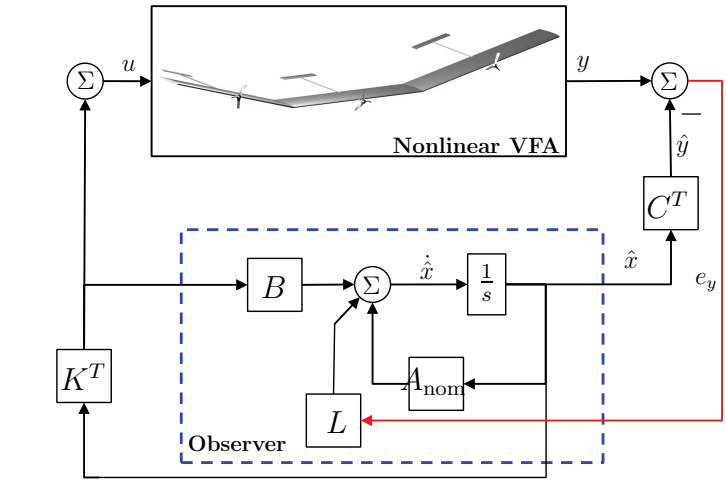

(a) Linear LQG/LTR

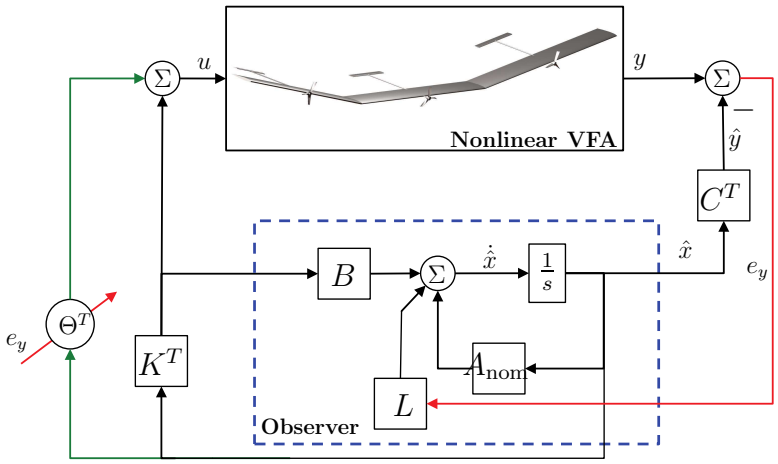

(b) Adaptive LQG/LTR

Figure 6-2: Comparison of adaptive and linear controller to dihedral disturbance.

6.4.1 Comparison of linear and adaptive controllers

Table 6.1: Control Design Parameters.

Variable	Value
Q_0	$I^{7\times 7}$
R_0	$I^{3\times 3}$
ν	0.04
Q_c	$\text{diag}\big([1\ 10\ 1\ 1\ 10\ 0.01\ 10]^T\big)$
R_c	$\text{diag}\big([10\ 100\ 100]^T\big)$;
Γ	$15 \cdot \text{diag}\left([0.01\ 0.1\ 0.0001\ 1\ 10\ 10\ 0.01]^T\right)$
ϑ	5
ε	0.1

Two simulation studies now follow that compare the a linear LQG/LTR Controller and an adaptive LQG/LTR controller. The first simulation study is without the presence of turbulence. The second simulation study is in the presence of turbulence using the same turbulence model as in Section **??** with $D = \sqrt{0.5}$ and $\Delta_t = 0.1$. For the simulation studies that follows the aircraft was initially trimmed at an altitude of 1,000 ft, a speed of 35 ft/s with a dihedral angle of 5 deg. Then, the initial condition on the dihedral angle was changed to 40 deg and then the simulation was started. Also, to ensure that the controllers were not achieving good performance while sacrificing robustness to actuator dynamics, a first order actuator model with a pole at -20 rad/s and a rate saturation limit of 60 deg/s was added to each control surface. A complete list of the free design parameters used to build the controllers can be found in Table 6.1.

Simulation results for the first study are displayed in Figures 6-3 through 6-5. Figure 6-3 shows the first 20 seconds of the simulation run, Figure 6-4 shows 80 seconds of the simulation run, and Figure 6-5 shows the adaptive control parameters over an 80 second time window. Figures 6-3 and 6-4 contain the dihedral angle, angle of attack, inner elevator position, and outer aileron position. The first thing to note in Figure 6-3 is that the adaptive controller is able to reduce the dihedral more rapidly than the linear controller. When only the linear controller is present the dihedral oscillates in a divergent fashion and exceeds 50 degrees. It is important to note that while the adaptive controller has superior stability properties as compared to the linear controller, the control action required by the adaptive controller is not excessive. The reason for the lack of stability in the linear controller is due to the fact that the linear controller is tuned for the VFA with a dihedral angle of 5 degrees. When the VFA model has a dihedral angle of 45 degrees, the phugoid mode is less stable and the actuators become less affective. Given that the linear controller was diverging, only 20 seconds of the linear control history are presented in Figure 6-4. Over the longer time window, Figure 6-4 illustrates that the adaptive controller is able to stabilize the VFA back to a dihedral angle of 5 degrees. Looking at Figure 6-5 it is interesting to note that the adaptive control gains do in fact hit the projection limit of 5. However, the adaptive controller maintaines stability.

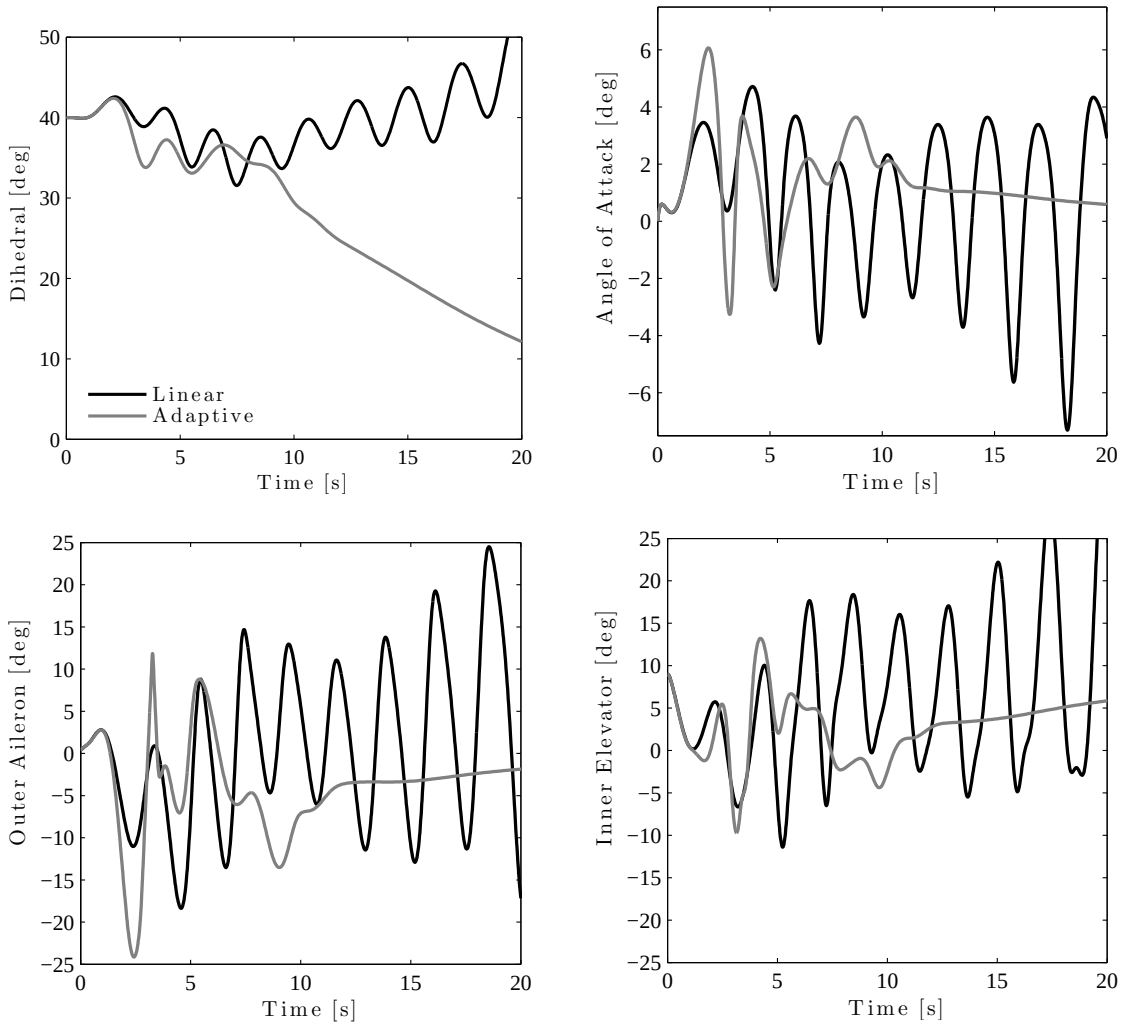

Figure 6-3: Comparison of adaptive and linear controller to dihedral disturbance $t \in [0, 20]$.

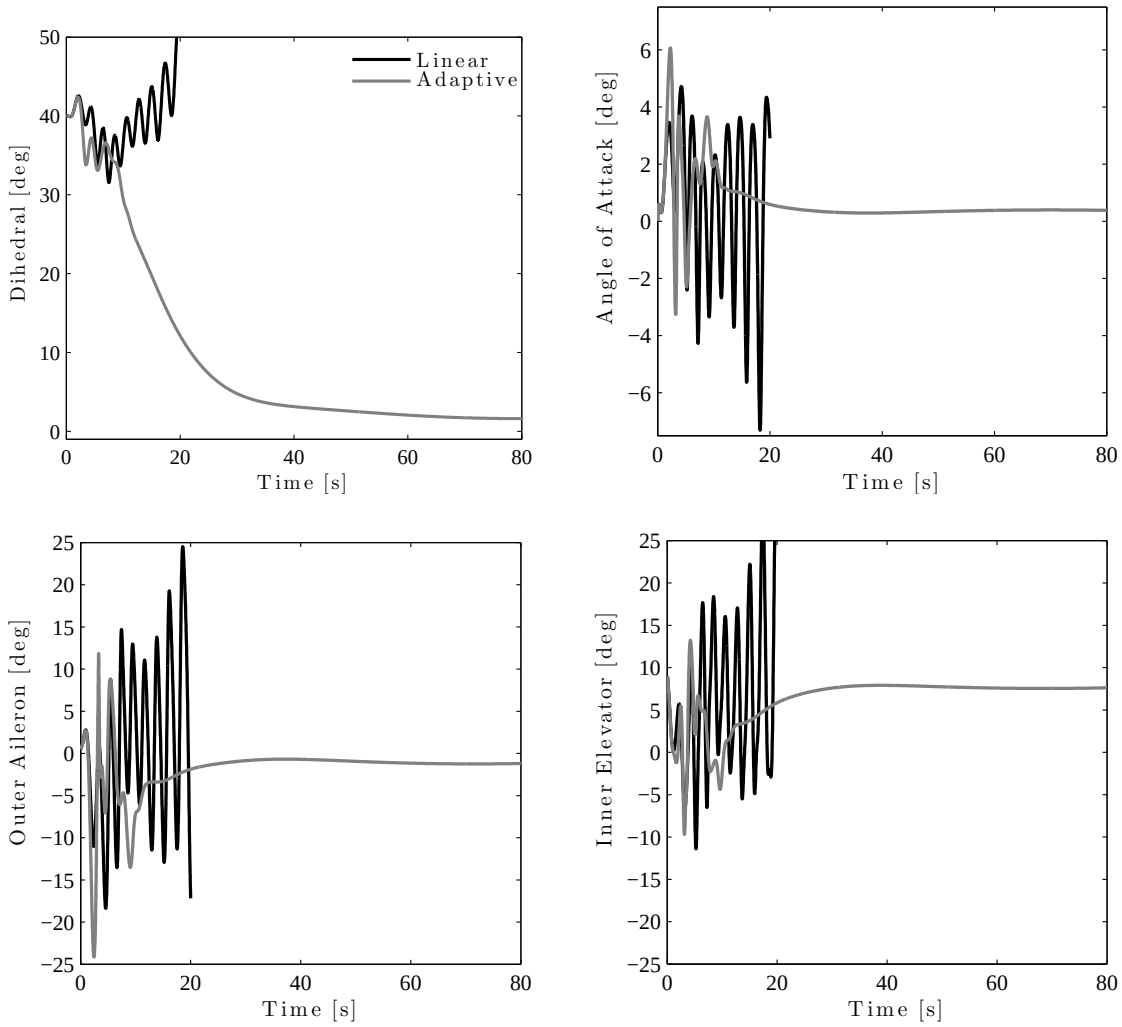

Figure 6-4: Comparison of adaptive and linear controller to dihedral disturbance $t \in [0, 80]$.

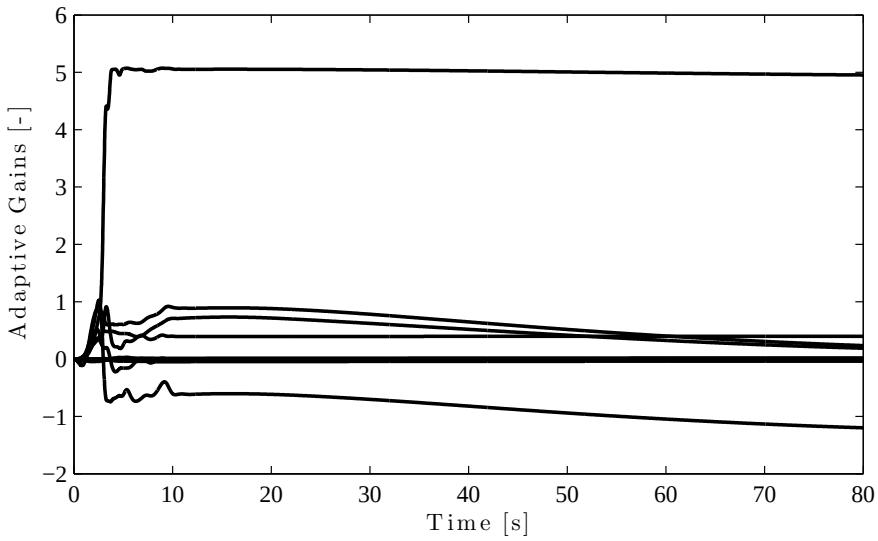

Figure 6-5: Adaptive gains without turbulence $t \in [0, 80]$.

Simulation results for the second study (in the presence of turbulence) are displayed in Figures 6-6 through 6-8. Figure 6-6 shows the first 20 seconds of the simulation run, Figure 6-7 shows 800 seconds of the simulation run, and Figure 6-8 shows the adaptive control parameters over an 800 second time window. Figures 6-6 and 6-7 contain the dihedral angle, angle of attack, inner elevator position, and outer aileron position. Inspecting Figure 6-6 we see that similar to the previous simulation study the linear controller quickly diverges and the simulation has to be stopped at 16 seconds as the dihedral angle diverges past 50 degrees and the VFA does not recover. Also, as before, the adaptive controller does not use excessive control force in stabilizing the system, and the angle of attack never exceeds 6 degrees in magnitude. Comparing the results in Figure 6-6 to those in 6-3 the control surfaces are more oscillatory due to the presence of turbulence. From Figure 6-7 it can be observered that adaptive controller is not able to have the dihedral asymptotically track 5 degrees. With the presence of turbulence the adaptive controller is only able to bring the dihedral to a bounded region near trim. Investigating Figure 6-8 we see that the adaptive parameters hit the projection limits on several occasions, yet stability is maintained.

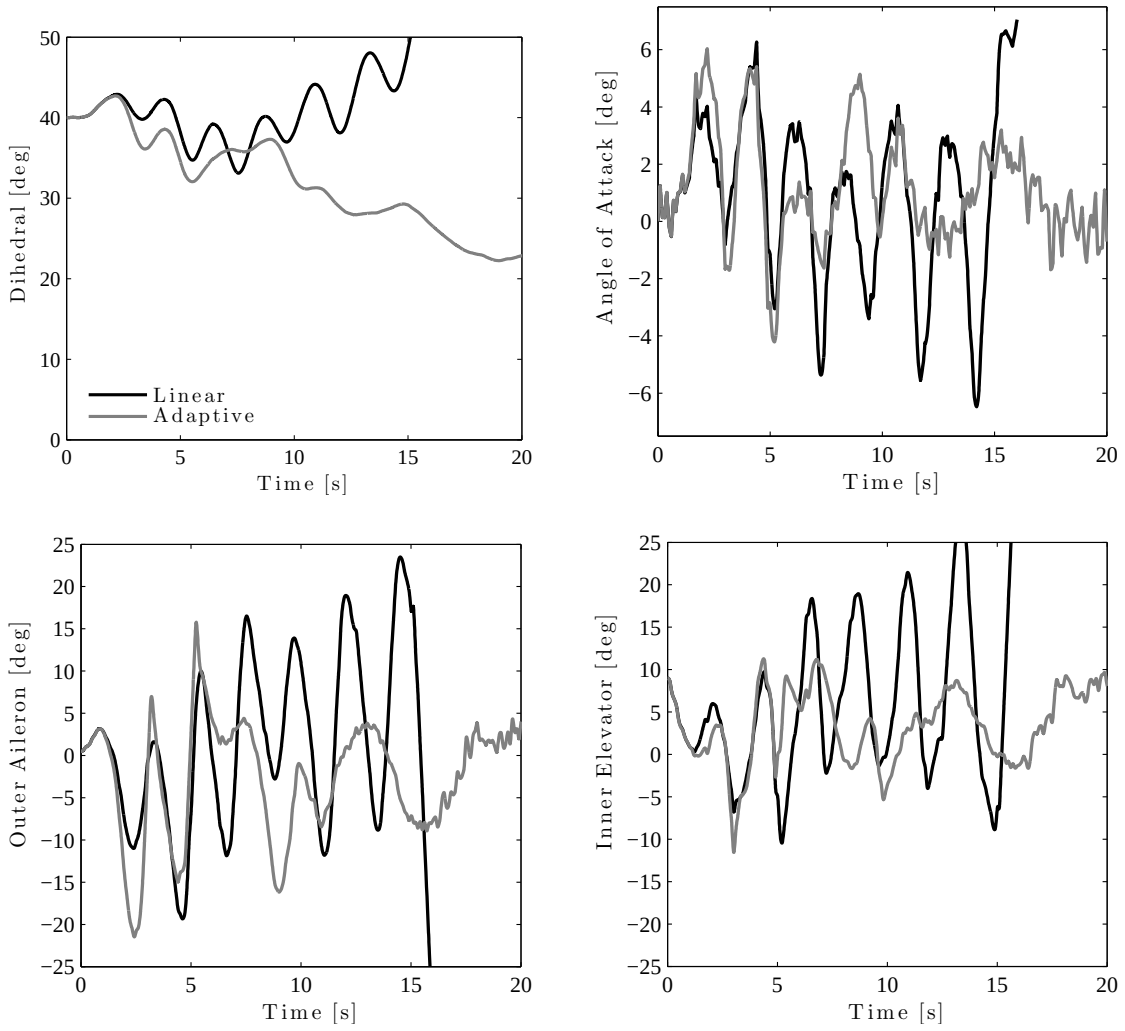

Figure 6-6: Comparison of adaptive and linear controller in the presence of turbulence over $t \in [0, 20]$.

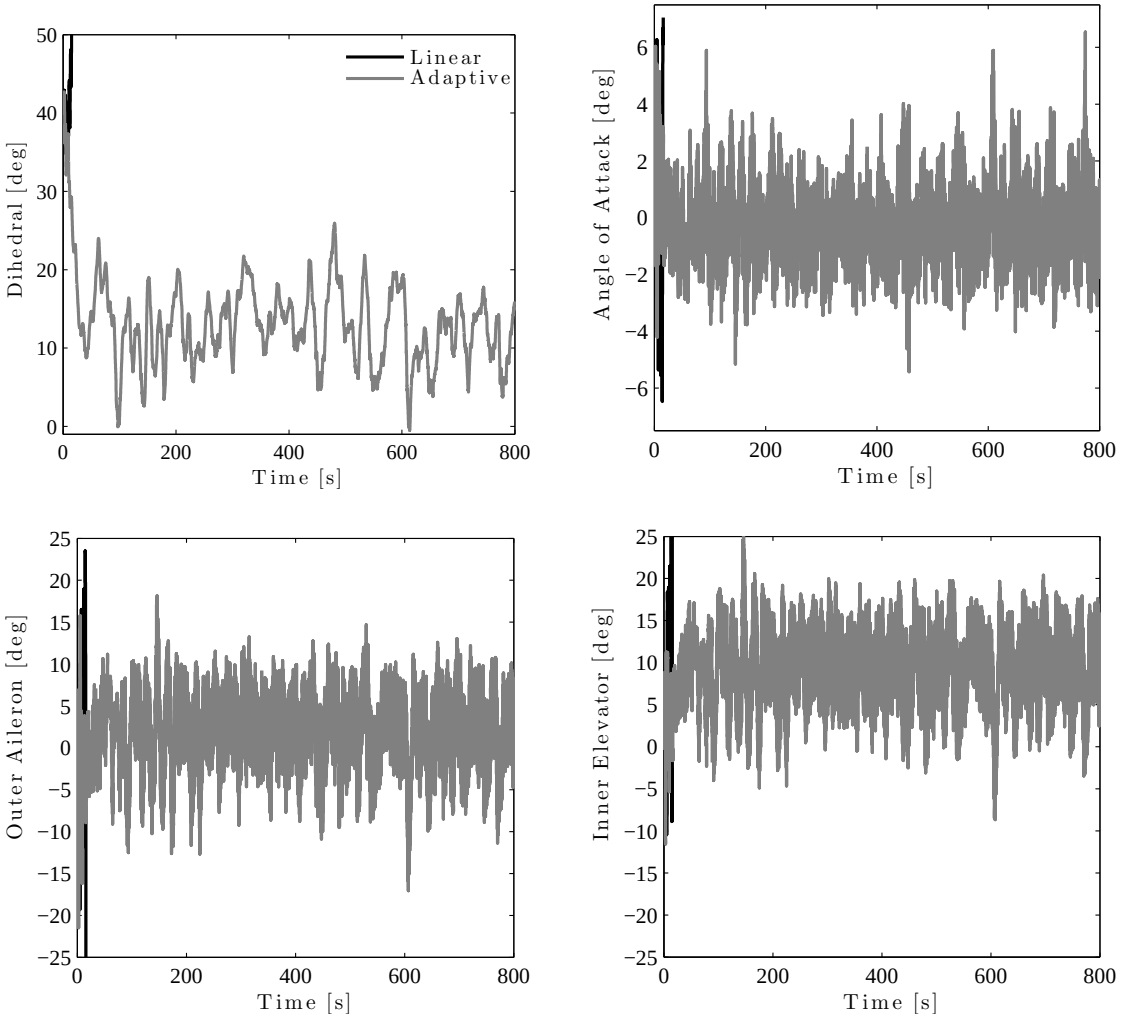

Figure 6-7: Comparison of adaptive and linear controller to dihedral disturbance in the presence of turbulence over $t \in [0, 800]$.

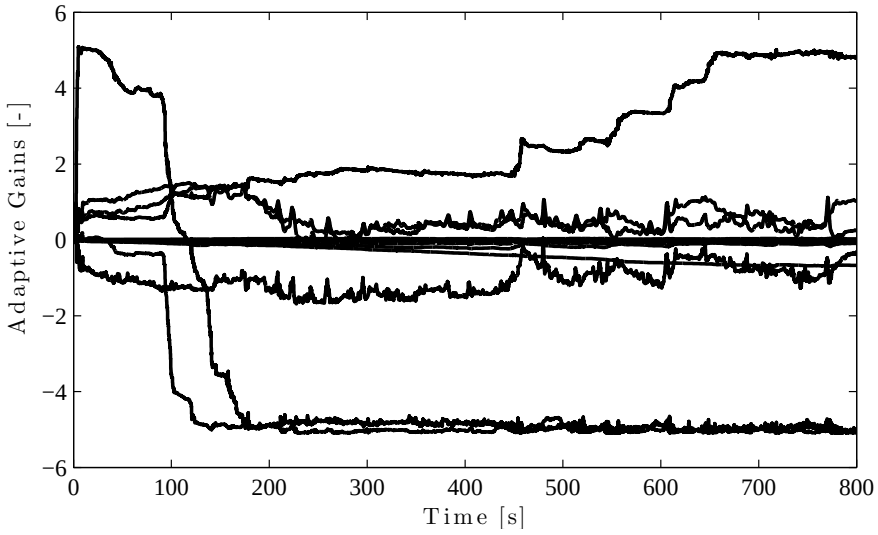

Figure 6-8: Adaptive gains in the presence of turbulence $t \in [0, 800]$.

Chapter 7

Conclusions

In this thesis the stability properties and transient performance of adaptive systems with closed loop reference models was explored. It was shown that CRM adaptive system have a transient performance improvement that is directly quantifiable by a reduction in the high frequency oscillations of the adaptive parameters. This result was shown to hold in scalar, full states accessible and output feedback systems. CRM adaptive systems can also be designed so as to have filtered regressor vector feedback, which results in improved performance in the presence of measurement noise and input disturbances.

A first principles control oriented model of a VFA was also presented. It was shown that VFA are susceptible to turbulence induced dihedral drift, the most likely catalyst to the Helios accident. A CRM adaptive system in the form of an LQG/LTR controller was shown to be a viable candidate for the adaptive control of VFA as well.

7.1 Future Work

One of the biggest observations from the analysis and simulations of CRM adaptive systems is that there is a trade off between synchronization and adaptation that can occur. This manifested itself in Chapter 3 when the peaking phenomenon was explored. When the observer gain is large in magnitude, the reference model can start to act as an observer more than a reference trajectory. This can have a negative impact on performance when the open-loop system is unstable as the reference model tracks the divergent plant. Also, due to the fact that the model following error is small with large observer gain, the adaptive parameters are not able to quickly stabilize the system. Thus, with large observer gain the closed-loop system with plant and reference model can be highly synchronized, and unless the adaptive tuning gain is chosen appropriately very little adaptation can occur, as was shown in Chapter 3. With the recent interest in complex systems [1, 50, 64] the notion of synchronization versus learning in complex networks would be an interesting endeavor.

Appendix A

Projection Algorithm

A.1 Properties of Convex Sets and Functions

Definition A.1. A set $E \subset \mathbb{R}^k$ is *convex* if

$$\lambda x + (1-\lambda)y \in E$$

whenever $x \in E$, $y \in E$, and $0 \leq \lambda \leq 1$

Remark A.1. Essentially, a convex set has the following property. For any two points $x, y \in E$ where E is convex, all the points on the connecting line from x to y are also in E.

Definition A.2. A function $f : \mathbb{R}^k \to \mathbb{R}$ is *convex* if

$$f(\lambda x + (1-\lambda)y) \leq \lambda f(x) + (1-\lambda) f(y)$$

$\forall 0 \leq \lambda \leq 1$.

Lemma A.1. *Let $f(\theta) : \mathbb{R}^k \to \mathbb{R}$ be a convex function. Then for any constant $\delta > 0$ the subset $\Omega_\delta = \{\theta \in \mathbb{R}^k | f(\theta) \leq \delta\}$ is convex.*

Proof. Let $\theta_1, \theta_2 \in \Omega_\delta$. Then $f(\theta_1) \leq \delta$ and $f(\theta_2) \leq \delta$. Since $f(x)$ is convex then for any $0 \leq \lambda \leq 1$

$$f\big(\underbrace{\lambda\theta_1 + (1-\lambda)\theta_2}_{\theta}\big) \leq \lambda \underbrace{f(\theta_1)}_{\leq\delta} + (1-\lambda)\underbrace{f(\theta_2)}_{\leq\delta} \leq \lambda\delta + (1-\lambda)\delta = \delta$$

$\therefore f(\theta) \leq \delta$, thus, $\theta \in \Omega_\delta$. □

Lemma A.2. *Let $f(\theta) : \mathbb{R}^k \to \mathbb{R}$ be a continuously differentiable convex function. Choose a constant $\delta > 0$ and consider $\Omega_\delta = \{\theta \in \mathbb{R}^k | f(\theta) \leq \delta\} \subset \mathbb{R}$. Let θ^* be an interior point of Ω_δ, i.e. $f(\theta^*) < \delta$. Choose θ_b as a boundary point so that $f(\theta_b) = \delta$. Then the following holds:*

$$(\theta^* - \theta_b)^T \nabla f(\theta_b) \leq 0 \tag{A.1}$$

where $\nabla f(\theta_b) = \left(\frac{\partial f(\theta)}{\partial \theta_1} \ \cdots \ \frac{\partial f(\theta)}{\partial \theta_k}\right)^T$ evaluated at θ_b.

Proof. $f(\theta)$ is convex $\therefore$

$$f\left(\lambda\theta^* + (1-\lambda)\theta_b\right) \leq \lambda f(\theta^*) + (1-\lambda) f(\theta_b)$$

equivalently,

$$f\left(\theta_b + \lambda(\theta^* - \theta_b)\right) \leq f(\theta_b) + \lambda\left(f(\theta^*) - f(\theta_b)\right)$$

For any $0 < \lambda \leq 1$:

$$\frac{f\left(\theta_b + \lambda(\theta^* - \theta_b)\right) - f(\theta_b)}{\lambda} \leq f(\theta^*) - f(\theta_b) \leq \delta - \delta = 0$$

and taking the limit as $\lambda \to 0$ yields (A.1). □

A.2 Projection

Definition A.3. The *Projection Operator* for two vectors $\theta, y \in \mathbb{R}^k$ is now introduced as

$$\text{Proj}(\theta, y, f) = \begin{cases} y - \frac{\nabla f(\theta)(\nabla f(\theta))^T}{\|\nabla f(\theta)\|^2} y f(\theta) & \text{if } f(\theta) > 0 \wedge y^T \nabla f(\theta) > 0 \\ y & \text{otherwise.} \end{cases} \tag{A.2}$$

where $f : \mathbb{R}^k \to \mathbb{R}$ is a convex function and $\nabla f(\theta) = \left(\frac{\partial f(\theta)}{\partial \theta_1} \cdots \frac{\partial f(\theta)}{\partial \theta_k}\right)^T$. Note that the following are notationally equivalent $\text{Proj}(\theta, y) = \text{Proj}(\theta, y, f)$ when the exact structure of the convex function f is of no importance.

Remark A.2. A geometrical interpretation of (A.2) follows. Define a convex set Ω_0 as

$$\Omega_0 \triangleq \left\{\theta \in \mathbb{R}^k | f(\theta) \leq 0\right\} \tag{A.3}$$

and let Ω_1 represent another convex set such that

$$\Omega_1 \triangleq \left\{\theta \in \mathbb{R}^k | f(\theta) \leq 1\right\} \tag{A.4}$$

From (A.3) and (A.4) $\Omega_0 \subset \Omega_1$. From the definition of the projection operator in (A.4) θ is not modified when $\theta \in \Omega_0$. Let

$$\Omega_{\mathcal{A}} \triangleq \Omega_1 \backslash \Omega_0 = \left\{\theta | 0 < f(\theta) \leq 1\right\}$$

represent an annulus region. Within $\Omega_{\mathcal{A}}$ the projection algorithm subtracts a scaled component of y that is normal to boundary $\left\{\theta | f(\theta) = \lambda\right\}$. When $\lambda = 0$, the scaled normal component is 0, and when $\lambda = 1$, the component of y that is normal to the boundary Ω_1 is entirely subtracted from y, so that $\text{Proj}(\theta, y, f)$ is tangent to the boundary $\left\{\theta | f(\theta) = 1\right\}$. This discussion is visualized in Figure A-1.

Remark A.3. Note that $(\nabla f(\theta))^T \text{Proj}(\theta, y) = 0 \forall \theta$ when $f(\theta) = 1$ and that the

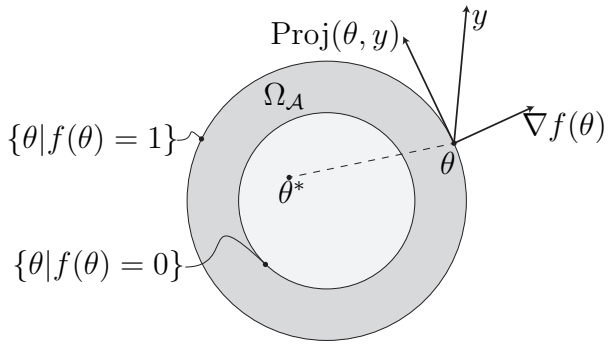

Figure A-1: Visualization of Projection Operator in $\mathbb{R}^2$.

general structure of the algorithm is as follows

$$\text{Proj}(\theta, y) = y - \alpha(t)\nabla f(\theta) \tag{A.5}$$

for some time varying α when the modification is triggered. Multiplying the left hand side of the equation by $(\nabla f(\theta))^T$ and solving for α one finds that

$$\alpha(t) = \left((\nabla f(\theta))^T \nabla f(\theta)\right)^{-1} (\nabla f(\theta))^T y \tag{A.6}$$

and thus the algorithm takes the form

$$\text{Proj}(\theta, y) = y - \nabla f(\theta) \left((\nabla f(\theta))^T \nabla f(\theta)\right)^{-1} (\nabla f(\theta))^T y f(\theta) \tag{A.7}$$

where the modification is active. Notice that the $f(\theta)$ has been added to the definition, making (A.7) continuous.

Lemma A.3. *One important property of the projection operator follows. Given* $\theta^* \in \Omega_0$*,*

$$(\theta - \theta^*)^T (\mathit{Proj}(\theta, y, f) - y) \leq 0. \tag{A.8}$$

Proof. Note that

$$(\theta - \theta^*)^T (\text{Proj}(\theta, y, f) - y) = (\theta^* - \theta)^T (y - \text{Proj}(\theta, y, f))$$

If $f(\theta) > 0 \wedge y^T \nabla f(\theta) > 0$, then

$$(\theta^* - \theta)^T \left(y - \left(y - \frac{\nabla f(\theta)(\nabla f(\theta))^T}{\|\nabla f(\theta)\|^2} y f(\theta) \right) \right)$$

and using Lemma A.2

$$\frac{\underbrace{(\theta^* - \theta)^T \nabla f(\theta)}_{\leq 0} \underbrace{(\nabla f(\theta))^T y}_{>0}}{\|\nabla f(\theta)\|^2} \underbrace{f(\theta)}_{\geq 0} \leq 0$$

otherwise $\text{Proj}(\theta, y, f) = y$. □

Definition A.4 (Projection Operator)**.** The general form of the projection operator is the $n \times m$ matrix extension to the vector definition above.

$$\text{Proj}(\Theta, Y, F) = [\text{Proj}(\theta_1, y_1, f_1) \ \dots \ \text{Proj}(\theta_m, y_m, y_m)]$$

where $\Theta = [\theta_1 \ \dots \ \theta_m] \in \mathbb{R}^{n\times m}, Y = [y_1 \ \dots \ y_m] \in \mathbb{R}^{n\times m}$, and $F = [f_1(\theta_1) \ \dots \ f_m(\theta_m)]^T \in \mathbb{R}^{m\times 1}$. Recalling (A.2)

$$\text{Proj}(\theta_j, y_j, f_j) = \begin{cases} y_j - \frac{\nabla f_j(\theta_j)(\nabla f_j(\theta_j))^T}{\|\nabla f_j(\theta_j)\|^2} y_j f_j(\theta_j) & \text{if } f_j(\theta_j) > 0 \wedge y_j^T \nabla f_j(\theta_j) > 0 \\ y_j & \text{otherwise} \end{cases}$$

$j = 1$ to m.

Lemma A.4. *Let $F = [f_1 \ \dots \ f_m]^T \in \mathbb{R}^{m\times 1}$ be a convex vector function and $\hat{\Theta} = [\hat{\theta}_1 \ \dots \ \hat{\theta}_m], \Theta = [\theta_1 \ \dots \ \theta_m], Y = [y_1 \ \dots \ y_m]$ where $\hat{\Theta}, \Theta, Y \in \mathbb{R}^{n\times m}$ then,*

$$\textit{trace}\Big\{\big(\hat{\Theta} - \Theta\big)^T \big(\textit{Proj}(\hat{\Theta}, Y, F) - Y\big)\Big\} \leq 0.$$

Proof. Using (A.8),

$$\begin{aligned} \text{trace}\Big\{\big(\hat{\Theta} - \Theta\big)^T \big(\text{Proj}(\hat{\Theta}, Y, F) - Y\big)\Big\} &= \sum_{j=1}^{m} (\hat{\theta}_j - \theta_j)^T (\text{Proj}(\hat{\theta}_j, y_j, f_j) - y_j) \\ &\leq 0. \end{aligned}$$

□

The application of the projection algorithm in adaptive control is explored below.

Lemma A.5. *If an initial value problem, i.e. adaptive control algorithm with adaptive law and initial conditions, is defined by:*

1. $\dot{\theta} = Proj(\theta, y, f)$
2. $\theta(t = 0) = \theta_0 \in \Omega_1 = \{\theta \in \mathbb{R}^k | f(\theta) \leq 1\}$
3. $f(\theta) : \mathbb{R}^k \to \mathbb{R}$ *is convex*

Then $\theta(t) \in \Omega_1 \forall t \geq 0$.

Proof. Taking the time derivative of the convex function

$$\dot{f}(\theta) = (\nabla f(\theta))^T \dot{\theta} = (\nabla f(\theta))^T \text{Proj}(\theta, y, f) \tag{A.9}$$

Substitution of (A.9) into (A.2) leads to

$$\begin{aligned} \dot{f}(\theta) &= (\nabla f(\theta))^T \text{Proj}(\theta, y, f) \\ &= \begin{cases} (\nabla f(\theta))^T y(1 - f(\theta)) & \text{if } f(\theta) > 0 \wedge y^T \nabla f(\theta) > 0 \\ (\nabla f(\theta))^T y & \text{if } f(\theta) \leq 0 \vee y^T \nabla f(\theta) \leq 0 \end{cases} \end{aligned}$$

therefore

$$\begin{cases} \dot{f}(\theta) > 0 & \text{if } 0 < f(\theta) < 1 \wedge y^T \nabla f(\theta) > 0 \\ \dot{f}(\theta) = 0 & \text{if } f(\theta) = 1 \wedge y^T \nabla f(\theta) > 0 \\ \dot{f}(\theta) < 0 & \text{if } f(\theta) \leq 0 \vee y^T \nabla f(\theta) \leq 0 \end{cases}.$$

Thus $f(\theta_0) \leq 1 \Rightarrow f(\theta) \leq 1 \forall t \geq 0$. □

Remark A.4. Given $\theta_0 \in \Omega_0$, θ may increase up to the boundary where $f(\theta) = 1$. However, θ never leaves the convex set Ω_1.

Example A.1 (Projection Algorithm in Adaptive Control Law)**.** Let $\Theta(t) : \mathbb{R}^+ \to \mathbb{R}^{m \times n}$ represent a time varying feedback gain in a dynamical system. This feedback gain is implemented as:

$$u = \Theta(t)^T x$$

where $u \in \mathbb{R}^n$ represents the control input and $x \in \mathbb{R}^m$ the state vector. The time varying feedback gain is adjusted using the following adaptive law

$$\dot{\Theta} = \text{Proj}(\Theta, -xe^T PB, F)$$

where $e \in \mathbb{R}^m$ is an error signal in the state vector space, $P \in \mathbb{R}^{m \times m}$ is a square matrix derived from a Lyapunov relationship and $B \in \mathbb{R}^{m \times n}$ is the input Jacobian for the LTI system to be controlled and $F(\Theta) = [f_1(\theta_1) \ \ldots \ f_m(\theta_m))]^T$. The projection algorithm operates with the family of convex functions

$$f(\theta; \vartheta, \varepsilon) = \frac{\|\theta\|^2 - \vartheta^2}{2\varepsilon\vartheta + \varepsilon^2}.$$

Then, the components of the convex vector function F are chosen as

$$f_i(\theta_i) = f(\theta_i; \vartheta_i, \varepsilon_i). \tag{A.10}$$

Each i–th component of F is associated with two constant scalar quantities ϑ_i and ε_i. From (A.10), $f_i(\theta_i) = 0$ when $\|\theta_i\| = \vartheta_i$, and $f_i(\theta_i) = 1$ when $\|\theta_i\| = \vartheta_i + \varepsilon_i$. If the initial condition for Θ is such that $\Theta(t = 0) \in \Theta_0 = [\theta_{0,1} \ \ldots \ \theta_{0,m}]$ where $\{\theta_{0,i} | f_i(\theta_i) \leq 0 \, i = 1 \text{ to } m\}$, then each θ_i satisfies all three conditions for Lemma A.5. Thus $\|\theta_i(t)\| \leq \vartheta_i + \epsilon_i \forall t \geq 0$.

A.3 Γ–Projection

Definition A.5. A variant of the projection algorithm, Γ–projection, updates the parameter along a symmetric positive definite gain Γ as defined below

$$\text{Proj}(\theta, y, f) = \begin{cases} \Gamma y - \Gamma \frac{\nabla f(\theta)(\nabla f(\theta))^T}{(\nabla f(\theta))^T \Gamma \nabla f(\theta)} \Gamma y f(\theta) & \text{if } f(\theta) > 0 \wedge y^T \Gamma \nabla f(\theta) > 0 \\ \Gamma y & \text{otherwise.} \end{cases} \tag{A.11}$$

This method was first introduced in [32].

Lemma A.6. *Given* $\theta^* \in \Omega_0$,

$$(\theta - \theta^*)^T(\Gamma^{-1}Proj(\theta, y, f) - y) \leq 0. \tag{A.12}$$

Proof. If $f(\theta) > 0 \wedge y^T\Gamma\nabla f(\theta) > 0$, then

$$(\theta^* - \theta)^T \left(y - \Gamma^{-1} \left(\Gamma y - \Gamma \frac{\nabla f(\theta)(\nabla f(\theta))^T}{(\nabla f(\theta))^T\Gamma\nabla f(\theta)} \Gamma y f(\theta) \right) \right)$$

and using Lemma A.2

$$\frac{\underbrace{(\theta^* - \theta)^T\nabla f(\theta)}_{\leq 0}\underbrace{(\nabla f(\theta))^T\Gamma y}_{>0}}{(\nabla f(\theta))^T\Gamma\nabla f(\theta)} \underbrace{f(\theta)}_{\geq 0} \leq 0$$

otherwise $\text{Proj}(\theta, y, f) = \Gamma y$. □

Appendix B

Bounds for Signals in SISO Adaptive System

B.1 Norm of $e_\chi(t)$

In this Appendix we compute the $\mathcal{L}_2$ norm of $e_\chi(t)$. The expression in (4.58) is equivalent to studying the equation

$$e_\chi(t) = \left[\overline{\theta}^T(t) - F(s)\overline{\theta}^T(t)F(s)^{-1}\right] F(s)I\bar{\omega}(t) \tag{B.1}$$

Given the definition of $F(s)$ in (4.69) we have that

$$F(s)\overline{\theta}^T(t)F(s)^{-1} = \overline{\theta}^T(t) - \frac{1}{s+f_1}\dot{\overline{\theta}}^T(t). \tag{B.2}$$

This allows (B.1) to be rewritten as

$$e_\chi(t) = \frac{1}{s+f_1}\dot{\overline{\theta}}^T(t)\frac{1}{s+f_1}I\bar{\omega}(t). \tag{B.3}$$

This is analyzed in 3 parts

$$|e_\chi(t)| \leq \chi_1(t) + \chi_2(t) + \chi_3(t) \tag{B.4}$$

where

$$\chi_1(t) = e_\chi(0)\Phi_f(t,0) \tag{B.5}$$

$$\chi_2(t) = \int_0^t \|\dot{\bar{\theta}}(\tau)\|\Phi_f(t,\tau)e_\chi(0)\Phi_f(\tau,0)d\tau \tag{B.6}$$

$$\chi_3(t) = \int_0^t \|\dot{\bar{\theta}}(\tau)\|\Phi_f(t,\tau)\int_0^\tau \Phi_f(\tau,z)\|\bar{\omega}(z)\|dzd\tau \tag{B.7}$$

and

$$\Phi_f(t,\tau) = \mathbf{e}^{(-f_1(t-\tau))}. \tag{B.8}$$

Then the $\mathcal{L}_2$ norm of $e_\chi(t)$ is obtained as

$$\|e_\chi(t)\|_{\mathcal{L}_2}^2 \leq 3\sum_{i=1}^{3}\int_0^\infty \chi_i^2(\tau)d\tau. \tag{B.9}$$

Squaring and integrating (B.5) we have that

$$\int_0^\infty \chi_1^2(\tau)d\tau \leq \frac{e_\chi^2(0)}{2f_1}. \tag{B.10}$$

Notice that $\Phi_f(t,0) = \Phi_f(t,\tau)\Phi_f(\tau,0)$ is not a function of τ and therefore can be pulled out of the integral in (B.6) resulting in

$$\chi_2(t) \leq e_\chi(0)\Phi_f(t,0)\int_0^t \|\dot{\bar{\theta}}(\tau)\|d\tau. \tag{B.11}$$

Using Youngs inequality

$$\int_0^t \|\dot{\bar{\theta}}(\tau)\|d\tau \leq \left(\int_0^t 1^2 d\tau\right)^{1/2}\left(\int_0^t \|\dot{\bar{\theta}}(\tau)\|^2 d\tau\right)^{1/2}$$

and therefore

$$\chi_2(t) \leq e_\chi(0)\sqrt{t}\Phi_f(t,0)\|\dot{\bar{\theta}}(\tau)\|_{\mathcal{L}_2}. \tag{B.12}$$

Squaring the result above and integrating we have that

$$\int_0^\infty \chi_2^2(\tau)d\tau \leq \frac{e_\chi(0)^2}{4f_1^2}\|\dot{\bar{\theta}}(\tau)\|_{\mathcal{L}_2}^2 \tag{B.13}$$

Integrating the inner integral in (B.7) we have that

$$\chi_3(t) \leq \frac{\|\bar{\omega}(t)\|_\infty}{f_1}\int_0^t \|\dot{\bar{\theta}}(\tau)\|\Phi_f(t,\tau)(1-\Phi_f(\tau,0))d\tau. \tag{B.14}$$

Noting that $[1-\Phi_f(t,0)] \leq 1$ for all t the above simplifies to

$$\chi_3(t) \leq \frac{\|\bar{\omega}(t)\|_\infty}{f_1}\int_0^t \|\dot{\bar{\theta}}(\tau)\|\Phi_f(t,\tau)d\tau. \tag{B.15}$$

Using Young's Inequality we have that

$$\int_0^t \|\dot{\bar{\theta}}(\tau)\|\Phi_f(t,\tau)d\tau \leq \left(\int_0^t \Phi_f(t,\tau)d\tau\right)^{1/2}\left(\int_0^t \Phi_f(t,\tau)\|\dot{\bar{\theta}}(\tau)\|^2 d\tau\right)^{1/2} \tag{B.16}$$

and bounding the first integral term we have that

$$\int_0^t \|\dot{\bar{\theta}}(\tau)\|\Phi_f(t,\tau)d\tau \leq \frac{1}{\sqrt{f_1}}\left(\int_0^t \Phi_f(t,\tau)\|\dot{\bar{\theta}}(\tau)\|^2 d\tau\right)^{1/2}. \tag{B.17}$$

Substitution of (B.17) into (B.15), squaring and integrating we have that

$$\int_0^\infty \chi_3^2(\tau)d\tau \leq \frac{\|\bar{\omega}(t)\|_\infty^2}{f_1^3}\|\dot{\tilde{\theta}}(t)\|_{\mathcal{L}_2}^2. \tag{B.18}$$

B.2 Norm of $e_a(t)$

Noting that $\frac{a}{1+b} \leq a$ for all $a, b \geq 0$, e_y in (4.44) can be bounded as

$$|e_y(t)| \leq |e_a(t)| + |W_f(s)e_\chi(t)|\,. \tag{B.19}$$

From (B.3) and the definition of $W_f(s)$ in (4.72) the filtered error state e_ζ from (4.75) satisfies the following equality

$$e_\zeta(t) = W_e(s)\dot{\tilde{\theta}}^T(t)\frac{1}{s+f_1}I\bar{\omega}(t). \tag{B.20}$$

We will also make use of the fact that there exist an $m \geq 1$ such that

$$\mathbf{e}^{(A_\ell t)} \leq m\mathbf{e}^{(-\mu t)}. \tag{B.21}$$

e_ζ is analyzed in 3 parts just as we did with e_χ

$$|e_\zeta(t)| \leq \zeta_1(t) + \zeta_2(t) + \zeta_3(t) \tag{B.22}$$

where

$$\zeta_1(t) = e_\zeta(0)m\Phi_\mu(t,0) \tag{B.23}$$

$$\zeta_2(t) = e_\chi(0)m\int_0^t \|\dot{\tilde{\theta}}(\tau)\|\Phi_\mu(t,\tau)\Phi_f(\tau,0)d\tau \tag{B.24}$$

$$\zeta_3(t) = m\int_0^t \|\dot{\tilde{\theta}}(\tau)\|\Phi_\mu(t,\tau)\int_0^\tau \Phi_f(\tau,z)\|\bar{\omega}(z)\|dzd\tau \tag{B.25}$$

and then the $\mathcal{L}_2$ norm of $e_\zeta(t)$ is obtained as

$$\|e_\zeta(t)\|_{\mathcal{L}_2}^2 \leq 3\sum_{i=1}^3 \int_0^\infty \zeta_i^2(\tau)d\tau. \tag{B.26}$$

Squaring and integrating (B.23) we have that

$$\int_0^\infty \zeta_1^2(\tau)d\tau \leq \frac{m^2 e_\zeta^2(0)}{2\mu}. \tag{B.27}$$

Using Young's inequality the integral in (B.24) can be upper bounded by

$$\left(\int_0^t \Phi_\mu^2(t,\tau)\Phi_f^2(\tau,0)d\tau\right)^{1/2} \|\dot{\bar{\theta}}(t)\|_{\mathcal{L}_2}$$

and after computing the integral in the first term reduces to $\left(\frac{\Phi_f(2t,0)-\Phi_\mu(2t,0)}{2(\mu-f_1)}\right)^{1/2} \|\dot{\bar{\theta}}(t)\|_{\mathcal{L}_2}$. Using this, squaring and integrating (B.24) we have that

$$\int_0^\infty \zeta_2^2(\tau)d\tau \leq \frac{m^2 e_\chi(0)^2}{4\mu f_1}\|\dot{\bar{\theta}}(\tau)\|_{\mathcal{L}_2}^2 \tag{B.28}$$

Integrating the inner integral in (B.25) we have that

$$\zeta_3(t) \leq \frac{m\|\bar{\omega}(t)\|_\infty}{f_1}\int_0^t \|\dot{\bar{\theta}}(\tau)\|\Phi_\mu(t,\tau)(1-\Phi_f(\tau,0))d\tau. \tag{B.29}$$

Noting that $[1-\Phi_f(t,0)] \leq 1$ for all t the above simplifies to

$$\zeta_3(t) \leq \frac{m\|\bar{\omega}(t)\|_\infty}{f_1}\int_0^t \|\dot{\bar{\theta}}(\tau)\|\Phi_\mu(t,\tau)d\tau. \tag{B.30}$$

Using Young's Inequality we have that

$$\begin{aligned}\int_0^t \|\dot{\bar{\theta}}(\tau)\|\Phi_\mu(t,\tau)d\tau \leq &\left(\int_0^t \Phi_\mu(t,\tau)d\tau\right)^{1/2} \\ &\cdot \left(\int_0^t \Phi_\mu(t,\tau)\|\dot{\bar{\theta}}(\tau)\|^2 d\tau\right)^{1/2}\end{aligned} \tag{B.31}$$

and bounding the first integral term we have that

$$\int_0^t \|\dot{\bar{\theta}}(\tau)\|\Phi_f(t,\tau)d\tau \leq \frac{1}{\sqrt{\mu}}\left(\int_0^t \Phi_\mu(t,\tau)\|\dot{\bar{\theta}}(\tau)\|^2 d\tau\right)^{1/2}. \tag{B.32}$$

Substitution of (B.32) into (B.30), squaring and integrating we have that

$$\int_0^\infty \zeta_3^2(\tau)d\tau \leq \frac{m^2\|\bar{\omega}(t)\|_\infty^2}{\mu f_1^2}\|\dot{\bar{\theta}}(t)\|_{\mathcal{L}_2}^2. \tag{B.33}$$

Appendix C

MIMO Adaptive Control Squaring Up Example

Three separate tools are needed for the modern output feedback adaptive controller. These tools are presented in Sections C.1-C.3. The adaptive control design is given in Section C.4.

C.1 Creating SPR Transfer Functions for Square Systems Using Observer Feedback

Consider the triple $\{A, B, C^T\}$ describing the n-dimensional dynamic system

$$\dot{x} = Ax + Bu, \quad y = C^T x$$

and

$$G(s) = C^T(sI - A)^{-1}B$$

as the transfer function form $u \in \mathbb{R}^q$ to $y \in \mathbb{R}^q$. Note that the input and output are the same dimension so this system is *Square*. We now present the same notation that is in [28].

Table C.1: Definitions

Symbol	Meaning
X^T	Transpose
X^*	Complex Conjugate Transpose
$X^\dagger$	Moore-Penrose Pseudoinverse
herm$\{X\}$	$\frac{1}{2}(X + X^*)$
$X_\perp$	Orthonormal, $X_\perp^T X = 0$, $[X, X_\perp]$ full rank, $X_\perp^T X_\perp = I$

Lemma C.1. *If $G(s)$ is minimum phase, $C^TB = B^TC > 0$, (A, B) is controllable and (A, C^T) is observable, then there exists an L such that*

$$C^T(sI - (A + LC^T))^{-1}B$$

is SPR, and

$$\begin{aligned} A_L^T P + PA_L &= -Q \\ PB &= C \end{aligned} \tag{C.1}$$

where $A_L \triangleq A + LC^T$ with L and P defined by the following relations

$$L \triangleq -BC^{\dagger} herm\{PA\}(I - C_{\perp}(C_{\perp}^T herm\{PA\}C_{\perp})^{-1}C_{\perp}^T)herm\{PA\}C^{\dagger T} - BS$$

where $S \in \mathbb{R}^{q\times q}$ is an arbitrary positive definite matrix, and

$$P \triangleq C(B^TC)^{-1}C^T + B_{\perp}XB_{\perp}^T$$

where X is such that the following LMI is satisfied

$$\begin{aligned} C_{\perp}^T herm\{B_{\perp}XB_{\perp}^T A\}C_{\perp} &< 0 \\ X &> 0 \end{aligned}$$

For any minimum phase system an X such that the above LMI is satisfied always exists. [5]

Proof. See [5, 28] □

C.2 Squaring Up

Consider the triple $\{A, B, C^T\}$ describing the n-dimensional dynamic system

$$\dot{x} = Ax + Bu, \quad y = C^Tx,$$

$u \in \mathbb{R}^m$ and $y \in \mathbb{R}^q$.

Definition C.1. Let $[z_1,\ z_2,\ \ldots,\ z_r]$ be the zeros of $G(s)$. $z_i \in [z_1,\ z_2,\ \ldots,\ z_r]$ is a transmission zero of $G(s)$ if $G(z_i)$ is rank deficient.

Assumption C.1. Assumptions for squaring up.

1. (A, B) is controllable
2. rank $(C^TB) = m$
3. $q > m$

Lemma C.2. *Given Assumption 1, a B_1 exists such that*

$$G(s) = C^T(sI - A)^{-1}\bar{B}$$

is square and has all of its transmission zeros in the left half plane (i.e. $G(s)$ is minimum phase) for $\bar{B} \triangleq [B, B_1]$.

Proof. See [56] □

C.3 Mixing the Outputs

Consider the triple $\{A, B, C^T\}$ describing the n-dimensional dynamic system

$$\dot{x} = Ax + Bu, \quad y = C^T x,$$

$u \in \mathbb{R}^q$ and $y \in \mathbb{R}^q$. Choosing

$$S = (C^T B)^{-1}$$

The system

$$G_1(s) = SC^T(sI - A)^{-1}B$$

has the following property

$$SC^T B = (SC^T B)^T = I$$

and furthermore the transmission zeros of $C^T(sI-A)^{-1}B$ are equal to the transmission zeros of $SC^T(sI - A)^{-1}B$. [70]

C.4 Adaptive Control Example

Considering the following system with control input $u \in \mathbb{R}^m$ and command signal $z_{\text{cmd}} \in \mathbb{R}^{n_e}$.

$$\begin{aligned}
\dot{x} &= Ax + B\Lambda u + B_{\text{cmd}} z_{\text{cmd}} \\
y &= C^T x \\
z &= C_z^T x.
\end{aligned}$$

The measured outputs are $y \in \mathbb{R}^p$, regulated outputs $z \in \mathbb{R}^{n_e}$, and also we have $x \in \mathbb{R}^n$, $\Lambda \in \mathbb{R}^{m\times m}$ is an unknown positive diagonal matrix of known sign, and $A \in \mathbb{R}^{n\times n}$, $B \in \mathbb{R}^{n\times m}$, $B_{\text{ref}} \in \mathbb{R}^{n\times n_e}$, $C_z \in \mathbb{R}^{n_e\times n}$, and $C \in \mathbb{R}^{p\times n}$ are all known matrices. The controller is defined as

$$u = K^T x_m + \theta^T(t) x_m. \tag{C.2}$$

where K^T is obtained from an LQR control design (i.e. Matlab -K'=LQR(A,B,Rxx,Ruu)) and $\theta(t)$ is the adaptive parameter. Note that feedback is through x_m and not x.

The reference model is chosen as

$$\begin{aligned} x_m &= A_m x_m + B_{\text{ref}} z_{\text{cmd}} + L(y - y_m) \\ y_m &= C^T x_m \end{aligned}$$

where $x_m \in \mathbb{R}^n$, $y_m \in \mathbb{R}^p$, $L \in \mathbb{R}^{n\times p}$ and $A_m \in \mathbb{R}^{n\times n}$, where $A_m \triangleq A + BK^T$. It is assumed that a θ^* exists such that

$$A_m = A + BK^T + B\theta^{*T}. \tag{C.3}$$

We now describe how L and the update law for $\theta(t)$ are found

Step 1

Using the squaring up result from Section 2 we find a B_1 such that

$$C^T(sI - A)\bar{B}$$

is square where

$$\bar{B} = [B,\ B_1] \tag{C.4}$$

and $C^T(sI - A)\bar{B}$ is minimum phase.

Step 2

Choose $S = (C^T\bar{B})^{-1}$.

Step 3

Using the results from Section 1, we choose an L such that

$$SC^T(sI - (A + LC^T))\bar{B}$$

is SPR.

Theorem C.1. *There exist a $P = P^T$, $Q = Q^T > 0$, S_1 such that*

$$\begin{aligned} A_L^T P + PA_L &= -Q, \quad A_L \triangleq A + LC^T \\ PB &= CS_1^T \end{aligned} \tag{C.5}$$

where $S^T = [S_1^T,\ S_2^T]$.

Proof. From (C.1) in Lemma C.1 we have that

$$\begin{aligned} A_L^T P + PA_L &= -Q \\ P\bar{B} &= CS^T \end{aligned}$$

Expanding $\bar{B}$ from (C.4) and S as defined in Step 2, we have that

$$P[B,\ B_1] = C[S_1^T,\ S_2^T]$$

Removing the right hand side columns we have that $PB = CS_1^T$. □

The update law is now given as

$$\dot{\hat{\theta}} = \dot{\theta} = -\Gamma x_m (S_1 e_y)^T \tag{C.6}$$

where $e = x - x_m$, $e_y = C^T e$ and $\Gamma = \Gamma > 0$.

The error dynamics can be described as:

$$\dot{e} = Ax + B\Lambda u + B_{\text{cmd}} z_{\text{cmd}} - A_m x_m - B_{\text{cmd}} z_{\text{cmd}} + L(y - y_m) \tag{C.7}$$

where

$$\tilde{\theta} = \theta - \theta^*. \tag{C.8}$$

Notice that the term $B_{\text{cmd}} z_{\text{cmd}}$ appears in addition and subtraction, and noting that $y - y_m = C^T e$ we have

$$\dot{e} = Ax + B\Lambda u - A_m x_m + LC^T e.$$

Expanding A_m from the matching condition in (C.3)

$$\dot{e} = Ax + B\Lambda u - (A + B\Lambda\theta^{*T} + B\Lambda K^T) x_m + LC^T e.$$

Substitution of u as defined in (C.2) results in

$$\dot{e} = Ae + B\Lambda K^T x_m + B\Lambda\theta^T x_m - B\Lambda\theta^{*T} x_m - B\Lambda K^T x_m + LC^T e.$$

Collecting the factors of e, noting the cancellation of the term $B\Lambda K^T x_m$, and using the definition of $\tilde{\theta}$ in (C.8), we have

$$\dot{e} = (A + LC^T)e + B\Lambda\tilde{\theta}^T x_m.$$

The stability result follows from analyzing the Lyapunov candidate

$$V = e^T P e + \text{Trace}\left(\tilde{\theta}^T \Gamma^{-1} \tilde{\theta} \Lambda\right)$$

and differentiating we have

$$\dot{V} = e^T (A_L^T P + P A_L) e + 2e^T P B \Lambda \tilde{\theta}^T x_m + 2\text{Trace}\left(\tilde{\theta}^T \Gamma^{-1} \dot{\theta} \Lambda\right)$$

Substituting the fact that $A_L^T P + P A_L = -Q$ and $PB = CS_1^T$ from (C.5),

$$\dot{V} = -e^T Q e + 2e^T C S_1^T \Lambda \tilde{\theta}^T x_m + 2\text{Trace}\left(\tilde{\theta}^T \Gamma^{-1} \dot{\theta} \Lambda\right).$$

Using the fact that $e^T C = e_y^T$ and the substitution of the update law for $\dot{\theta}$ in (C.6) we have that

$$\dot{V} = -e^T Q e + 2e_y^T S_1^T \Lambda \tilde{\theta}^T x_m - 2\text{Trace}\left(\tilde{\theta}^T x_m (S_1 e_y)^T \Lambda\right)$$

and expanding the transpose

$$\dot{V} = -e^T Q e + 2e_y^T S_1^T \Lambda \tilde{\theta}^T x_m - 2\text{Trace}\left(\tilde{\theta}^T x_m e_y^T S_1^T \Lambda\right). \tag{C.9}$$

Note that the Trace operator has the following property

$$\text{Trace}\left(\tilde{\theta}^T x_m e_y^T S_1^T \Lambda\right) = e_y^T S_1^T \Lambda \tilde{\theta}^T x_m. \tag{C.10}$$

Using (C.10), (C.9) simplifies to

$$\dot{V} = -e^T Q e.$$

Thus our adaptive system is stable and $\lim_{t\to\infty} e(t) = 0$.

Bibliography

[1] Reka Albert and Albert-Laszlo Barabasi. Statistical mechanics of complex networks. *Reviews of modern physics*, 74(1):47, 2002.

[2] Brian Allen. Winged victory of "gossamer albatross". *National Geographic*, 1979.

[3] K. J. Aström and R. M. Murray. *Feedback Systems: An Introduction for Scientists and Engineers*. Princeton University Press, 2010.

[4] K. J. Astrom and B. Wittenmark. *Adaptive Control*. Dover, 2008.

[5] I. Barkana. Comments on "design of strictly positive real systems using constant output feedback". *Automatic Control, IEEE Transactions on*, 49(11):2091–2093, Nov. 2004.

[6] R. Bellman. The stability of solutions of linear differential equations. *Duke Math J.*, 1943.

[7] Stuart Bennett. A brief history of automatic control. *Control Systems, IEEE*, 16(3):17–25, 1996.

[8] C. E. S. Cesnik, P. J. Senatore, W. Su, E. M. Atkins, C. M. Shearer, and N. A. Pitcher. X–hale: A very flexible uav for nonlinear aeroelastic tests. In *AIAA 2010–2715*, 2010.

[9] C. E. S. Cesnik and W. Su. Nonlinear aeroelastic simulation of x–hale: a very flexible uav. In *AIAA 2011–1226*, 2011.

[10] A. Datta and P.A. Ioannou. Performance analysis and improvement in model reference adaptive control. *IEEE Trans. Automat. Contr.*, 39(12), Dec. 1994.

[11] E. J Davison and S. H Wang. Properties and calculation of transmission zeros of linear multivariable systems. *Automatica*, 10(6):643–658, 12 1974.

[12] C. A. Desoar and M. Vidyasagar. *Feedback systems: input-output properties*. Academic Press, 1975.

[13] M. Drela. Aerodynamics of human–powered flight. *Annu. Rev. Fluid Mech.*, 23, 1991.

[14] M. Drela. Integrated simulation model for preliminary aerodynamic, structural, and control–law design of aircraft. In *AIAA–99–1394*, 1999.

[15] Mark Drela. Method for simultaneous wing aerodynamic and structural load prediction. *J. Aircraft*, 1990.

[16] M. A. Duarte and K. S. Narendra. Combined direct and indirect approach to adaptive control. *IEEE Trans. Automat. Contr.*, 34(10):1071–1075, 1989.

[17] Z.T. Dydek, A.M. Annaswamy, and E. Lavretsky. Adaptive control and the nasa x-15-3 flight revisited. *Control Systems, IEEE*, 30(3):32–48, june 2010.

[18] B. Egardt. *Stability of adaptive controllers*. Springer, 1979.

[19] T. E. Gibson, A. M. Annaswamy, and E. Lavretsky. Modeling for control of very flexible aircraft. In *AIAA Guidance Navigation and Control Conference*, 2011.

[20] T. E. Gibson, A. M. Annaswamy, and E. Lavretsky. Improved transient response in adaptive control using projection algorithms and closed loop reference models. In *AIAA Guidance Navigation and Control Conference*, 2012.

[21] T. E. Gibson, A. M. Annaswamy, and E. Lavretsky. Closed–loop Reference Model Adaptive Control: Composite control and Observer Feedback. In *11th IFAC International Workshop on Adaptation and Learning in Control and Signal Processing*, 2013.

[22] T. E. Gibson, A. M. Annaswamy, and E. Lavretsky. Closed–loop Reference Model Adaptive Control, Part I: Transient Performance. In *American Control Conference*, 2013.

[23] T. E. Gibson, A. M. Annaswamy, and E. Lavretsky. Closed-loop reference models for output–feedback adaptive systems. In *European Control Conference*, 2013.

[24] T. E. Gibson, A. M. Annaswamy, and E. Lavretsky. Closed–loop reference model adaptive control: Stability, performance and robustness. *IEEE Trans. Automat. Contr.*, (*submitted*) 2012 ArXiv:1201.4897 `http://arxiv.org/abs/1201.4897`.

[25] Travis E. Gibson. Adaptive control of hypersonic vehicles. Master's thesis, Massachusetts Institute of Technology, 2008.

[26] G Goodwin, P Ramadge, and P Caines. Discrete-time multivariable adaptive control. *Automatic Control, IEEE Transactions on*, 25(3):449–456, 1980.

[27] W. Hahn. *Stability of Motion*. Springer–Verlag, New York NY, 1967.

[28] C. H. Huang, P. A. Ioannou, J. Maroulas, and M. G. Safonov. Design of strictly positive real systems using constant output feedback. *Automatic Control, IEEE Transactions on*, 44(3):569–573, Mar 1999.

[29] H. S. Hussain, M. Matsutani, A. M. Annaswamy, and E. Lavretsky. Adaptive control of scalar plants in the presence of unmodeled dynamics. In *IFAC International Workshop on Adaptation and Learning in Control and Signal Processing*, 2013.

[30] H. S. Hussain, M. Matsutani, A. M. Annaswamy, and E. Lavretsky. Robust adaptive control in the presence of unmodeled dynamics: A counter to rohrs's counterexample. In *AIAA Guidance Navigation and Control Conference*, 2013.

[31] P. A. Ioannou and A. Datta. Robust adaptive control: a unified approach. *Proc. IEEE*, 79:1736–1768, 1991.

[32] P.A. Ioannou and J. Sun. *Robust Adaptive Control*. Dover, 2013.

[33] P.A. Ioannou and G. Tao. Frequency domain conditions for strictly positive real functions. *IEEE Trans. Automat. Contr.*, 32(1):53–54, January 1987.

[34] R. E. Kalman. Mathematical description of linear dynamical systems. *J.S.I.A.M. Control*, 1(2), 1963.

[35] R. E. Kalman and J. E. Bertram. Control systems analysis and design via the 'second method' of liapunov, i. continuous-time systems. *Journal of Basic Engineering*, 82:371–393, 1960.

[36] G. Kreisselmeier and K. S. Narendra. Stable model reference adaptive control in the presence of bounded disturbances. *IEEE Trans. Automat. Contr.*, 27:1169–1175, Dec 1982.

[37] M. Krstic, I. Kanellakopoulos, and P. Kokotovic. *Nonlinear and Adaptive Control Design*. John Wiley and Sons, 1995.

[38] M. Krstic and P. V. Kokotovic. Transient–performance improvement with a new class of adaptive controllers. *Syst. Contr. Lett.*, 21:451–461, 1993.

[39] A. Krupadanam, A. M. Annaswamy, and R. Mangoubi. A viable multivariable adaptive controller with application to autonomous helicopters. *AIAA Journal of Guidance Control and Dynamics*, 2002.

[40] H. Kwakernaak and R. Sivan. The maximally achievable accuracy of linear optimal regulators and linear optimal filters. *IEEE Trans. Automat. Contr.*, 17(1):79–86, February 1972.

[41] Y. D. Landau. *Adaptive Control: The Model Reference Approach*. Marcel Dekker Incorporated, 1979.

[42] J. Langford. The daedalus project: A summary of lessons learned. In *AIAA 89–2048*, 1989.

[43] E. Lavretsky. Combined / composite model reference adaptive control. *IEEE Trans. Automat. Contr.*, 54(11):2692–2697, 2009.

[44] E. Lavretsky. Adaptive output feedback design using asymptotic properties of lqg/ltr controllers. In *AIAA 2010–7538*, 2010.

[45] E. Lavretsky. Adaptive output feedback design using asymptotic properties of lqg/ltr controllers. *IEEE Trans. Automat. Contr.*, 57(6), 2012.

[46] E. Lavretsky, R. Gadient, and I. M. Gregory. Predictor–based model reference adaptive control. *AIAA JGCD*, 2010.

[47] E. Lavretsky and K. A. Wise. *Robust and Adaptive Control: With Aerospace Applications*. Springer, 2013.

[48] P. D. Lax. *Functional Analysis*. Wiley-Interscience, 2002.

[49] Tea-Gyoo Lee and Uk-Youl Huh. An error feedback model based adaptive controller for nonlinear systems. In *Proceedings of the IEEE International Symposium on Industrial Electronics*, 1997.

[50] Y.-Y. Liu, J.-J.E. Slotine, and A.-L. Barabasi. Controllability of complex networks. *Nature*, 478:167–173, 2013.

[51] A.M. Lyapunov. Problème général de la stabilité du mouvement (translation of the russian original, 1892). *Ann. Fac. Sci. Toulouse*, 2(9):203–474, 1907.

[52] J. S. Massera. Contributions to stability theory. *Annals of Mathematics*, 64(1), 1956 (Erratum, Ann. of Math, 1958).

[53] M. Matsutani. *Robust adaptive flight control systems in the presence of time delay*. PhD thesis, Massachusetts Institute of Technology, 2013.

[54] M. Matsutani, A. M. Annaswamy, and E. Lavretsky. Guaranteed delay margins for adaptive control of scalar plants. In *IEEE, Conference on Decision and Control*, 2012.

[55] MdeVicente. Centrifugal governor. Wikipedia (Creative Commons CC0 1.0 Universal Public Domain Dedication), July 2011.

[56] P. Misra. A computational algorithm for squaring-up. i. zero input-output matrix. In *Proceedings of the 31st IEEE Conference on Decision and Control*, 1992.

[57] C. Moler and C.V. Loan. Nineteen dubious ways to compute the matrix exponential of a matrix, twenty-five years later. *SIAM Review*, 2003.

[58] R Monopoli. Model reference adaptive control with an augmented error signal. *Automatic Control, IEEE Transactions on*, 19(5):474–484, 1974.

[59] K. S. Narendra and A. M. Annaswamy. Robust adaptive control in the presence of bounded disturbances. *IEEE Trans. Automat. Contr.*, 31:306–315, 1986.

[60] K. S. Narendra and A. M. Annaswamy. A new adaptive law for robust adaptation without persistent excitation. *IEEE Trans. Automat. Contr.*, 1987.

[61] K. S. Narendra and A. M. Annaswamy. *Stable Adaptive Systems*. Dover, 2005.

[62] K. S. Narendra and P. Kudva. Stable adaptive schemes for system identification and control - parts I & II. *IEEE Transactions on Systems, Man and Cybernetics*, 4:542–560, Nov 1972.

[63] K. S. Narendra, Y. H. Lin, and L. S. Valavani. Stable adaptive controller design - part II: proof of stability. *IEEE Trans. Automat. Contr.*, 25:440–448, 1980.

[64] M. Newman. The structure and function of complex networks. *SIAM Review*, 45(2):167–256, 2013/08/08 2003.

[65] Thomas E. Noll, John M. Brown, Marla E. Perez-Davis, Stephen D. Ishmael, Geary C. Tiffany, and Matthew Gaier. Investigation of the helios prototype aircraft mishap volume i: Mishap report. In *NASA*, 2004.

[66] M. J. Patil and D. H. Hodges. Flight dynamics of highly flexible flying wings. *Journal of Aircraft*, 43(6), 2006.

[67] J. Pomet and L. Praly. Adaptive nonlinear regulation: Estimation from the lyapunov equation. *IEEE Trans. Automat. Contr.*, 37(6), June 1992.

[68] B. Raghavan and M. Patil. Flight dynamics of high aspect–ratio flying wings: Effect of large trim deformation. In *AIAA 2007–6386*, 2007.

[69] Walter Rudin. *Principles of Mathematical Analysis*. McGraw–Hill, 1976.

[70] A. Saberi, P. Kokotovic, and H. Sussmann. Global stabilization of partially linear composite systems. *SIAM Journal on Control and Optimization*, 28(6):1491–1503, 2013/05/03 1990.

[71] C. M. Shearer and C. E. S. Cesnik. Nonlinear flight dynamics of very flexible aircraft. *Journal of Aircraft*, 44(5), 2007.

[72] J.-J.E. Slotine and W. Li. Composite adaptive control of robot manipulators. *Automatica*, 25(4):509–519, 1989.

[73] J.-J.E. Slotine and W. Li. *Applied Nonlinear Control*. Prentice Hall, 1995.

[74] V. Stepanyan and K. Krishnakumar. Mrac revisited: guaranteed perforamance with reference model modification. In *American Control Conference*, 2010.

[75] V. Stepanyan and K. Krishnakumar. M–mrac for nonlinear systems with bounded disturbances. In *Conference on Decision and Control*, 2011.

[76] W. Su and C. E. S. Cesnik. Dynamic response of highly flexible flying wings. *AIAA Journal*, 49(2), 2011.

[77] H. J. Sussmann and P. V. Kokotovic. The peaking phenomonen and the global stabilization of nonlinear systems. *IEEE Trans. Automat. Contr.*, 36(4), 1991.

[78] M. C. van Schoor and A. H. von Flotow. Aeroelastic characteristics of a highly flexible aircraft. *J. Aircraft*, 20(10), 1990.

[79] H.P. Whitaker, J. Yamron, and A Kezer. Design of model reference adaptive control systems for aircraft. Technical Report R-164, Instrumentation Laboratory, Massachusetts Institute of Technology, 1958.

[80] N. Wiener. *Cybernetics: Or, Control and Communication in the Animal and the Machine*. Mit Press, 2 edition, 1965.

[81] Zhuquan Zang and R.R. Bitmead. Transient bounds for adaptive control systems. *IEEE Trans. Automat. Contr.*, 39(1), 1994.

[82] S. H. Zerweckh, A. H. von Flotow, and J. E. Murray. Flight testing a highly flexible aircraft: Case study on the mit light eagle. *J. Aircraft*, 1990.